Old Dominion University

ODU Digital Commons

Summer 2021

Finite Difference Schemes for Integral Equations with Minimal Regularity Requirements

Wesley Cameron Davis
Old Dominion University, wdavi002@odu.edu

FINITE DIFFERENCE SCHEMES FOR INTEGRAL EQUATIONS WITH

MINIMAL REGULARITY REQUIREMENTS

by

Wesley Cameron Davis
B.S. May 2014, Virginia Wesleyan College
M.S. December 2016, Old Dominion University

A Dissertation Submitted to the Faculty of
Old Dominion University in Partial Fulfillment of the
Requirements for the Degree of

DOCTOR OF PHILOSOPHY

COMPUTATIONAL AND APPLIED MATHEMATICS

OLD DOMINION UNIVERSITY
August 2021

Approved by:

Richard D. Noren (Director)

Gangfeng Ma (Member)

Gordon Melrose (Member)

Ke Shi (Member)

Xiang Xu (Member)

ABSTRACT

FINITE DIFFERENCE SCHEMES FOR INTEGRAL EQUATIONS WITH MINIMAL REGULARITY REQUIREMENTS

Wesley Cameron Davis
Old Dominion University, 2021
Director: Dr. Richard D. Noren

Volterra integral equations arise in a variety of applications in modern physics and engineering, namely in interactions that contain a memory term. Classical formulations of these problems are largely inflexible when considering non-homogeneous media, which can be problematic when considering long term interactions of real-world applications. The use of fractional derivative and integral terms naturally relax these restrictions in a natural way to consider these problems in a more general setting. One major drawback to the use of fractional derivatives and integrals in modeling is the regularity requirement for functions, where we can no longer assume that functions are as smooth or as well behaved as their classical counterparts.

This work outlines the derivation and application of a class of stable and convergent finite difference methods to discretize weakly singular integrals which occur in Volterra integral equations. This derivation is motivated by classical discretizations that arise in Caputo fractional derivatives. We present a time-fractional diffusion equation as a case study to develop the finite difference scheme, where the Laplace transform is used to pose the problem equivalently as a Volterra integral equation, which is then discretized. A generalized scheme is presented to consider a much wider class of integral equations, which allows for the consideration of applications of the Fourier transform. This ultimately allows for a natural discretization of both time- and space-fractional diffusion and differential equations. Some natural physical applications are considered to fully utilize these schemes.

The novelty of these schemes is in its simplicity and efficiency when compared to classic methods of discretization, especially for Caputo fractional derivatives. Typical discretizations in the fractional derivative form over-assume regularity to discretize a full derivative term, which subsequently restricts the admissible solution space. Other considerations from discretizing the fractional derivative form include negatively impacting the rate of convergence from the remaining fractional integration term, which is recovered by the use of

non-uniform mesh partitions to recover some of the order of convergence.

I dedicate this dissertation to my wife, Katie. Please don't call me "doctor" in the airport. To my family and friends, thank you for your undying support and dedication through everything.

ACKNOWLEDGEMENTS

I extend my many thanks and deepest gratitude to...

Dr. Richard Noren

If only I could sum up him to others as he has been to me. He has been a wonderful mentor, guide, and most of all, friend. There were countless times where he could have given up on me, but he saw something in me and helped me become who I am today. He always challenged me to go above and to do better, not just to do enough.

Dr. Gordon Melrose

It was Dr. Melrose's transform methods class that inspired me to pursue this subject matter in such a zealous manner. There were many times where I could have given up, but Dr. Melrose wouldn't give up on me. I still believe I'm his favorite problem child to this day.

Drs. Ke Shi and Xiang Xu

Drs. Shi and Xu have been wonderful mentors through and through, and gave me a new-found appreciation of mathematics as a whole. It has been a true pleasure working with them and learning from them over the years.

My wife, Katie

I'd write a love letter in this if it wasn't going to be published for all to see. This achievement is as much mine as it is yours, since you've supported me without end for year after year while I babble on about how cool I think math is. You have been there through the highs and the lows, and you've been an unending source of love and reassurance that I was capable of doing this.

My family and friends

I would not be where I am today if it was not for your love and support. You being there was more than enough to keep me going and sane. I owe a piece of this to each of you for being an anchor for me. I think I've probably lost my mind several times over the years, but somehow you keep me going and put me back together.

TABLE OF CONTENTS

LIST OF TABLES

Table   Page

LIST OF FIGURES

Figure   Page

Figure   Page

CHAPTER 1

INTRODUCTION AND RELATED WORKS

Fractional derivatives naturally generalize the classical definition of the derivative to convey the rate of change of a function in non-homogeneous material. This presents a much wider class of differential equations and partial differential equations with fractional derivative terms that naturally arise in many areas of physic and engineering ([1],[4], [18],[22], [23],[30], [32], [40], and [56]). These types of equations have been studied over the last several decades in various manners, beginning with the nature and derivation of systems of equations that arise from the physical phenomena. One of the major goals in its infancy was to demonstrate the existence and uniqueness of solutions to many of these equations, as well as any of the semigroups of the equations to consider a wider class of physical phenomena, as seen in [2], [16], [17], and [28].

The existence and uniqueness of solutions to these types of equations impose regularity restrictions based on the order of derivative present in the differential equations. In particular, for fractional derivative terms, then fractional orders of regularity are imposed on the solutions to satisfy a classical solution in general. Some of the framework for this discussion can be found in [12], [16], [17], [25], [26], [44], and [51], and the problem in over-assuming regularity of the function is discussed further in [45] and [46]. As a result, solutions to these types of equations can run into regularity issues depending on the order of fractional derivative imposed. The regularity of the solutions is paramount to how physically viable these solutions are, and how practical they are in terms of modeling physical phenomena, as seen in [13], [29] [22], [45], [55]. While the existence and uniqueness of solutions is still an ongoing topic as newer partial differential equations arise, over time the interest has shifted to numerically discretizing fractional differential equations and fractional partial differential equations.

The numerical analysis of these fractional differential equations and fractional partial differential equations has been an ongoing discussion over the past several decades. Classical methods of discretization include deriving finite difference methods and linear interpolation for the fractional derivative terms, as showcased in [43], [56], and [47]. Finite difference methods have served as the standard for a great number of years, but one of the largest drawbacks is the over-assumption of regularity in full differential form. This suggests that

the problem is forced to be too unique, as seen in [45], which means that not all physical phenomena can be simulated numerically in a stable manner. Linear interpolation suffers from the same issues, generally speaking, but the difference between the two lies in the derivation of the scheme. This difference is highlighted because classical finite difference methods are derived by using Taylor series expansions of functions to obtain an estimate for any given point on a grid [9], [20], [21], [53]. This tool is highly effective in practice, but without careful consideration, can force the scheme to be too rigid.

More recent work involving fractional differential and fractional partial differential equations focus on analyzing a time-fractional diffusion equation with a simple Laplacian operator in the space variable. In particular, the most popular method of discretizing a fractional diffusion equation is the so-called L1-method, where a second order linear interpolation is applied to the Caputo fractional derivative to discretize the derivative under the integral. This time stepping method is a natural approach, but it suffers on the regularity and the rate of convergence approach, as seen in [8], [9], [22], [23], and [34]. One of the ways to mitigate the rate of convergence concern is to re-discretize the problem on non-uniform and quasi-uniform meshes to minimize the error term on certain subintervals [34], [35], [46], [56]. As a consequence, the weak singularity near the origin for these problems is better approximated, and attains a better rate of convergence in this ad-hoc method.

Another area of improvement presented for the L1-method is the re-writing of the scheme to consider nonsmooth initial data, as seen in [22],[23], and [29]. These results presented have lasting implications, and allow for a greater class of functions to be approximated, but ultimately suffers from some of the same issues as before. Since the scheme is rewritten to better handle nonsmooth initial data, the scheme is more complex, and ultimately takes much longer to numerically simulate experiments as a result.

Fast solver methods have been another focus in recent years, where the memory term from the fractional derivative is approximated with a minimal amount of points [33]. Since the memory term is discretized as a summation of all of the previous time steps, many operations are devoted to storing the information from previous time steps and summing the new data. One flaw is the over-assumption of regularity in the memory term, which can lead to instability if not carefully treated. In short, in differential form, fractional differential equations and fractional partial differential equations suffer from the regularity requirement when numerically discretizing them.

This work bridges the gap between sensibility and practicality in its approach in discretizing differential equations with a fractional derivative term. This is highlighted by allowing

for a much wider class of functions to be numerically approximated that would normally fail to converge numerically in differential form, while maintaining an optimal rate of convergence. As seen in the literature, this is also accomplished by solving a weak formulation of the given problem, but typically fractional derivatives still prove problematic in a weak sense. Since the methods outlined here completely relax the regularity assumptions on the objective function and on the integral kernel, far more physical problems can be modeled, and with exact regularity.

This work begins by analyzing the L1-method and applying a Laplace transform to a Caputo time-fractional diffusion equation to obtain a Volterra Integral equation with a Laplacian term in Chapter 1. From there, a C^α and C^1 in-time schemes are constructed analogously to the lemmas in [56], with an optimal rate of convergence in both scenarios. Due to the nature of the convolution Volterra integral, term, the truncation error aids in the numerical convergence for certain forcing functions f. The stability and convergence of both schemes is proven, followed by some numerical examples illustrating these findings. Of particular interest is the reduction in condition number from the scheme outlined in [56] by a large factor, which is detailed further in Appendix C. One of the major questions that necessitate the findings in Chapter 2 is why the C^1 in-time scheme provided a rate of convergence of $O(\tau^{1+\alpha})$, where τ is the size of uniform subinterval of the time mesh, and whether other schemes can be constructed analogously.

In Chapter 2, Volterra integral equations with convolution kernels are considered, where a Taylor series expansions is used to construct schemes that are γ-order accurate, where now $0 < \gamma \leq 5$. In particular, any order γ scheme can be derived under this construction, however for $\gamma > 5$ the schemes are not always stable, hence are no longer guaranteed to numerically converge. Fractional-order regularity is addressed with regularity barriers, which further supports the findings in Chapter 1 and from [8]. Additionally, an invertibility criterion in derived to properly implement the schemes numerically, but does not outright prevent numerical convergence, as demonstrated in the numerical examples for Chapter 2. Further, the stability and convergence of the γ-order accurate schemes is proven with mild assumptions on the integral kernel. Notably, the standard assumption of a decreasing integral kernel is only required for γ-order accurate approximation for $\gamma > 2$, which allows for a wide class of problems to be approximated with minimal regularity assumed.

The link between Chapters 2 and 3 are readily apparent from the Laplace transform of the time-fractional diffusion equation, where Volterra integral equations can be obtained from time-fractional differential equations in a similar form. Chapter 4 addresses how this notion

can extend in a rather natural way to consider the Fourier transform instead, namely with the ultimate goal to address space-fractional differential equations. By applying a Fourier transform to the time-fractional diffusion equation instead, we find that the resulting integral equation is now a Fredholm integral equation with a convolution integral kernel as well.

Interestingly enough, the resulting Fredholm equation can be rewritten as a Volterra equation from the convolution integral kernel, so the results in Chapter 3 and from Chapter 2 can be applied similarly. Some numerical results are presented that validate the findings of the finite difference schemes and their results under this new construction. For real-analytic functions, often seen in the heat equation and other physical problems, simple trigonometric interpolation can be used on the resulting Fredholm equation with an optimal order of convergence, as seen in [26].

Chapters 5 and 6 present two case studies on applying these techniques in a meaningful way to physical problems. Chapter 5 considers the works in [1] and [49] and applies a Laplace transform to a time-fractional version of Theis's groundwater flow equation to obtain a Volterra equation in one-dimensional cylindrical coordinates. One major consideration is inclusion of a aquifer, which suggests a mild singularity near the origin. By applying Neumann boundary conditions on Theis's fractional partial differential equation, axi-symmetric diffusion of water can be modeled and discretized meaningfully as a Volterra integral equation. The full discrete problem is derived using a C^1 order accurate scheme.

Chapter 6 contrasts the previous chapters by considering a nonlinear Volterra integral equation from the works in [15] and [13]. The Taylor series expansion argument is now recast to approximate any nonlinear function, where in there a quartic function is the objective function to discretize under the integral. Two prospective methods are proposed that are founded in the results in the previous chapters, where the positive and negative aspects are presented for both methods.

CHAPTER 2

AN α-ORDER STABLE AND CONVERGENT FINITE DIFFERENCE SCHEME FOR THE TIME-FRACTIONAL DIFFUSION EQUATION

We begin with a treatment of the Caputo time-fractional diffusion equation, by using the Laplace transform, to obtain a Volterra integro-differential equation. We derive and utilize a numerical scheme that is derived in parallel to the L1-method for the time variable and a standard fourth order approximation in the spatial variable. The main method derived in this paper has a rate of convergence of $O(k^\alpha + h^4)$ for $u(x,t) \in C^\alpha([0,T]; C^6(\Omega))$, $0 < \alpha < 1$, which improves previous regularity assumptions that require $C^2[0,T]$ regularity in the time variable. We also present a novel alternative method for a first order approximation in time, under a regularity assumption of $u(x,t) \in C^1([0,T]; C^6(\Omega))$, while exhibiting order of convergence slightly more than $O(k)$ in time. This allows for a much wider class of functions to be analyzed which was previously not possible under the L1-method. We present numerical examples demonstrating these results and discuss future improvements and implications by using these techniques.

2.1 INTRODUCTION

Fractional differential equations have been of great interest to various fields in physics, engineering, and mathematics over the past several decades, as seen in [10,11] and many others. Many applications of fractional diffusion equations are studied due to their physical applications, we refer to [10-16] for a small survey of relevant and related works. In their 2014 article [56], Zhang et al. established a numerical scheme for the one-dimensional time-fractional order diffusion equation with initial and boundary conditions

$$\mathcal{D}_t^\alpha u(\mathbf{x},t) = \frac{\partial^2}{\partial x^2} u(\mathbf{x},t) + f(\mathbf{x},t), \ \mathbf{x} \in \Omega, \ t \in [0,T], \tag{1}$$

$$u(x,0) = \phi(x), \ x \in [0,1] \text{ and } u(0,t) = u(1,t) = 0,$$

with $\alpha \in (0,1)$ order Caputo fractional time derivative defined by

$$\mathcal{D}_t^\alpha u(\mathbf{x},t) = \frac{1}{\Gamma(1-\alpha)} \int_0^t \frac{\partial u(\mathbf{x},s)}{\partial s} (t-s)^{-\alpha} \, ds,$$

where $\Gamma(x) = \int_0^\infty e^{-t} t^{x-1}\, dt$. Various authors have placed various hypotheses on the PDE in their analysis, see [1,2,15,16]. This problem was solved numerically in [56] on the domain $[0,1] \times [0,T]$ with numerical accuracy of order $O(k^{2-\alpha} + h^4)$ by application of a 4th order spatial and a 2nd-order in time scheme, where k denotes the time mesh size and h denotes the space mesh size, with a constant that depends on T^α. The 2nd-order time scheme is the so-called L1-method, which has been studied extensively in previous works, see [22], [29], [46],[55], and [56] for further discussion. One of the main issues with the L1-method is the strength of regularity it requires, namely that the function must lie in $u(x, \cdot) \in C^2[0,T]$ because of the derivative under the integral. Typical solutions to (1) may only lie in $C^\alpha[0,T]$ due to the nature of the fractional derivative (c.f [46] and [17]), see [22], [23], [29], [45], and [55] for further discussion. In contrast, our response to this issue is to apply the Laplace transform to reformulate the problem (1) into an equivalent form. Based on the new formulation, we are able to construct two time discretizations tailored towards the weaker regularity assumptions of $C^\alpha[0,T]$ and $C^1[0,T]$ for both $u(x, \cdot) \in C^\alpha[0,T]$ and $u(x, \cdot) \in C^1[0,T]$, respectively. We will use the same 4th order discrete spatial Laplacian operator as in [56]. Under such weaker regularity setting, when $u(x, \cdot) \in C^\alpha[0,T]$, our analysis shows that the order of convergence is $\mathcal{O}(k^\alpha)$. This is achieved by utilizing a fractional Taylor series expansion of the objective function, which is further detailed in [53]. It's worth to mention that for a class of functions in $C^\alpha[0,T]$, a convergence rate of $O(k)$ can be obtained using the results outlined in [11],[30], [34], and [35]. In addition, by slightly strengthening the regularity assumption to have $u(x, \cdot) \in C^1[0,T]$, we can modify the scheme such that it provides an optimal convergence rate of $O(h^4 + k^1)$ but numerical experences show an even better convergence rate of $\mathcal{O}(h^4 + k^{1+\alpha})$.

Existence, uniqueness, and monotonicity results were established in [17] by A. Friedman for the solution of a generalization of equation (2), see Corollary 1 of [2, p.143]. Applications are referenced as well in [2, p.146-147]. More recently, M. Stynes et al were able to obtain existence and uniqueness for the solution of a generalization of equation (2) in [46], see Theorem 2.1 of [46] for further discussion.

The remainder of the paper is organized as follows. Section 2 presents the preliminaries and the existence and uniqueness of a solution to this newly transformed equation. Section 3 defines the numerical schemes and establishes the necessary lemmas for our a priori error estimates. Section 4 contains the statements of our main theorems presented. Section 5 presents some numerical examples illustrating our results. Finally, we conclude our findings in Section 6.

2.2 PRELIMINARIES

We will transform (1) into its equivalent form

$$u(x,t) = \phi(x) + \left(a_{1-\alpha} * \left(\frac{\partial^2 u}{\partial x^2} + f \right) \right)(x,t), \tag{2}$$

where $a_{1-\alpha}(t) = \dfrac{t^{\alpha-1}}{\Gamma(\alpha)}$ by application of the Laplace transform under the hypotheses of Theorem A from [46], which we state below. Let $\{(\lambda_i, \psi_i) : i = 1, 2, ...\}$ be the eigenvalues and eigenfunctions for the Sturm-Liouville two-point boundary value problem

$$\mathcal{L}\psi_i = -p\frac{\partial^2 \psi_i}{\partial x^2} + c\psi_i = \lambda_i \psi_i \ \text{ on } (0,1), \quad \psi_i(0) = \psi_i(1) = 0,$$

where the eigenfunctions are normalized by requiring $\|\psi_i\|_2 = 1$ for all i. Let $\langle f, g \rangle = \int_\Omega f(x)g(x)\, dx$ denote the usual L^2 inner product over a given domain Ω. Define the fractional power $\mathcal{L}^\gamma$ of the operator $\mathcal{L}$ for each $\gamma \in \mathbb{R}$ with corresponding domain

$$D(\mathcal{L}^\gamma) = \left\{ g \in H_0^2(0,1) : \sum_{i=1}^\infty \lambda_i^{2\gamma} |\langle g, \psi_i \rangle| < \infty \right\} \subset L^2(0,1).$$

Further, we will use the Sobolev space norm

$$\|g\|_{\mathcal{L}^\gamma} = \left(\sum_{i=1}^\infty \lambda_i^{2\gamma} |\langle g, \psi_i \rangle| \right)^{1/2}, \text{ for all } g \in D(\mathcal{L}^\gamma).$$

Theorem (2.1 of [46]). *Let* $\phi \in D(\mathcal{L}^{5/2})$, $f(\cdot, t) \in D(\mathcal{L}^{5/2})$, $f_t(\cdot, t) \in D(\mathcal{L}^{1/2})$, *and* $f_{tt}(\cdot, t) \in D(\mathcal{L}^{1/2})$ *for each* $t \in (0,T]$ *with*

$$\|f(\cdot, t)\|_{\mathcal{L}^{5/2}} + \|f_t(\cdot, t)\|_{\mathcal{L}^{1/2}} + t^\rho \|f_{tt}(\cdot, t)\|_{\mathcal{L}^{1/2}} \le C_1$$

for all $t \in (0,T]$ *and some constant* $\rho < 1$ *where* C_1 *is a constant independent of t. Then,* (1) *has a unique solution u that satisfies the initial and boundary conditions pointwisely, and there exists a constant C such that*

$$\left| \frac{d^k u}{dx^k} \right| \le C \text{ for } k=0,1,2,3,4 \tag{3}$$

$$\left| \frac{d^l u}{dt^l} \right| \le C(1 + t^{\alpha-l}) \text{ for } l=0,1,2. \tag{4}$$

Lemma 2.2.1. *Assume the hypothesis of Theorem 2.1 of [46]. Then the function* $u = u(x,t)$ *satisfies* (1) *if and only if it satisfies* (2).

Proof. We use the convolution theorem (see Chapter 6, Section 1.3 of [4, p.135])

$$\mathscr{L}(a * b) = \mathscr{L}(a)\mathscr{L}(b) \text{ if } (a * b)(t) = \int_0^t a(t-s)b(s)\,ds$$

and the facts

$$\mathscr{L}(a_\alpha)(z) = z^{\alpha-1} \text{ and } \mathscr{L}(h')(z) = z\mathscr{L}(h)(z) - h(0)$$

to obtain

$$\mathscr{L}(\mathcal{D}_t^\alpha u(x,t)) = (z\mathscr{L}(u(x,\cdot))(z) - \phi(x))z^{\alpha-1}$$

Applying the Laplace transform to equation (1) we obtain after some algebra,

$$(z\mathscr{L}(u(x,\cdot))(z) - \phi(x))z^{\alpha-1} = \left[\mathscr{L}\left(\frac{\partial^2 u}{\partial x^2}(x,\cdot)\right) + \mathscr{L}(f(x,\cdot))(z)\right]$$

$$\mathscr{L}(u(x,\cdot))(z) = z^{-1}\phi(x) + z^{-\alpha}\left[\mathscr{L}\left(\frac{\partial^2 u}{\partial x^2}(x,\cdot)\right) + \mathscr{L}(f(x,\cdot))(z)\right].$$

By inverting the Laplace transform, we get the equivalent Volterra integral equation

$$u(x,t) = \phi(x) + a_{1-\alpha} * \left(\frac{\partial^2 u}{\partial x^2} + f\right)(x,t).$$

Since the steps are reversible and our formal manipulations are valid by Theorem A, then the result follows. □

Remark 2.2.2. *The manipulations in the prior lemma use the assumptions from Theorem 2.1 of [46] in order to guarantee our a priori estimates that are derived in sections 3 and 4.*

With the equivalence established between (1) and (2), next we provide the finite difference schemes and the a priori error estimates in the following sections. The existence and uniqueness of a solution to (2) is presented in Appendix A. We now examine the consistency, stability, and convergence of multiple numerical schemes for (2) based on the regularity of the solution in the time-variable.

2.3 FULLY DISCRETIZED NUMERICAL SCHEMES

In [22], [23],[29], and [56], a fully discrete scheme was derived for the L1-method in the time variable and analyzed as such. By utilizing the Laplace transform, we are able to derive an equation with a different integral kernel than the fractional derivative operator as defined before. Therefore, we will derive two convergent numerical schemes for this newly transformed equation for both a first and an α-order approximation to (2) in time. The schemes are defined by the degree of regularity that will be assumed, therefore we will

construct an α-order accurate scheme for functions that are $C^\alpha[0, T]$ in time and a first-order accurate scheme for functions that are $C^1[0, T]$ in time. From there, we will utilize a standard fourth-order stable spatial operator that was utilized in [56] to arrive at the fully discretized equations.

We will use the notations and state key results from [56] that extend to our work. Divide the time interval [0,T] into N intervals where $0 = t_0 < t_1 < ... < t_N = T$. Denote the time steps as

$$\tau_n = t_n - t_{n-1}, \quad 1 \le n \le N,$$

and the mesh size of the partition

$$\tau_{max} = \max_{1 \le j \le N} \tau_j.$$

We will derive the numerical results for any temporal mesh provided, see Theorems 3.1, 3.2, 4.3, and 4.6 for these results. Having established the unique solution to (2) in section 2.1, we shall denote the grid function by

$$v = \{v_i : \ 0 \le i \le M\}, \text{ where } M > 0, \ h = \frac{1}{M}, \text{ and } x_i = ih,$$

and the grid operator

$$\mathcal{H}_h v_i = \begin{cases} \dfrac{1}{12}(v_{i+1} + 10v_i + v_{i-1}), & 1 \le i \le M - 1, \\ v_i, & i = 0 \text{ or } i = M. \end{cases} \tag{5}$$

When $1 \le i \le M - 1$,

$$\mathcal{H}_h u(x_i, t_n) = \frac{1}{12}u(x_{i-1}, t_n) + \frac{10}{12}u(x_i, t_n) + \frac{1}{12}u(x_{i+1}, t_n)$$

$$= \mathcal{H}_h \left[u(x_i, 0) + \frac{1}{\Gamma(\alpha)} \int_0^{t_n} (t_n - s)^{\alpha-1} \left(\frac{\partial^2 u}{\partial x^2}(x_i, s) + f(x_i, s) \right) ds \right]$$

$$= \mathcal{H}_h u(x_i, 0) + \frac{1}{\Gamma(\alpha)} \int_0^{t_n} (t_n - s)^{\alpha-1} \left(\mathcal{H}_h \frac{\partial^2 u}{\partial x^2}(x_i, s) + \mathcal{H}_h f(x_i, s) \right) ds. \tag{6}$$

We present the discretization in the space variable for (2), which was used in [56].

Lemma (4.1 of [56]). *Let $f(x)$ and $\xi(s)$ be functions such that $f(x) \in C^6[x_{i-1}, x_{i+1}]$ and $\xi(s) = 5(1 - s)^3 - 3(1 - s)^5$, then*

$$\frac{f''(x_{i+1}) + 10f''(x_i) + f''(x_{i-1})}{12} = \frac{f(x_{i+1}) - 2f(x_i) + f(x_{i-1})}{h^2}$$

$$+ \frac{h^4}{360} \int_0^1 [f^{(6)}(x_i - sh) + f^{(6)}(x_i + sh)]\xi(s) \, ds.$$

2.3.1 A $C^\alpha[0,T]$ IN TIME SCHEME

In general, the solution to (1) has a regularity of $C^\alpha[0,T]$ in the time variable, so we must also consider an appropriate scheme with that regularity. We achieve such relaxation by utilizing a fractional Taylor series expansion, which is presented in [53]. The following is an analogue of Lemma 2.1 of [56].

Theorem 2.3.1. *For $0 < \alpha < 1$ and for $g(t) \in C^\alpha[0,T]$, it follows that for $C > 0$ and for each $1 \le n \le N$,*

$$\int_0^{t_n} g(s)(t_n - s)^{\alpha-1}\, ds = \sum_{k=1}^n \int_{t_{k-1}}^{t_k} g(t_k)(t_n - s)^{\alpha-1}\, ds + R_t^n, \tag{7}$$

where

$$|R_t^n| \le C \max_{0 \le t \le t_n} |\mathcal{D}_t^\alpha g(t)|(\tau_{max})^\alpha$$

Proof. We begin with the fractional derivative Taylor expansion of $g(s)$ at the point $s = t_k$, see Theorem 3.1 of [53], where $s \in [t_{k-1}, t_k]$, $t_k \in [0, t_n]$ for each $k = 1, 2, ..., N$. Utilizing Corollary 2.4 of [12], we then have for some $\xi \in (t_{k-1}, t_k)$,

$$g(s) - g(t_k) = \frac{(t_k - s)^\alpha}{\Gamma(\alpha + 1)} \mathcal{D}_t^\alpha g(\xi).$$

Define

$$(R_t)^n = \sum_{k=1}^{n-1} \int_{t_{k-1}}^{t_k} (g(s) - g(t_k))(t_n - s)^{\alpha-1}\, ds.$$

Then,

$$|(R_t)^n| \le \max_{0 \le t \le t_n} |\mathcal{D}_t^\alpha g(t)| \sum_{k=1}^n \int_{t_{k-1}}^{t_k} \frac{|(t_k - s)^\alpha|}{\Gamma(\alpha + 1)} (t_n - s)^{\alpha-1}\, ds$$

$$\le \max_{0 \le t \le t_n} |\mathcal{D}_t^\alpha g(t)| \int_0^{t_n} \frac{(\tau_{max})^\alpha (t_n - s)^{\alpha-1}}{\Gamma(\alpha + 1)}\, ds$$

$$= \frac{(\tau_{max})^\alpha}{\Gamma(\alpha + 1)} \max_{0 \le t \le t_n} |\mathcal{D}_t^\alpha g(t))| \frac{(t_n - 0)^\alpha}{\alpha}$$

$$\le \frac{T^\alpha (\tau_{max})^\alpha}{\alpha \Gamma(\alpha + 1)} \max_{0 \le t \le t_n} |\mathcal{D}_t^\alpha g(t)|. \tag{8}$$

Therefore, for a uniform mesh, we further have the result $|R_t^n| \le C\tau^\alpha$. $\qquad\square$

Define

$$a_k^n = \frac{1}{\Gamma(\alpha)} \int_{t_{k-1}}^{t_k} (t_n - s)^{\alpha-1} ds, \tag{9}$$

$$= \frac{1}{\Gamma(\alpha+1)} \left[(t_n - t_{k-1})^\alpha - (t_n - t_k)^\alpha \right].$$

We further define

$$f_{1-\alpha}(x,t) = \int_0^t \frac{(t-s)^{\alpha-1}}{\Gamma(\alpha)} f(x,s) \, ds \tag{10}$$

to denote the forcing function term in the approximate equation. By applying the $\mathcal{H}_h$ operator, Lemma 4.1 of [56], Lemma 2.2, and the previously stated discretization to (2), we have the fully discretized approximate equation for $u_i^n \approx u(x_i, t_n)$ with initial and boundary conditions

$$\begin{cases} \mathcal{H}_h u_i^n = \mathcal{H}_h \phi(x_i) + \mathcal{H}_h f_{1-\alpha}(x_i, t_n) + \sum_{k=1}^n \frac{a_k^n}{h^2} \left[u_{i+1}^k - 2u_i^k + u_{i-1}^k \right] \\ u_i^0 = 0, \quad u_0^n = u_M^n = 0, \end{cases} \tag{11}$$

for each $n = 0, 1, ..., N$, $i = 0, 1, ..., M$.

2.3.2 A $C^1[0,T]$ IN TIME SCHEME

Previously we saw that for $g \in C^\alpha[0,T]$, we can construct a one-point scheme in time that has the corresponding error of $O(k^\alpha)$. We now derive a two-point first-order scheme for $g \in C^1[0,T]$ that has the corresponding error of $O(k^1)$.

Theorem 2.3.2. *For $0 < \alpha < 1$ and for $g(t) \in C^1[0,T]$, it follows that*

$$\int_0^{t_n} g(s)(t_n - s)^{\alpha-1} \, ds = \sum_{k=1}^n \frac{g(t_{k-1}) + g(t_k)}{2} \int_{t_{k-1}}^{t_k} (t_n - s)^{\alpha-1} \, ds + R_t^n, \tag{12}$$

for each n, $1 \leq n \leq N$, where

$$|R_t^n| \leq (\tau_n + \tau_{max}) \frac{T^\alpha}{2\alpha} \max_{0 \leq t \leq t_n} |g'(t)|, .$$

Proof. We begin by writing the integral as

$$\int_0^{t_n} g(s)(t_n - s)^{\alpha-1} \, ds = \int_0^{t_{n-1}} g(s)(t_n - s)^{\alpha-1} \, ds + \int_{t_{n-1}}^{t_n} g(s)(t_n - s)^{\alpha-1} \, ds.$$

The first integral on the right hand side is rewritten as

$$\int_0^{t_{n-1}} g(s)(t_n - s)^{\alpha-1}\, ds = \sum_{k=1}^{n-1} \int_{t_{k-1}}^{t_k} g(s)(t_n - s)^{\alpha-1}\, ds$$

$$= \sum_{k=1}^{n-1} \int_{t_{k-1}}^{t_k} \left(g(s) - \frac{g(t_{k-1}) + g(t_k)}{2} \right) (t_n - s)^{\alpha-1}\, ds$$

$$+ \int_{t_{k-1}}^{t_k} \left(\frac{g(t_{k-1}) + g(t_k)}{2} \right) (t_n - s)^{\alpha-1}\, ds$$

$$= \sum_{k=1}^{n-1} \frac{g(t_{k-1}) + g(t_k)}{2} \int_{t_{k-1}}^{t_k} (t_n - s)^{\alpha-1}\, ds + (R_1)^n,$$

where

$$(R_1)^n = \sum_{k=1}^{n-1} \int_{t_{k-1}}^{t_k} \left(g(s) - \frac{g(t_{k-1}) + g(t_k)}{2} \right) (t_n - s)^{\alpha-1}\, ds.$$

By utilizing the Taylor expansion of $g(s)$ for $s \in (0, t_{n-1})$,

$$|(R_1)^n| \leq \max_{0 \leq t \leq t_{n-1}} |g'(t)| \sum_{k=1}^{n-1} \int_{t_{k-1}}^{t_k} \left| t_k - s - \frac{\tau_k}{2} \right| (t_n - s)^{\alpha-1}\, ds$$

$$\leq \frac{\tau_{max}}{2} \max_{0 \leq t \leq t_{n-1}} |g'(t)| \int_0^{t_{n-1}} (t_n - s)^{\alpha-1}\, ds$$

$$= \frac{\tau_{max}}{2} \max_{0 \leq t \leq t_{n-1}} |g'(t)| \left(\frac{t_n^\alpha}{\alpha} - \frac{\tau_n^\alpha}{\alpha} \right)$$

$$\leq \frac{\tau_{max} T^\alpha}{2\alpha} \max_{0 \leq t \leq t_{n-1}} |g'(t)|. \tag{13}$$

In a similar manner, by the Taylor expansion of g(s) for $s \in (t_{n-1}, t_n)$, we have

$$\left| g(s) - \frac{g(t_{n-1}) + g(t_n)}{2} \right| \leq \frac{\tau_n}{2} \max_{t_{n-1} \leq t \leq t_n} |g'(t)|, \quad t_{n-1} < s < t_n.$$

Therefore, the approximation error in the interval $[t_{n-1}, t_n]$ satisfies

$$|(R_2)^n| = \left| \int_{t_{n-1}}^{t_n} \left(g(s) - \frac{g(t_{k-1}) + g(t_k)}{2} \right) (t_n - s)^{\alpha-1}\, ds \right|$$

$$\leq \frac{\tau_n T^\alpha}{2\alpha} \max_{t_{n-1} \leq t \leq t_n} |g'(t)|. \tag{14}$$

Finally, since

$$R_t^n = (R_1)^n + (R_2)^n = \sum_{k=1}^{n} \int_{t_{k-1}}^{t_k} \left(g(s) - \frac{g(t_{k-1}) + g(t_k)}{2} \right) (t_n - s)^{\alpha-1}\, ds,$$

by combining the error estimates (13) and (14), we have the desired result. $\qquad \square$

We remark that under these assumptions, we may obtain a first order accurate scheme for $g(t) \in C^1[0,T]$. The L1-method requires the function $g(t) \in C^2[0,T]$ based on a Taylor series argument, so the regularity assumption for the L1-method cannot be relaxed to allow $g(t) \in C^1[0,T]$ due to the nature of the Caputo Fractional Derivative. In section 5, we will see that this scheme exhibits superconvergence for this $C^1[0,T]$ scheme. In a similar manner to the C^α scheme, we may now write the discrete approximate equation for $u_i^n \approx u(x_i, t_n)$ with initial and boundary conditions as

$$
\begin{cases}
\mathcal{H}_h u_i^n = \mathcal{H}_h \phi(x_i) + \mathcal{H}_h f_{1-\alpha}(x_i, t_n) \\
\qquad\quad + \sum_{k=1}^{n} \frac{a_k^n}{2h^2} \left[u_{i+1}^k - 2u_i^k + u_{i-1}^k \right] + \frac{a_k^n}{2h^2} \left[u_{i+1}^{k-1} - 2u_i^{k-1} + u_{i-1}^{k-1} \right], \\
u_i^0 = 0 \quad , \quad u_0^n = u_M^n = 0,
\end{cases}
\tag{15}
$$

which is to be solved for $\{u_i^n\}_{n=0,1,\ldots,N,\ i=0,1,\ldots,M}$ as before. We now examine the stability of each of these methods presented in order to guarantee the convergence of each scheme.

2.4 ERROR ESTIMATES

Before we establish stability and convergence of the numerical methods used, we will make use of the definitions in [1, p.202]. Let

$$
\mathcal{V}_h = \{v = (v_0, v_1, \ldots, v_M) | v_0 = v_M = 0\}.
$$

For any grid function $v, w \in \mathcal{V}_h$, we will define the following (c.f [56]):

$$
\delta_x v_{i-1/2} = \frac{1}{h}(v_i - v_{i-1})
$$

$$
\delta_x^2 v_i = \frac{1}{h}(\delta_x v_{i+1/2} - \delta_x v_{i-1/2})
$$

$$
\langle v, v \rangle_h = h \sum_{i=0}^{M} v_i \cdot v_i
$$

$$
L_2 \text{ norm } \|v\|_h = \sqrt{\langle v, v \rangle_h}
$$

$$
H^1 \text{ semi-norm } \|\delta_x v\|_h = \sqrt{h \sum_{i=1}^{M} (\delta_x v_{i-1/2})^2}
$$

$$
H^1 \text{ norm } \|v\|_{1,h} = \sqrt{\|v\|_h^2 + \|\delta_x v\|_h^2}
$$

Where $\|\mathcal{H}_h v\|_h$ and $\|\delta_x^2 v\|_h$ are defined in a similar manner. By applying Lemma 4.2 of [56], then

$$
\|v\|_h \leq \frac{1}{\sqrt{6}} \|\delta_x v\|_h.
$$

Following [56], define

$$\langle v, w \rangle_A = h \sum_{i=1}^{M} (\delta_x v_{i-1/2} \cdot \delta_x w_{i-1/2}) - \frac{h^2}{12} h \sum_{i=1}^{M-1} \delta_x^2 v_i \cdot \delta_x^2 w_i,$$

and

$$\|v\|_A = \sqrt{\langle v, v \rangle_A}.$$

They further go on to show that, by Lemma 4.3 of [56],

$$-h \sum_{i=1}^{M-1} (\mathcal{H}_h v_i) \cdot \delta_x^2 w_i = \langle v, w \rangle_A,$$

which establishes that $\|\cdot\|_A$ and $\|\delta_x \cdot\|_h$ are equivalent.

2.4.1 CONSISTENCY, STABILITY, AND CONVERGENCE RESULTS

With the preliminaries established in section 2, we will present the main theorems of this paper. We begin with deriving the consistency of the schemes (11) and (15) and then the stability for each. With both these proofs, we are able to assert the convergence of each scheme, which is then demonstrated in the next section. We have a similar set of results for the numerical scheme (11) for functions $g(t) \in C^\alpha[0, T]$. Beginning with the consistency results, we will provide each theorem as follows:

Theorem 2.4.1. *Let* $u(x, t) \in C^\alpha([0, T]; C^6(\Omega))$ *and let* $\{u_i^n | 0 \leq i \leq M, 1 \leq n \leq N\}$ *be the solution of the scheme* (11), *with a uniform grid used in the spatial domain. Further, let* $\phi \in D(\mathcal{L}^{5/2})$, $f(\cdot, t) \in D(\mathcal{L}^{5/2})$, $f_t(\cdot, t) \in D(\mathcal{L}^{1/2})$, *and* $f_{tt}(\cdot, t) \in D(\mathcal{L}^{1/2})$ *for each* $t \in (0, T]$. *Then,* u *is a unique solution to* (2), *with resulting approximation error*

$$\|u(x_i, t_n) - u_i^n\|_\infty \leq \frac{T^\alpha}{\Gamma(\alpha+1)} \left(\frac{h^4}{180} \left\| \frac{\partial^6 u}{\partial x^6} \right\|_\infty + \frac{(\tau_{max})^\alpha}{\alpha} \max_{0 \leq t \leq T} |\mathcal{D}_t^\alpha u(x, t)| \right). \qquad (16)$$

Proof. By Theorem A, there exists a unique solution to (2). Denote the residual of the approximation in space $(R_x)^n(x_i, t_n)$ by

$$(R_x)^n(x_i, t_n) = \frac{h^4}{360} \int_0^1 \left[\frac{\partial^6 u}{\partial x^6}(x_i - sh, t_n) + \frac{\partial^6 u}{\partial x^6}(x_i + sh, t_n) \right] ds \qquad (17)$$

for all $t \in [0, 1]$. We may then bound $(R_x)^n(x_i, t_n)$ by

$$\left| (R_x)^n(x_i, t_n) \right| = \left| \frac{h^4}{360} \int_0^1 \left(\frac{\partial^6 u}{\partial x^6}(x_i - sh, t_n) + \frac{\partial^6 u}{\partial x^6}(x_i + sh, t_n) \right) ds \right|$$

$$\left| (R_x)^n(x_i, t_n) \right| \leq \frac{h^4}{360} \int_0^1 \left(\left\| \frac{\partial^6 u}{\partial x^6} \right\|_\infty + \left\| \frac{\partial^6 u}{\partial x^6} \right\|_\infty \right) ds$$

$$= \frac{h^4}{180} \left\| \frac{\partial^6 u}{\partial x^6} \right\|_\infty.$$

In a similar manner, we bound the residual of the approximation in time $(R_t)^n(x_i, t_n)$ by

$$(R_t)^n(x_i, t_n) \leq \frac{T^\alpha (\tau_{max})^\alpha}{\alpha \Gamma(\alpha + 1)} \max_{0 \leq t \leq t_n} |\mathcal{D}_t^\alpha u(x, t)|, \tag{18}$$

as seen in Theorem 3.1. By combining the above, we have

$$\|u(x_i, t_n) - u_i^n\|_\infty = \left\| \int_0^{t_n} \frac{(t_n - s)^{\alpha - 1}}{\Gamma(\alpha)} R_x^n(x_i, s)\, ds + R_t^n \right\|_\infty \tag{19}$$

$$\leq \|R_x^n(x_i, t_n)\|_\infty \left\| \frac{t_n^\alpha}{\Gamma(\alpha + 1)} \right\|_\infty + \|R_t^n(x_i, t_n)\|_\infty \tag{20}$$

$$\leq \frac{T^\alpha}{\Gamma(\alpha + 1)} \left(\frac{h^4}{180} \left\| \frac{\partial^6 u}{\partial x^6} \right\|_\infty + \frac{(\tau_{max})^\alpha}{\alpha} \max_{0 \leq t \leq t_n} |\mathcal{D}_t^\alpha u(x, t)| \right). \tag{21}$$

Therefore, under a uniform partition of the time domain, the approximation error of (11) is $O(h^4 + \tau^\alpha)$. $\qquad \square$

Theorem 2.4.2. *Suppose $\{u_i^n | 0 \leq i \leq M, 1 \leq n \leq N\}$ is the solution of the scheme (11). Then, for any size temporal mesh described before, the discrete difference scheme (11) is unconditionally stable to f and ϕ, where*

$$\|u^n\|_A^2 \leq \|\phi\|_A^2 + \frac{T^\alpha}{\Gamma(\alpha + 1)} \max_{1 \leq l \leq N} \|\mathcal{H}_h f^l\|_h^2$$

Proof. Recall that

$$a_k^n = \frac{1}{\Gamma(\alpha)} \int_{t_{k-1}}^{t_k} (t_n - s)^{\alpha - 1} ds,$$

$$= \frac{1}{\Gamma(\alpha + 1)} \left[(t_n - t_{k-1})^\alpha - (t_n - t_k)^\alpha \right].$$

We consider the scheme (11) after combining the initial and boundary conditions. By omitting the residual term R_i^n and by substituting the exact solution U_i^k with its approximation u_i^k into (11), we have:

$$\mathcal{H}_h u_i^n = \mathcal{H}_h u_i^0 + \sum_{k=1}^n a_k^n \left(\delta_x^2 u_i^k + \mathcal{H}_h f_i^n \right).$$

By multiplying both sides by $-2h\delta_x^2 u_i^n$ and summing over each i, then

$$2 \|u^n\|_A^2 + 2 \sum_{k=1}^{n-1} a_k^n \|\delta_x^2 u^k\|_h^2 = 2\langle u^0, u^n \rangle_A - 2 \sum_{k=1}^n a_k^n \langle \mathcal{H}_h f, \delta_x^2 u^n \rangle_h$$

$$\leq \left(\|u^0\|_A^2 + \|u^n\|_A^2 \right) + \sum_{k=1}^n a_k^n \left(\|\mathcal{H}_h f^n\|_h^2 + \|\delta_x^2 u^n\|_h \right)$$

$$\Rightarrow \|u^n\|_A^2 \leq \|\phi\|_A^2 + \sum_{k=1}^n a_k^n \max_{1 \leq l \leq N} \|\mathcal{H}_h f^l\|_h^2 \quad 1 \leq n \leq N.$$

Finally, since $\sum_{k=1}^n a_k^n = \frac{T^\alpha}{\Gamma(\alpha + 1)}$ when $n = N$, we see the result holds. $\qquad \square$

To further see the convergence of the numerical scheme, denote $\epsilon_i^n := u(x_i, t_n) - u_i^n$. The error equations are then obtained:

$$\mathcal{H}_h \epsilon_i^n = \sum_{k=1}^{n} a_k^n \delta_x^2 \epsilon_i^n + R_i^n \tag{22}$$

$$\epsilon_0^n = \epsilon_M^n = 0, \ 1 \leq n \leq N$$

$$\epsilon_i^0 = 0, \ 0 \leq i \leq M.$$

We present the error convergence rate for the scheme (11):

$$\|\epsilon^n\|_\infty^2 \leq \|\epsilon^0\|_A^2 + \frac{T^\alpha}{\Gamma(\alpha+1)} \|R_i^n\|_h^2$$

$$\leq \frac{T^\alpha}{\Gamma(\alpha+1)} \left(\frac{h^4}{180} \left\| \frac{\partial^6 u}{\partial x^6} \right\|_\infty + \left(\frac{\tau_{max}^\alpha}{\Gamma(\alpha+1)} \right) \max_{0 \leq t \leq T} |\mathcal{D}_t^\alpha u(x,t)| \right)^2$$

$$\|\epsilon^n\|_\infty \leq \sqrt{\frac{T^\alpha}{\Gamma(\alpha+1)}} \left(\frac{h^4}{180} \left\| \frac{\partial^6 u}{\partial x^6} \right\|_\infty + \left(\frac{\tau_{max}^\alpha}{\Gamma(\alpha+1)} \right) \max_{0 \leq t \leq T} |\mathcal{D}_t^\alpha u(x,t)| \right).$$

Hence, the scheme (11) is both stable and consistent, hence it is convergent. Therefore, by [3, theorem 2.1] we have the following immediate results:

Theorem 2.4.3. *Let* $u(x,t) \in C^\alpha([0,T]; C^6(\Omega))$ *and let* $\{u_i^n | 0 \leq i \leq M, 1 \leq n \leq N\}$ *be the solution of the scheme* (11), *with a uniform grid used in the spatial domain and any grid spacing used in the temporal direction. Further, let* $\phi \in D(\mathcal{L}^{5/2})$, $f(\cdot, t) \in D(\mathcal{L}^{5/2})$, $f_t(\cdot, t) \in D(\mathcal{L}^{1/2})$, *and* $f_{tt}(\cdot, t) \in D(\mathcal{L}^{1/2})$ *for each* $t \in (0, T]$. *Then, it holds for some* $C > 0$

$$\|u(x_i, t_n) - u_i^n\|_\infty \leq \sqrt{\frac{T^\alpha}{\Gamma(\alpha+1)}} C \left(h^4 + \tau_{max}^\alpha \right), \quad 1 \leq n \leq N. \tag{23}$$

We now examine the consistency and stability results for the scheme (15).

Theorem 2.4.4. *Let* $u(x,t) \in C^1([0,T]; C^6(\Omega))$ *and let* $\{u_i^n | 0 \leq i \leq M, 1 \leq n \leq N\}$ *be the solution of the scheme* (15), *with a uniform grid used in the spatial domain. Further, let* $\phi \in D(\mathcal{L}^{5/2})$, $f(\cdot, t) \in D(\mathcal{L}^{5/2})$, $f_t(\cdot, t) \in D(\mathcal{L}^{1/2})$, *and* $f_{tt}(\cdot, t) \in D(\mathcal{L}^{1/2})$ *for each* $t \in (0, T]$. *Then,* u *is a unique solution to* (2), *with resulting approximation error*

$$\|u(x_i, t_n) - u_i^n\|_\infty \leq \frac{T^\alpha}{\Gamma(\alpha+1)} \left(\frac{h^4}{180} \left\| \frac{\partial^6 u}{\partial x^6} \right\|_\infty + \left(\frac{\tau_n + \tau_{max}}{2} \right) \left\| \frac{\partial u}{\partial t} \right\|_\infty \right). \tag{24}$$

Proof. The proof is identical to Theorem 4.1 and is therefore omitted. $\square$

We remark that as $\alpha \to 0$ then $\frac{T^\alpha}{\Gamma(1+\alpha)} \to 1$. Also, as $\alpha \to 1$ then $\frac{T^\alpha}{\Gamma(1+\alpha)} \to T$. The following corollary is immediate from the previous theorem.

Corollary 2.4.4.1. *Under a uniform partition of the time domain where $\tau_n = \tau$ for all n, then the approximation error of (15) is $O(h^4 + \tau)$.*

We also have a theorem asserting the stability of the discrete scheme and derives the corresponding error equations of the scheme:

Theorem 2.4.5. *Suppose $\{u_i^n | 0 \leq i \leq M, 1 \leq n \leq N\}$ is the solution of the scheme (15). Then, for any size temporal mesh described before, the discrete difference scheme (15) is unconditionally stable to f and ϕ, where*

$$\|u^n\|_A^2 \leq \|\phi\|_A^2 + \frac{T^\alpha}{\Gamma(\alpha+1)} \max_{1 \leq l \leq N} \left\|\mathcal{H}_h f^l\right\|_h^2$$

Proof. The proof is identical to Theorem 4.2, and is therefore omitted. $\qquad\square$

The error equations are then obtained:

$$\mathcal{H}_h \epsilon_i^n = \sum_{k=1}^{n} a_k^n \delta_x^2 \epsilon_i^n + a_n^n R_i^n \tag{25}$$

$$\epsilon_0^n = \epsilon_M^n = 0, \ 1 \leq n \leq N$$

$$\epsilon_i^0 = 0, \ 0 \leq i \leq M.$$

By applying (17) and by applying the previous stability analysis, we have the immediate error convergence result

$$\|\epsilon^n\|_A^2 \leq \|\epsilon^0\|_A^2 + \frac{T^\alpha}{\Gamma(\alpha+1)} \|R_i^n\|_h^2$$

$$\leq \frac{T^\alpha}{\Gamma(\alpha+1)} \left(\frac{h^4}{180} \left\|\frac{\partial^6 u}{\partial x^6}\right\|_\infty + \left(\frac{\tau_n + \tau_{max}}{2}\right) \left\|\frac{\partial u}{\partial t}\right\|_\infty \right)^2,$$

$$\|\epsilon^n\|_A \leq \sqrt{\frac{T^\alpha}{\Gamma(\alpha+1)}} \left(\frac{h^4}{180} \left\|\frac{\partial^6 u}{\partial x^6}\right\|_\infty + \left(\frac{\tau_n + \tau_{max}}{2}\right) \left\|\frac{\partial u}{\partial t}\right\|_\infty \right).$$

That is, the scheme (15) is both stable and consistent, hence it is convergent, see [7-9] for further details. Therefore, by [3, theorem 2.1] we have the following immediate results:

Theorem 2.4.6. *Let $u(x,t) \in C^1([0,T]; C^6(\Omega))$ and let $\{u_i^n | 0 \leq i \leq M, 1 \leq n \leq N\}$ be the solution of the scheme (15), with a uniform grid used in the spatial domain and any grid spacing used in the temporal direction. Further, let $\phi \in D(\mathcal{L}^{5/2})$, $f(\cdot, t) \in D(\mathcal{L}^{5/2})$, $f_t(\cdot, t) \in D(\mathcal{L}^{1/2})$, and $f_{tt}(\cdot, t) \in D(\mathcal{L}^{1/2})$ for each $t \in (0, T]$. Then, it holds for some $C > 0$*

$$\|u(x_i, t_n) - u_i^n\|_\infty \leq \sqrt{\frac{T^\alpha}{\Gamma(\alpha+1)}} C \left(h^4 + \tau_{max}\right), \quad 1 \leq n \leq N. \tag{26}$$

We also have a corollary detailing the use of a truncation of the exact solution to generate the data at $u(x, t_1)$.

Corollary 2.4.6.1. *Let* $u_{h,1}(x, t_1) = \phi(x) + \dfrac{\phi''(x)t_1^\alpha}{\Gamma(\alpha + 1)} + (f * a_{1-\alpha})(x, t_1)$. *Then, the truncation error*

$$\|e_{h,1}\|_\infty = \|u(x, t_1) - u_{h,1}(x, t_1)\|_\infty \leq C\tau_{max}^{2\alpha} \left(\left\|\phi^{(4)}(x)\right\|_\infty + \|f(x, t_1)\|_\infty\right)$$

Proof. Consider the exact solution $u(x, t)$ of (2) which is generated from (110). That is,

$$u(x, t) = \phi(x) + \frac{\phi''(x)t^\alpha}{\Gamma(\alpha + 1)} + \frac{\phi^{(4)}(x)t^{2\alpha}\Gamma(1/2)}{4^\alpha\Gamma(\alpha + 1/2)} + O(t^{3\alpha}\phi^{(6)}(x))$$
$$+ (f * a_{1-\alpha})(x, t) + ((f * a_{1-\alpha}) * a_{1-\alpha})(x, t) + O(t^{3\alpha}).$$

Hence, the truncation error at the first time step t_1 is, after ignoring the higher order terms,

$$
\begin{aligned}
\|e_{h,1}\|_\infty &= \left\| \frac{\phi^{(4)}(x)t_1^{2\alpha}\Gamma(1/2)}{4^\alpha\Gamma(\alpha + 1/2)} + ((f * a_{1-\alpha}) * a_{1-\alpha})(x, t_1) \right\|_\infty \\
&\leq Ct_1^{2\alpha}\|\phi(x)\|_\infty \\
&\quad + \left\| \int_0^{t_1} \frac{(t_1 - s)^{\alpha-1}}{\Gamma(\alpha)} \left(\int_0^s \frac{(s - v)^{\alpha-1}f(x, v)}{\Gamma(\alpha)} dv \right) ds \right\| \\
&\leq Ct_1^{2\alpha}\|\phi(x)\|_\infty + \|f(x, t_1)\|_\infty \left\| \int_0^{t_1} \frac{s^\alpha(t_1 - s)^{\alpha-1}}{\Gamma(\alpha)} \right\|_\infty \\
&= Ct_1^{2\alpha}\|\phi(x)\|_\infty + \|f(x, t_1)\|_\infty \left\| \frac{\Gamma(1/2)t_1^{2\alpha}}{4^\alpha\Gamma(\alpha + 1/2)} \right\|_\infty \\
&\leq Ct_1^{2\alpha}\left(\|\phi(x)\|_\infty + \|f(x, t_1)\|_\infty\right),
\end{aligned}
$$

which yields the desired results. □

Remark. *By letting* $t_1 = \tau$, $\phi(x) = 0$, *and where* $f(x, \tau) = (\tau + O(\tau^{1+\alpha}))X(x)$, *we have the truncation error in corollary 2.4.6.1 after neglecting the terms of order* $O(\tau^{1+\alpha})$ *:*

$$\|e_{h,1}\|_\infty = \|u(x, t_1) - u_{h,1}(x, t_1)\|_\infty \leq C\tau^{1+2\alpha}\|X(x)\|_\infty.$$

We now have two convergent schemes that were previously not possible under the usual L1-method. Further, when compared to the L1-method, we do not lose any order of convergence due to the integral kernel. That is, we are able to relax the L1-method hypothesis of $g(t) \in C^2[0, T]$ to $g(t) \in C^1[0, T]$ and further to $C^\alpha[0, T]$ while obtaining an order of convergence equal to the order of regularity.

2.4.2 CONDITIONING OF THE SCHEME

Given the numerical approximation schemes (15) and (11), we wish to investigate the condition number of the matrix of coefficients attached to the u_i^n term. In appendix B, the numerical scheme was rewritten as a matrix equation to be solved for all time and space steps. In particular, the coefficient matrices $\mathbf{I}_\alpha^*$ and $\mathbf{I}_2^*$ are inverted to solve the numerical approximation schemes (11) and (15). We define the condition numbers in a similar fashion to [50] by

$$\kappa_{2,\alpha} = \left\|\mathbf{I}_\alpha^*\right\|_2 \left\|\mathbf{I}_\alpha^{*\,-1}\right\|_2$$

$$\kappa_{2,2} = \left\|\mathbf{I}_2^*\right\|_2 \left\|\mathbf{I}_2^{*\,-1}\right\|_2,$$

where the matrix p-norm is defined for any matrix $\mathbf{I}^* \in C^{m,n}$ by

$$\left\|\mathbf{I}^*\right\|_p = \sup_{x \neq 0} \frac{\left\|\mathbf{I}_2^*\mathbf{x}\right\|_p}{\left\|\mathbf{x}\right\|_p},$$

with corresponding vector norm for the vector $\mathbf{x}$

$$\left\|\mathbf{x}\right\|_p = \left(\sum_i x_i^p\right)^{1/p}.$$

We remark that the constructions for the matrices $\mathbf{I}_\alpha^*$ and $\mathbf{I}_2^*$ depend entirely on τ, h, and α. Given the C^1 approximation scheme (15), we compute the condition number $\kappa_{2,2}$ for a numerical experiment with $u(x,t) = \sin(\pi x)t^{1.01}$, $\phi(x) = 0$, $u(0,t) = u(1,t) = 0$, given $N = 10, 20, 40, 80, 160$ and $M = 100$. In a similar manner, we can also compute the condition number $\kappa_{2,\alpha}$ for a numerical experiment with $u(x,t) = \sin(\pi x)t^\alpha$, $\phi(x) = 0$, $u(0,t) = u(1,t) = 0$, given $N = 10, 20, 40, 80, 160$ and $M = 100$. The table of condition numbers $\kappa_{2,2}$ and $\kappa_{2,\alpha}$ for $0 < \alpha < 1$ are detailed in full in appendix C. In the next section, we shall consider a simple numerical experiment that illustrates our theoretical results.

2.5 NUMERICAL EXPERIMENT

We will consider the following two test problems for our numerical experiments:

$$\begin{cases} u(x,t) & = \sin(\pi x)t^{1.01},\ u(0,t) = u(1,t) = 0,\ \phi = u(x,0) = 0, \\ f_{1-\alpha}(x,t) & = \sin(\pi x)\left[t + \dfrac{\Gamma(2.01)\pi^2 t^{\alpha+1.01}}{\Gamma(\alpha+2.01)}\right] = a_{1-\alpha}(t) * f(x,t), \end{cases} \tag{27}$$

$$\begin{cases} u(x,t) & = \sin(\pi x)t^\alpha,\ u(0,t) = u(1,t) = 0,\ \phi = u(x,0) = 0, \\ f_{1-\alpha}(x,t) & = \sin(\pi x)\left[t^\alpha + \dfrac{4^{-\alpha}\pi^{5/2}t^{2\alpha}}{\Gamma(\alpha+1/2)}\right] = a_{1-\alpha}(t) * f(x,t), \end{cases} \tag{28}$$

which will satisfy $u(x,t) \in C^1[0,T]$ in time for the first problem and $u(x,t) \in C^\alpha[0,T]$ for the second problem. We define M to be the number of partitions of the spatial domain, $E_1(M,N)$ to be the L^∞ error norm over the total mesh for functions in $C^1[0,T]$, and $\text{rate}_1 = log_2\left(\frac{E_1(M,N/2)}{E_1(M,N)}\right)$ under a uniform time mesh. In this manner, E_α and rate_α are defined analogously. For all numerical experiments, we fix $M = 25$ space grid points and and $T = 1$.

We have the following results when considering the first problem using the first-order scheme:

Table 1: Numerical error for $u(x,t) = \sin(\pi x)t^{1.01}$ using a midpoint scheme

Numerical Error for $u(x,t) = \sin(\pi x)t^{1.01}$, using scheme (15)			
α	N	$E_1(M,N)$	rate$_1$
0.05	10	0.15621	–
	20	0.07707	1.092
	40	0.03802	1.0195
	80	0.01875	1.0197
	160	0.00925	1.02
	320	0.00456	1.0203
0.25	10	0.13324	–
	20	0.06321	1.0757
	40	0.02981	1.0844
	80	0.01397	1.0938
	160	0.00650	1.1037
	320	0.00300	1.114
0.5	10	0.11029	–
	20	0.04762	1.2117
	40	0.01996	1.2543
	80	0.00812	1.2792
	160	0.00321	1.338
	320	0.00124	1.3747
0.75	10	0.08773	–
	20	0.03230	1.4416
	40	0.01118	1.5309
	80	0.00368	1.6043
	160	0.00116	1.6588
	320	3.5928e–4	1.6962
0.95	10	0.06893	–
	20	0.02145	1.6839
	40	0.00619	1.7932
	80	0.00170	1.8655
	160	4.5245e–4	1.9085
	320	1.1852e–4	1.9326

The results for the second problem utilizing the α-order scheme is as follows:

Table 2: Numerical error for $u(x,t) = \sin(\pi x)t^\alpha$, using an α-order scheme

Numerical Error for $u(x,t) = \sin(\pi x)t^\alpha$, using scheme (11)			
α	N	$E_\alpha(M,N)$	rate$_\alpha$
0.05	10	0.0260	–
	20	0.0250	0.0551
	40	0.0240	0.0552
	80	0.0231	0.0554
	160	0.0223	0.0556
0.25	10	0.0588	–
	20	0.0481	0.2878
	40	0.0393	0.2937
	80	0.0319	0.3003
	160	0.0258	0.3077
0.5	10	0.0385	–
	20	0.0249	0.6265
	40	0.0158	0.6618
	80	0.0097	0.7017
	160	0.0058	0.7443
0.75	10	0.0370	–
	20	0.0208	0.8356
	40	0.0114	0.8618
	80	0.0062	0.8904
	160	0.0033	0.9178
0.95	10	0.0470	–
	20	0.0238	0.979
	40	0.0120	0.9863
	80	0.0061	0.9916
	160	0.0030	0.9953

The previous table shows that for various values of α, the error estimate improves with an increase in the number of space and time steps used in the mesh partitioning while preserving a rate of convergence approaching $O(k^{1+\alpha})$ in the first example. For the second example, we exhibit a rate of convergence that is better than expected, which is especially noticeable for $\alpha \geq 0.5$. As a result, our method exhibits a better rate of convergence than predicted, under these relaxed regularity assumptions. We remark that such examples are not numerically stable by utilizing the traditional L1 method, as outlined in [56]. We further remark that for the numerical example with exact solution as in (28), full order of convergence in time can be obtained by using a linear interpolant scheme [11, 30, 34, 35]. However, their results do not extend to general functions in $C^{\alpha}[0, T]$.

By corollary 2.4.6.1, if we instead replace $u(x_i, t_1)$ with its approximation derived from the exact solution, we instead have the following improved results for a small amount of time steps due to the truncation error. For this example, we have $u(x_i, t_1) = f_{1-\alpha}(x_i, t_1)$ These results are summarized in the following table:

Table 3: Numerical Error for $u(x, t) = \sin(\pi x)t^2$ with truncation error for $u(x, t_1)$

Numerical Error for $u(x, t) = \sin(\pi x)t^2$ with truncation error for $u(x, t_1)$			
α	N	$E_1(M, N)$	rate$_1$
0.05	10	0.0840	–
	20	0.0370	1.1821
	40	0.0179	1.046
0.25	10	0.0435	–
	20	0.0157	1.4744
	40	0.0067	1.222
0.5	10	0.0189	–
	20	0.0046	2.0227
	40	0.0017	1.4294
0.75	10	0.0079	–
	20	0.0014	2.4636
	40	2.7567e–4	2.3859
0.95	10	0.0050	–
	20	7.76962e–4	2.6739
	40	1.1287e–4	2.7832

CHAPTER 3

THE GENERALIZED METHOD FOR UP TO FIFTH ORDER ACCURACY

We obtain new numerical schemes for weakly singular integrals of convolution type called Caputo fractional order integrals using Taylor and fractional Taylor series expansions and grouping terms in a novel manner. A fractional Taylor series expansion argument is utilized to provide fractional-order approximations for functions with minimal regularity. The resulting schemes allow for the approximation of functions in $C^\gamma[0, T]$, where $0 < \gamma \leq 5$. A mild invertibility criterion is provided for the implicit schemes. Consistency and stability are proven separately for the whole-number-order approximations and the fractional-order approximations. The rate of convergence in the time variable is shown to be $O(\tau^\gamma)$, $0 < \gamma \leq 5$ for $u \in C^\gamma[0, T]$, where τ is the size of the partition of the time mesh. Crucially, the assumption of the integral kernel K being decreasing is not required for the scheme to converge in second-order and below approximations. Optimal convergence results are then proven for both sets of approximations, where fractional-order approximations can obtain up to whole-number rate of convergence in certain scenarios. Finally, numerical examples are provided that illustrate our findings.

3.1 INTRODUCTION

We begin by recalling the Caputo fractional time-derivative [9,10] of a given function $f(t)$ is

$$_0^C D_t^\alpha f(t) = \frac{1}{\Gamma(1-\alpha)} \int_0^t \frac{df(s)}{ds} (t-s)^{-\alpha} \, ds, \quad 0 < \alpha < 1, \tag{29}$$

which is a fractional derivative of order α. In [8], the Laplace transform was applied to the fractional order diffusion initial-boundary value problem

$$_0^C D_t^\alpha u(x,t) = \frac{\partial^2}{\partial x^2} u(x,t) + g(x,t), \quad x \in [0,1], t \in [0,T], \tag{30}$$

$$u(x,0) = \phi(x), \quad u(0,t) = u(1,t) = 0, \tag{31}$$

to obtain the integral equation

$$u(x,t) = \phi(x) + \int_0^t \frac{(t-s)^{\alpha-1}}{\Gamma(\alpha)} \left(\frac{\partial^2}{\partial x^2} u(x,s) + g(x,s) \right) ds. \tag{32}$$

Equation (32) was then studied numerically and convergent schemes were developed for this integral equation inspired by the works presented in [36]-[41], [46], [47], and [56]. The regularity of equation (2) has been considered in [8], [40], [46], and others. Our discussion of the regularity of these schemes is motivated by the findings in [16], [17], and [28]. We will derive and examine numerical schemes to discretize integrals of the form (32), motivated by the principles in [17], [26], [43], [44], and [48]. Equations of the form (32) have numerous engineering and physics applications, see [46], [47] and [56]. One of the major advantages of applying the Laplace Transform to a fractional derivative term, as seen in [8], is the ability to relax the regularity assumption for fractional derivative discretizations in the time variable while preserving an optimal convergence rate. Namely, we now have the ability to relax the regularity assumption from requiring the objective function $u(t) \in C^2[0, T]$ under the well known L1-method (c.f [56]) to $u(t) \in C^\gamma[0, T]$, where $0 < \gamma \leq 2$. Further, we can strengthen this assumption to $u(t) \in C^\gamma[0, T]$, where $2 < \gamma \leq 5$ while obtaining optimal rate of convergence. This is achieved by a Taylor series expansion to obtain convergence results for whole number values of γ, and by using a fractional Taylor series expansion to approximate functions with a fractional order of regularity, see [53]. By requiring more regularity than $u(t) \in C^2[0, T]$ in the usual L1-method, we are able to obtain a higher order of convergence, as seen in Theorems 3.6 and 3.7. This method naturally generalizes to any convolution type-quadrature where the kernel function K is positive, nonincreasing, and satisfies $K \in L^1[0, T]$, as seen in Theorems 3.4 and 3.5. The space variable can be discretized by a stable finite difference operator presented in [8] and [56] to obtain a rate of convergence in the space variable of $O(h^4)$, where h denotes the size of the partition of the space variable interval. This ultimately yields a rate of convergence in both space and time for $u(x, t) \in C^\gamma([0, T]; C^6[0, 1])$ of $O(\tau^\gamma + h^4)$, where τ is the size of the partition of the time variable interval. We remark that a standard finite difference operator in the space variable can relax the regularity in space to $u(x, t) \in C^\gamma([0, T]; C^4[0, 1])$, where special consideration must be taken to ensure stability in the space variable.

The remainder of this chapter is organized as follows. Section 2 will provide discretizations for fractional integrals of the form found in (32), and a general scheme is established for convolution integrals based on the integral kernel. We obtain general schemes of orders up to 5th order of accuracy in time. Section 3 establishes all of the necessary consistency, stability, and convergence results for each of these schemes, in addition to a discussion of the implementation of the schemes. We also prove optimal order of convergence of our stable schemes, and the instability of schemes of order 6 and above are presented as well. The

main results are featured in Theorems 3.4 through 3.7. Section 4 presents numerical solutions of fractional integral equations demonstrating orders of convergence predicted by our theoretical results.

3.2 DISCRETIZED NUMERICAL SCHEMES

In order to discretize the Caputo fractional integral (32), let $0 = t_0 < t_1 < ... < t_N = T$ be a uniform partition, define $\tau = \dfrac{T}{N} = t_k - t_{k-1}, k = 1, ..., N$ where N is the number of partitions of the time interval $[0, T]$ and let $s \in (0, T)$. Then,

$$f(s) = f(t_k) + (s - t_k)f'(t_k) + \frac{(s - t_k)^2}{2!}f''(t_k) + \frac{(s - t_k)^3}{3!}f'''(t_k) + ... \tag{33}$$

From the above, similar Taylor expansions centered at any given t_k can be constructed for each of the previous points $t_{k-1}, t_{k-2}, ..., t_1, t_0 \in [0, t_k]$. We will use the notation $A = O(h)$ if $\dfrac{A}{h}$ is bounded. We obtain

$$f(t_k) = f(t_k) \tag{34}$$

$$f(t_{k-1}) = f(t_k) - \tau f'(t_k) + \frac{\tau^2}{2!}f''(t_k) - \frac{\tau^3}{3!}f'''(t_k) + O(\tau^4)$$

$$f(t_{k-2}) = f(t_k) - 2\tau f'(t_k) + \frac{(2\tau)^2}{2!}f''(t_k) - \frac{(2\tau)^3}{3!}f'''(t_k) + O(\tau^4)$$

$$...$$

$$f(t_0) = f(t_k) - k\tau f'(t_k) + \frac{(k\tau)^2}{2!}f''(t_k) - \frac{(k\tau)^3}{3!}f'''(t_k) + O(\tau^4).$$

We will use the following equations to find the j-th order approximation of $f(s)$ for any point $s \in (0, T)$ and each $k = 0, ..., N$

$$\sum_{i=0}^{j-1} c_i^k f(t_{k-i}) = f(s) + O((s - t_k)^j) \tag{35}$$

$$\sum_{i=0}^{j-1} c_i^k f(t_{k-i}) = \sum_{i=0}^{j-1} \frac{(s - t_k)^i}{i!}f^{(i)}(t_k) + O((s - t_k)^j). \tag{36}$$

We replace each $f(t_{k-i})$ by its Taylor expansion about the point t_k, neglect the higher order terms and solve the system resulting from equating coefficients of $f(t_k), f'(t_k), ..., f^{(j-1)}(t_k)$. For example, a second order approximation of $f(s)$ is obtained from

$$c_0^k f(t_k) + c_1^k \left(f(t_k) - \tau f'(t_k) \right) = f(t_k) + (s - t_k)f'(t_k),$$

by equating the coefficients of $f(t_k)$ and $f'(t_k)$ to obtain the system of equations

$$c_0^k + c_1^k = 1$$
$$-c_1^k \tau = (s - t_k).$$

Solving the above yields $c_1^k = \dfrac{t_k - s}{\tau}$, $c_0^k = 1 - \dfrac{t_k - s}{\tau}$. As an example, we may numerically approximate the integral as seen in [8] using c_0^k and c_1^k as solved for above:

$$\int_0^{t_n} \frac{(t_n - s)^{\alpha-1}}{\Gamma(\alpha)} f(s)\, ds = \sum_{k=1}^{n} \int_{t_{k-1}}^{t_k} \frac{(t_n - s)^{\alpha-1}}{\Gamma(\alpha)} f(s)\, ds$$

$$\approx \sum_{k=1}^{n} \int_{t_{k-1}}^{t_k} \frac{(t_n - s)^{\alpha-1}}{\Gamma(\alpha)} \left(c_0^k f(t_k) + c_1^k f(t_{k-1}) \right)\, ds.$$

We remark that under this construction, we satisfy the condition $s \in [t_{k-1}, t_k]$. This directly implies that the coefficients c_0 and c_1 presented above are nonnegative. We now provide the values of the coefficients for each scheme up to 4th order accuracy. Higher order schemes can be derived using the equation (35). In this way, the general method is outlined below. We remark that in general, $c_i = c_i(s)$ for each $i = 0, 1, ..., j - 1$. For fixed $k = 1, 2, ..., N$

First order accurate:

$$c_0^k = 1,$$
$$f(s) = f(t_k) + O(\tau).$$

Second order accurate:

$$c_0^k = 1 - \frac{t_k - s}{\tau},\ c_1^k = \frac{t_k - s}{\tau}, \quad k \geq 1,$$
$$f(s) = c_0^k f(t_k) + c_1^k f(t_{k-1}) + O(\tau^2).$$

Third order accurate:

$$c_0^k = \frac{(\tau + s - t_k)(2\tau + s - t_k)}{2\tau^2},\ c_1^k = \frac{(t_k - s)(2\tau + s - t_k)}{\tau^2},$$
$$c_2^k = \frac{(s - t_k)(\tau + s - t_k)}{2\tau^2}, \quad k \geq 2,$$
$$f(s) = c_0^k f(t_k) + c_1^k f(t_{k-1}) + c_2^k f(t_{k-2}) + O(\tau^3).$$

Fourth order accurate:

$$c_0^k = \frac{(\tau + s - t_k)(2\tau + s - t_k)(3\tau + s - t_k)}{6\tau^3},$$

$$c_1^k = \frac{(t_k - s)(2\tau + s - t_k)(3\tau + s - t_k)}{2\tau^3},$$

$$c_2^k = \frac{(s - t_k)(\tau + s - t_k)(3\tau + s - t_k)}{2\tau^3},$$

$$c_3^k = \frac{(t_k - s)(\tau + s - t_k)(2\tau + s - t_k)}{6\tau^3}, \quad k \geq 3,$$

$$f(s) = c_0^k f(t_k) + c_1^k f(t_{k-1}) + c_2^k f(t_{k-2}) + c_3^k f(t_{k-3}) + O(\tau^4).$$

Fifth order accurate:

$$c_0^k = \frac{(\tau + s - t_k)(2\tau + s - t_k)(3\tau + s - t_k)(4\tau + s - t_k)}{24\tau^4},$$

$$c_1^k = \frac{(t_k - s)(2\tau + s - t_k)(3\tau + s - t_k)(4\tau + s - t_k)}{6\tau^4},$$

$$c_2^k = \frac{(s - t_k)(\tau + s - t_k)(3\tau + s - t_k)(4\tau + s - t_k)}{4\tau^4},$$

$$c_3^k = \frac{(t_k - s)(\tau + s - t_k)(2\tau + s - t_k)(4\tau + s - t_k)}{6\tau^4}$$

$$c_4^k = \frac{(t_k - s)(\tau + s - t_k)(2\tau + s - t_k)(3\tau + s - t_k)}{24\tau^4}, \quad k \geq 4,$$

$$f(s) = c_0^k f(t_k) + c_1^k f(t_{k-1}) + c_2^k f(t_{k-2}) + c_3^k f(t_{k-3}) + c_4^k f(t_{k-4}) O(\tau^5).$$

As a generalization of the previous examples, after replacing each $f(t_{k-i})$ with its Taylor series, we equate the coefficients of $f(t_k)$, $f'(t_k)$, ..., $f^{(j-1)}(t_k)$ and neglect the higher order terms to obtain the following system of equations from (35)

$$V_\tau^T \vec{c_j^k} = \vec{y_j^k}, \tag{37}$$

where

$$V_\tau^T = \begin{bmatrix} 1 & 1 & 1 & ... & 1 \\ 0 & -\tau & -2\tau & ... & -(j-1)\tau \\ 0 & (-\tau)^2 & (-2\tau)^2 & ... & (-(j-1)\tau)^2 \\ & & ... & & \\ 0 & (-\tau)^{j-1} & (-2\tau)^{j-1} & ... & (-(j-1)\tau)^{j-1} \end{bmatrix} \tag{38}$$

$$\vec{c_j^k} = \begin{bmatrix} c_0^k \\ c_1^k \\ c_2^k \\ ... \\ c_{j-1}^k \end{bmatrix}, \vec{y_j^k} = \begin{bmatrix} 1 \\ (s-t_k) \\ (s-t_k)^2 \\ ... \\ (s-t_k)^{j-1} \end{bmatrix}. \tag{39}$$

Notice that V_τ^T is the transpose of the usual Vandermonde matrix [52] which has the determinant

$$\det(V_\tau^T) = \det(V_\tau) = \prod_{1 \le i < n \le j} (x_n - x_i)$$
$$= \prod_{1 \le i < n \le j} (n-i)\tau \ne 0,$$

because, recall $x_j = \dfrac{jT}{N}$ and $\tau = \dfrac{T}{N} \ne 0$. This directly implies that the matrix V_τ^T is invertible under this condition. The following lemma is immediate from the above considerations.

Lemma 3.2.1. *Equation* (37) *has a unique solution,* $\vec{c_n^k}$ *for each* $n \le N, n \in \mathbb{N}$ *and each* $k = 1, ..., N$.

We now compute the unique solution ensured by the previous lemma. From [52], we can establish the generalized inverse of the Vandermonde matrix to solve (37).

Theorem 3.2.2. *Let* $\tau > 0$. *Then,* (37) *has a unique solution* $\vec{c_n^k}$ *for each* $j = 1, 2, ..., N$, $N \in \mathbb{N}$ *and* $k \ge j$, *with the solution*

$$\vec{c_i^k} = \begin{cases} \displaystyle\sum_{1 \le n \le j} (s-t_k)^{n-1}(-1)^{j-i} \left(\dfrac{\displaystyle\sum_{\substack{1 \le m_1 < ..., m_{j-i} \le j \\ m_1, ..., m_{j-1} \ne n}} x_{m_1}...x_{m_{j-i}}}{\displaystyle\prod_{1 \le i < n \le j} (\tau(n-i))} \right), & 1 \le i < j, \\[40pt] \displaystyle\sum_{1 \le n \le j} (s-t_k)^{n-1} \dfrac{1}{\displaystyle\prod_{1 \le i < n \le j} (\tau(n-i))}, & i = j, \end{cases} \tag{40}$$

where $x_n = n\tau$.

Proof. From Lemma 3.2.1, we may invert the matrix V_τ^T to obtain the solution

$$\vec{c_j^k} = (V_\tau^T)^{-1}\vec{y_j^k},$$

which, from [52], each entry of $(V_\tau^T)^{-1} = [v_{in}]$, $1 \le i, j \le n$ is calculated by

$$v_{in} = \begin{cases} (-1)^{j-i}\left(\dfrac{\displaystyle\sum_{\substack{1\le m_1<...,m_{j-i}\le j \\ m_1,...,m_{j-1}\ne n}} x_{m_1}...x_{m_{j-i}}}{\displaystyle\prod_{1\le i<n\le j}(\tau(n-i))}\right), & 1 \le i < j, \\[2em] \dfrac{1}{\displaystyle\prod_{1\le i<n\le j}(\tau(n-i))}, & i = j, \end{cases}$$

so we may solve component-wise to find each entry of $\vec{c_j}$, from

$$(V_\tau^T)^{-1}\vec{y_j^k} = \sum_{1\le n\le j} v_{in}y_n^k.$$

Thus,

$$\vec{c_i^k} = (V_\tau^T)^{-1}\vec{y_j^k} = \sum_{1\le n\le j} v_{in}y_n^k \tag{41}$$

$$= \begin{cases} \displaystyle\sum_{1\le n\le j}(s-t_k)^{n-1}(-1)^{j-i}\left(\dfrac{\displaystyle\sum_{\substack{1\le m_1<...,m_{j-i}\le j \\ m_1,...,m_{j-1}\ne n}} x_{m_1}...x_{m_{j-i}}}{\displaystyle\prod_{1\le i<n\le j}(\tau(n-i))}\right), & 1 \le i < j, \\[2em] \displaystyle\sum_{1\le n\le j}(s-t_k)^{n-1}\dfrac{1}{\prod_{1\le i<n\le j}(\tau(n-i))}, & i = j. \end{cases}$$

$\square$

Remark 3.2.3. *By utilizing the fractional Taylor series expansion instead for $f(s)$ on $[0,T]$, as discussed in [53], we obtain similar results to those outlined in Theorem 2.2. This can further relax the regularity assumption to $f(s) \in C^\alpha[0,T]$ for $0 < \alpha < 1$.*

Using the fractional Taylor series expansion, we define an α-order scheme by the following: α order accurate:

$$c_0^k = 1,$$

$$f(s) = f(t_k) + O(\tau^\alpha).$$

We now examine the consistency, stability, and convergence of these schemes based on the generalized scheme

$$f(s) = \sum_{i=0}^{n-1} c_i^k f(t_{k-i}) + O((s - t_k)^n). \tag{42}$$

3.3 NUMERICAL CONSISTENCY, STABILITY, AND CONVERGENCE

3.3.1 NUMERICAL CONSISTENCY

We motivate our discussion of stability and convergence by examining the results presented in [2]. The main results of this paper are established in Theorems 3.3 through 3.7. The quadrature studied in [2] is of the form

$$\int_0^T \phi(s)\, ds = \tau \sum_{j=0}^N w_j \phi(j\tau) + O(\tau^R), \tag{43}$$

where $R \in \mathbb{N}$. From [2], if $\phi \in C^R[0, T]$ then there exists of a sequence of constants, $\{c_l\}$, such that

$$\int_0^T \phi(s)\, ds - \tau \sum_{j=0}^N w_j \phi(j\tau)$$

$$= \sum_{l=\rho+1}^R \tau^l (r^l c_l)\{\phi^{(l-1)}(T) - \phi^{(l-1)}(0)\} + O(\tau^R).$$

We will compare these results to the ones established in the previous section to prove stability and assert convergence. Our goal is to rewrite the integrand $\phi(s) = K(t_n - s)f(s)$ as a convolution integral, where we may relax the continuity assumptions on the kernel function K. We begin by recalling some basic definitions for quadrature methods. From (1.15) of [2], a quadrature method of the form (43) is said to be consistent if it satisfies

$$\sum_{j=0}^N w_j = N.$$

We will relate (43) and our findings in the previous section. We use the notation $\lceil \gamma \rceil = a$, where a is the smallest integer that satisfies $a \geq \gamma$.

Lemma 3.3.1. *Let $\gamma > 0$, $f \in C^\gamma[0,T]$, and $K \in L^1[0,T]$. Then, if w_j^k is given by (46) for any t_n*

$$\int_0^{t_n} f(s)K(t_n - s)\, ds = \sum_{k=1}^{n} \sum_{j=0}^{\lceil \gamma \rceil - 1} w_j^k f(t_{k-j}) + O(\tau^\gamma). \tag{44}$$

Proof. By utilizing the Taylor expansion for $f(s)$ about the point t_k, we may readily obtain a similar quadrature rule by using Theorem 3.2.2 and the definition of each $c_j(s)$ defined in (40). By further remarking that for each $s \in [t_{k-1}, t_k]$, then we may write $O((t_k - s)^\gamma) = O(\tau^\gamma)$ to find

$$\int_0^{t_n} f(s)K(t_n - s)\, ds = \sum_{k=1}^{n} \int_{t_{k-1}}^{t_k} f(s)K(t_n - s)\, ds \tag{45}$$

$$= \sum_{k=1}^{n} \int_{t_{k-1}}^{t_k} \left(\sum_{j=0}^{\lceil \gamma \rceil - 1} c_j^k(s) f(t_{k-j}) + O((s - t_k)^\gamma) \right) K(t_n - s)\, ds$$

$$= \sum_{k=1}^{n} \sum_{j=0}^{\lceil \gamma \rceil - 1} f(t_{k-j}) \int_{t_{k-1}}^{t_k} c_j^k(s) K(t_n - s)\, ds + O(\tau^\gamma).$$

By letting

$$w_j^k = \int_{t_{k-1}}^{t_k} c_j^k(s) K(t_n - s)\, ds, \tag{46}$$

we arrive at the conclusion. $\qquad \square$

The following remark is a natural extension of the first lemma, which allows for direct comparison to prove stability using the Theorem 3.7 in [2].

Remark 3.3.2. *By expanding the series*

$$\sum_{k=1}^{n} \sum_{j=0}^{\lceil \gamma \rceil - 1} w_j^k f(t_{k-j}) + O(\tau^\gamma),$$

and by collecting all of the repeating terms for each $f(t_{k-j})$, we may condense the double summation into a single summation term

$$\sum_{k=1}^{n} \sum_{j=0}^{\lceil \gamma \rceil - 1} w_j^k f(t_{k-j}) = \sum_{k=0}^{n} (w_0^k + w_1^{k+1} + ... + w_{\gamma-1}^{k+\gamma-1}) f(t_k), \tag{47}$$

where we define $w_0^0 = 0$ to satisfy the previous lemma. Further, by defining, for fixed $0 < \gamma \le 5$,

$$\tilde{w}_k^\gamma = w_0^k + w_1^{k+1} + ... + w_{\gamma-1}^{k+\gamma-1}, \tag{48}$$

we arrive at a form identical to the generalized quadrature rule posed in [2], namely

$$\sum_{k=1}^{n} \sum_{j=0}^{\lceil\gamma\rceil-1} w_j^k f(t_{k-j}) + O(\tau^\gamma) = \sum_{k=0}^{n} \tilde{w}_k^\gamma f(t_k) + O(\tau^\gamma). \tag{49}$$

Theorem 3.3.3. *The approximation scheme (44) combined with (49) is consistent for any $0 < \gamma \le 5$, where γ is the order of approximation.*

Proof. From the consistency requirement in [2], we must show that the scheme (49) satisfies, for any time step $\tau > 0$,

$$\begin{cases} \int_0^{t_n} \phi(s)\, ds = \tau \sum_{j=0}^{n} w_{n-j}\phi(j\tau) + O(\tau^R), \\ \sum_{j=0}^{n} w_j = n, \end{cases} \tag{50}$$

for any fixed γ. That is, we have from Remark 3.3.2

$$\sum_{k=0}^{n} \tilde{w}_k^\gamma = \sum_{k=0}^{n} w_0^k + w_1^{k+1} + ... + w_{\gamma-1}^{k+\gamma-1}$$

$$= \sum_{k=1}^{n} \sum_{j=0}^{\lceil\gamma\rceil-1} w_j^k$$

$$= \sum_{k=1}^{n} \sum_{j=0}^{\lceil\gamma\rceil-1} \int_{t_{k-1}}^{t_k} c_j^k(s) K(t_n - s)\, ds$$

$$= \sum_{k=1}^{n} \int_{t_{k-1}}^{t_k} \left(\sum_{j=0}^{\lceil\gamma\rceil-1} c_j^k(s) \right) K(t_n - s)\, ds.$$

From (37), the first equation in the Vandermonde matrix requires

$$\sum_{j=0}^{\lceil\gamma\rceil-1} c_j^k(s) = 1,$$

hence,

$$\sum_{k=0}^{n} \tilde{w}_k^\gamma = \sum_{k=1}^{n} \int_{t_{k-1}}^{t_k} K(t_n - s)\, ds = \int_0^{t_n} K(t_n - s)\, ds.$$

On the other hand, by relabelling the coefficients of (50) and by noting that $k\tau = t_k$,

$$\int_0^{t_n} f(s)K(t_n - s)\, ds = \tau \sum_{j=0}^n w_{n-j} f(j\tau) K(t_n - j\tau) + O(\tau^R)$$

$$= \tau \sum_{k=0}^n w_{n-k} f(t_k) K(t_n - t_k) + O(\tau^R). \tag{51}$$

By equating (49) and (51), we have

$$\tau \sum_{k=0}^n w_{n-k} K(t_n - t_k) = \sum_{k=0}^n \tilde{w}_k^\gamma = \int_0^{t_n} K(t_n - s)\, ds.$$

Since each $w_{n-k} \geq 0$ under this construction, we select $\{w_k\}_{k=0}^n$ to satisfy $\sum_{k=0}^n w_k = n$. Thus, we have for the scheme (49)

$$\begin{cases} \int_0^{t_n} f(s)K(t_n - s)\, ds = \tau \sum_{k=0}^n w_{n-k} f(t_k) K(t_n - t_k) + O(\tau^R) \\ \sum_{k=0}^n w_k = n, \end{cases}$$

hence the scheme (49) is consistent. For simplicity and for implementation, we take $w_k = 1$ for each k to trivially satisfy these conditions since $w_0^0 = w_0 = 0$. $\qquad \square$

3.3.2 INVERTIBILITY CRITERIA

Given a Volterra integral equation of the second kind

$$u(t) = f(t) + \int_0^t K(t, s)u(s)\, ds,$$

the numerical approximation of order γ to the integral is at the time $t = t_k$

$$u(t_k) \approx f(t_k) + \int_0^{t_k} K(t, s) \left(\sum_{i=0}^{\lceil \gamma \rceil - 1} c_i^k(s) u(t_{k-i}) \right) ds$$

$$= f(t_k) + \sum_{i=0}^{\lceil \gamma \rceil - 1} u(t_{k-i}) \int_0^{t_k} K(t, s) c_i^k(s)\, ds,$$

which is solved for each $k = 1, 2, ..., N$. As a result, we can rearrange the above to yield the

approximate equation

$$u(t_k) \left(1 - \int_{t_{k-1}}^{t_k} K(t_k, s)\, c_0^k(s)\, ds \right) = f(t_k)$$

$$+ \int_{t_{k-1}}^{t_k} K(t_k, s) \left(\sum_{i=1}^{\lceil \gamma \rceil - 1} c_i^k(s) u(t_{k-i}) \right) ds$$

$$+ \sum_{j=1}^{k-1} \int_{t_{j-1}}^{t_j} K(t_k, s) \left(\sum_{i=0}^{\lceil \gamma \rceil - 1} c_i^k(s) u(t_{j-i}) \right) ds,$$

hence,

$$u(t_k) = \left(1 - \int_{t_{k-1}}^{t_k} K(t_k, s)\, c_0^k(s)\, ds \right)^{-1} \left(f(t_k) \right.$$

$$+ \int_{t_{k-1}}^{t_k} K(t_k, s) \left(\sum_{i=1}^{\lceil \gamma \rceil - 1} c_i^k(s) u(t_{k-i}) \right) ds$$

$$+ \left. \sum_{j=1}^{k-1} \int_{t_{j-1}}^{t_j} K(t_k, s) \left(\sum_{i=0}^{\lceil \gamma \rceil - 1} c_i^k(s) u(t_{j-i}) \right) ds \right).$$

That is, for an implicit scheme, we must restrict

$$1 - \int_{t_{k-1}}^{t_k} K(t_k, s)\, c_0^k(s)\, ds \neq 0,$$

or equivalently,

$$\int_{t_{k-1}}^{t_k} K(t_k, s)\, c_0^k(s)\, ds \neq 1.$$

In practice, since γ is the pre-determined order of approximation and K is given, we can select an appropriate order of approximation or an appropriate choice of parameters for K. Additionally, when considering a traditional Volterra integral equation of the form

$$u(t) + \lambda \int_0^t K(t, s) u(s)\, ds = f(t), \quad \lambda > 0,$$

where K is a positive integral kernel and $K \in L^1[0, T]$, a routine discretization using the method above yields the invertibility criterion

$$1 + \lambda \int_{t_{k-1}}^{t_k} K(t_k, s)\, c_0^k(s)\, ds \neq 0,$$

which is never obtained since λ, K, and c_0^k are positive on the interval $[t_{k-1}, t_k]$. Therefore, the application of the schemes in this case is trivial without need for further consideration. The implementation of these schemes is detailed further in appendix B.

3.3.3 NUMERICAL STABILITY AND CONVERGENCE

As a remark, the consistency results hold for any $\gamma > 0$ using this argument, but the stability results do not hold in general for $\gamma > 5$. We must further satisfy stability requirements in order to prove the convergence of these schemes for any order $0 < \gamma \leq 5$. From [2], we have the following theorem asserting stability under arbitrary quadrature rules.

Theorem. *(3.7 of [2]) The stability polynomial*

$$\Sigma(\mu; \lambda\tau) = (1 - \lambda\tau w_0 K(0))\mu^N - \lambda\tau w_1 K(\tau)\mu^{N-1} - ...$$
$$- \lambda\tau w_N K(n\tau) \tag{52}$$

is Schur, if $|\lambda\tau| \sum_{k=0}^{N} |w_k K(k\tau)| < 1$. Assuming each $w_k \geq 0$ and satisfy $\sum_{k=0}^{N} w_k = N$, the recurrence for

$$y(t) = f(t) + \lambda \int_{t_n - T}^{t_n} K(t_n - s)y(s)\,ds$$

when $K(t) \equiv 1$ for $t \in [0, T]$ is stable whenever $|\lambda T| < 1$, given $\tau > 0$.

The Schur polynomial $\beta(\mu)$ in [2] is said to satisfy the requirement that the zeros of β lie inside the complex unit disc, namely $|\mu_n| < 1$ for all $n = 0, 1, ..., N$. This proof is achieved by the use of Rouche's theorem (c.f Theorem 3.8 of [6]), which requires that for α and β analytic functions in μ inside and on the contour $\Gamma \subset \mathbb{C}$, we have $|\beta(\mu)| < |\alpha(\mu)|$ for each $\mu \in \Gamma$. This proof is completed by letting Γ be the unit disc such that $|\mu| = 1$, $\alpha(\mu) = \mu^N$, and $\beta(\mu) = -\lambda h \left(w_0 k(0)\mu^N + w_1 k(h)\mu^{N-1} + ... + w_N k(\tau) \right)$. We remark that under these results, we must simply satisfy the requirement that each $\tilde{w}_k^\gamma \geq 0$ in (49) to satisfy a similar stability criterion for this generalized quadrature. This immediately leads to two stability results.

Theorem 3.3.4. *Let K be a positive function in $L^1[0, T]$ and let $\tau > 0$. Then, the approximation scheme (49) is stable for $0 < \gamma \leq 2$, where γ is the order of approximation.*

Proof. The case where $\gamma = 1$ is immediate since $c_0^k = 1$, hence $\tilde{w}_1^k \geq 0$. For $\gamma = 2$, recall

that since $c_0^k(s) > 0$ on $[t_{k-1}, t_k]$, $c_1^{k+1}(s) > 0$ on $[t_k, t_{k+1}]$, and $K(s) > 0$, then

$$\tilde{w}_2^k = w_0^k + w_1^{k+1} \tag{53}$$

$$= \int_{t_{k-1}}^{t_k} c_0^k(s)K(s)\, ds + \int_{t_k}^{t_{k+1}} c_1^{k+1}(s)K(s)\, ds$$

$$\geq \min_{s \in [t_1, T]} (K(s)) \left(\int_{t_{k-1}}^{t_k} c_0^k(s)\, ds + \int_{t_k}^{t_{k+1}} c_1^{k+1}(s)\, ds \right)$$

$$= \min_{s \in [t_1, T]} (K(s)) \left(\int_{t_k}^{t_{k+1}} c_0^{k+1}(s)\, ds + \int_{t_k}^{t_{k+1}} c_1^{k+1}(s)\, ds \right)$$

$$= \min_{s \in [t_1, T]} (K(s)) \left(\int_{t_k}^{t_{k+1}} c_0^{k+1}(s) + c_1^{k+1}(s)\, ds \right)$$

$$= \min_{s \in [t_1, T]} (K(s)) \tau \geq 0.$$

Using similar analysis we are able to come to the same conclusion for $\gamma = \alpha$ and $\gamma = 1 + \alpha$, given $0 < \alpha < 1$. Therefore, when $\gamma \in [1, 2]$, the scheme (49) is stable. $\qquad \square$

We require additional assumptions on the integral kernel K to ensure that the scheme is stable in the case where the order of approximation to (49) is any order $2 < \gamma \leq 5$.

Theorem 3.3.5. *Let K be a positive, nonincreasing function in $L^1[0, T]$ and let $\tau > 0$. The approximation scheme (49) is stable for any $2 < \gamma \leq 5$ order of accuracy.*

Proof. We begin by showing that $\tilde{w}_k^\gamma \geq 0$ for each $k = 1, 2, ..., n$. That is, we use the relationship established in Remark 3.3.2. We will present the argument for the cases where $\gamma = 3, 4, 5$ and deduce the pattern from there. We remark that under the construction found in Theorem 3.2.2 that for $j = 2, 4, 6, ...$ then $c_j^k(s) < 0$, provided $s \in [t_{k-1}, t_k]$. Therefore, when $\gamma = 3$, we have

$$\tilde{w}_3^k = w_0^k + w_1^{k+1} + w_2^{k+2}$$

$$= \int_{t_{k-1}}^{t_k} c_0^k(s)K(s)\, ds + \int_{t_k}^{t_{k+1}} c_1^{k+1}(s)K(s)\, ds + \int_{t_{k+1}}^{t_{k+2}} c_2^{k+2}(s)K(s)\, ds$$

$$\geq K(t_{k+1}) \left(\int_{t_{k-1}}^{t_k} c_0^k(s)\, ds + \int_{t_k}^{t_{k+1}} c_1^{k+1}(s)\, ds + \int_{t_{k+1}}^{t_{k+2}} c_2^{k+2}(s)\, ds \right)$$

$$= K(t_{k+1}) \left(\int_{t_{k+1}}^{t_{k+2}} c_0^{k+2}(s)\, ds + \int_{t_{k+1}}^{t_{k+2}} c_1^{k+2}(s)\, ds + \int_{t_{k+1}}^{t_{k+2}} c_2^{k+2}(s)\, ds \right)$$

$$= K(t_{k+1}) \left(\int_{t_{k+1}}^{t_{k+2}} c_0^{k+2}(s) + c_1^{k+2}(s) + c_2^{k+2}(s)\, ds \right)$$

$$= K(t_{k+1})\tau \geq 0.$$

Hence, when $\gamma = 3$, the scheme (49) is stable. When $\gamma = 4$, the argument is similar, but we must account for the extra positive term in w_3^{k+3}. That is, by recalling from (48) that $\tilde{w}_4^k = \tilde{w}_3^k + w_3^{k+3}$, where

$$\tilde{w}_3^k \geq K(t_{k+1}) \left(\int_{t_{k-1}}^{t_k} c_0^k(s)\,ds + \int_{t_k}^{t_{k+1}} c_1^{k+1}(s)\,ds + \int_{t_{k+1}}^{t_{k+2}} c_2^{k+2}(s)\,ds \right).$$

Here,

$$\begin{aligned}
\tilde{w}_4^k &= w_0^k + w_1^{k+1} + w_2^{k+2} + w_3^{k+3} \\
&\geq K(t_{k+1}) \left(\int_{t_k}^{t_{k+1}} c_0^{k+1}(s) + c_1^{k+1}(s) + c_2^{k+1}(s)\,ds \right) \\
&\quad + \int_{t_{k+2}}^{t_{k+3}} c_3^{k+3}(s) K(t_{k+3})\,ds \\
&= K(t_{k+1}) \left(\int_{t_{k+2}}^{t_{k+3}} 1 - c_2^{k+3}(s)\,ds \right) + \int_{t_{k+2}}^{t_{k+3}} c_2^{k+3}(s) K(t_{k+3})\,ds \\
&= \int_{t_{k+2}}^{t_{k+3}} K(t_{k+1}) + (K(t_{k+1}) - K(t_{k+3})) c_2^{k+3}(s)\,ds \geq 0.
\end{aligned}$$

Since K is nonincreasing, $K(t_{k+1}) \geq K(t_{k+3})$, and since $c_2^{k+3}(s) < 0$ where $s \in [t_{k+2}, t_{k+3}]$ by translating over to the correct interval, we then require $-1 \leq c_2^{k+3}(s)$, $s \in [t_{k+2}, t_{k+3}]$ to ensure that

$$\int_{t_{k+2}}^{t_{k+3}} K(t_{k+1}) + (K(t_{k+1}) - K(t_{k+3})) c_2^{k+3}(s)\,ds \geq \int_{t_{k+2}}^{t_{k+3}} K(t_{k+3})\,ds,$$

$$\geq 0.$$

To satisfy the requirement, we find that the minimum attained on the interval $s \in [t_{k+2}, t_{k+3}]$ for the function $c_2^{k+3}(s)$ is found at $s = t_{k+3} + \dfrac{-4 + \sqrt{7}}{3}\tau$ by the Extreme Value Theorem and by evaluating the derivative of $c_2^{k+3}(s)$ on the interval $s \in [t_{k+2}, t_{k+3}]$. Hence, the minimum value for $c_2^{k+3}(s)$ is

$$\begin{aligned}
c_2^{k+3}&\left(t_{k+3} + \frac{-4 + \sqrt{7}}{3}\tau\right) = \\
&\frac{\left(\dfrac{-4 + \sqrt{7}}{3}\right)\left(1 + \dfrac{-4 + \sqrt{7}}{3}\right)\left(3 + \dfrac{-4 + \sqrt{7}}{3}\right)}{2\tau^2} \\
&= \frac{20 - 14\sqrt{7}}{54} \approx -0.31 \geq -1.
\end{aligned}$$

Therefore, when $\gamma = 4$, the scheme is stable. We now consider the case where $\gamma = 5$. In this case, we have a similar argument where $\gamma = 4$, but we add an additional negative term in $w_4^{k+4}(s) < 0$ for $s \in [t_{k+3}, t_{k+4}]$. Thus, by recalling that

$$\tilde{w}_5^k = \tilde{w}_3^k + w_3^{k+3} + w_4^{k+4},$$

we have

$$
\begin{aligned}
\tilde{w}_5^k =& w_0^k + w_1^{k+1} + w_2^{k+2} + w_3^{k+3} + w_4^{k+4} \\
\geq& K(t_{k+1}) \left(\int_{t_{k+1}}^{t_{k+2}} c_0^{k+2}(s) + c_1^{k+2}(s) + c_3^{k+2}(s) \, ds \right) \\
& + K(t_{k+3}) \left(\int_{t_{k+1}}^{t_{k+2}} c_2^{k+3}(s) + c_4^{k+2}(s) \, ds \right) \\
=& K(t_{k+1}) \left(\int_{t_{k+1}}^{t_{k+2}} 1 - c_2^{k+2}(s) - c_4^{k+2}(s) \, ds \right) \\
& + K(t_{k+3}) \left(\int_{t_{k+1}}^{t_{k+2}} c_2^{k+3}(s) + c_4^{k+2}(s) \, ds \right) \\
=& \int_{t_{k+1}}^{t_{k+2}} K(t_{k+1}) + (K(t_{k+1}) - K(t_{k+3})) \left(c_2^{k+2}(s) + c_4^{k+2}(s) \right) \, ds.
\end{aligned}
$$

We must restrict $-1 \leq c_2^{k+2}(s) + c_4^{k+2}(s) < 0$ to ensure the stability of the scheme. We remark that under the construction of the coefficients c_2^{k+2} and c_4^{k+2}, there is a common factor of $(s - t_{k+2})$ and $(s - t_{k+2} + \tau)$, hence $c_2^{k+2}(s) + c_4^{k+2}(s) = 0$ when $s = t_{k+2}$ and $s = t_{k+2} - \tau = t_{k+1}$. Since $c_2^{k+2}, c_4^{k+2} < 0$ for $s \in (t_{k+1}, t_{k+2})$, then we may apply the extreme value theorem again to assert that $c_2^{k+2}(s) + c_4^{k+2}(s)$ attains a minimum value on $[t_{k+1}, t_{k+2}]$. Hence, the minimum of $c_2^{k+2}(s) + c_4^{k+2}(s)$ is attained at $s \approx t_{k+2} - 0.416\tau$, with a minimum value of

$$c_2^{k+2}(t_{k+2} - 0.416\tau) + c_4^{k+2}(t_{k+2} - 0.416\tau) \approx -0.603912 \geq -1.$$

Therefore, the scheme is stable when $\gamma = 5$.

We will now show that the above condition no longer holds when $\gamma = 6$. By repeating

the same argument for when $\gamma = 6$, we have

$$
\begin{aligned}
\tilde{w}_6^k =& w_0^k + w_1^{k+1} + w_2^{k+2} + w_3^{k+3} + w_4^{k+4} + w_5^{k+5} \\
\geq& K(t_{k+1}) \left(\int_{t_{k+1}}^{t_{k+2}} c_0^{k+2}(s) + c_1^{k+2}(s) + c_3^{k+2}(s) + c_5^{k+2} \, ds \right) \\
&+ K(t_{k+3}) \left(\int_{t_{k+1}}^{t_{k+2}} c_2^{k+3}(s) + c_4^{k+2}(s) \, ds \right) \\
=& K(t_{k+1}) \left(\int_{t_{k+1}}^{t_{k+2}} 1 - c_2^{k+2}(s) - c_4^{k+2}(s) \, ds \right) \\
&+ K(t_{k+3}) \left(\int_{t_{k+1}}^{t_{k+2}} c_2^{k+3}(s) + c_4^{k+2}(s) \, ds \right) \\
=& \int_{t_{k+1}}^{t_{k+2}} K(t_{k+1}) + \left(K(t_{k+1}) - K(t_{k+3}) \right) \left(c_2^{k+2}(s) + c_4^{k+2}(s) \right) \, ds,
\end{aligned}
$$

where we again must satisfy $-1 \leq c_2^{k+2}(s) + c_4^{k+2}(s) < 0$ to ensure the stability of the scheme. Using the same argument as before, we find that there exists a minimum for $s \in (t_{k+1}, t_{k+2})$, then we may apply the extreme value theorem again to assert that $c_2^{k+2}(s) + c_4^{k+2}(s)$ attains a minimum value on $[t_{k+1}, t_{k+2}]$. Using the definition of the coefficients c_2^{k+2} and c_4^{k+2} as defined by (40), we find that the minimum exists at the point $s = t_{k+2} - 0.38843\tau$ with the minimum value $c_2^{k+2}(s) + c_4^{k+2}(s) = -1.05315 \not\geq -1$. A similar analysis holds for each of the fractional order schemes and is therefore omitted. Hence, the condition is no longer satisfied and thus the scheme fails to be stable for when $\gamma = 6$, which completes the proof. $\qquad\square$

With the consistency and stability results, we are now ready to present the convergence analysis. We first define the infinity norm by $\|\cdot\|_\infty = \max\{\cdot\}$.

3.3.4 NUMERICAL CONVERGENCE

We now consider an arbitrary stable scheme of the form (49) up to order γ where $0 < \gamma \leq 5$. We present the convergence results for the usual Taylor series expansion first, followed by the fractional Taylor series expansion results.

Theorem 3.3.6. *Let $0 \leq s \leq t_n$ for any prescribed $t_n \in [0, T]$. Let $K \in L^1[0, T]$ be positive and nonincreasing on $[0, T]$ and let $\tau > 0$. Let $f(s) \in C^\gamma[0, T]$ satisfy the stable scheme (49) up to some order $\gamma = 1, 2, 3, 4, 5$, where γ is the order of approximation. Then, for some $C > 0$,*

$$
\left\| \int_0^{t_n} f(s) K(t_n - s) \, ds - \sum_{k=0}^{n} \tilde{w}_k^\gamma f(t_k) \right\|_\infty \leq C\tau^\gamma. \tag{54}
$$

Proof. We fix $\gamma \geq 1$ such that for some $C > 0$ by utilizing (44) and (49),

$$\left\| \int_0^{t_n} f(s) K(t_n - s)\, ds - \sum_{k=1}^n \tilde{w}_k^\gamma f(t_k) \right\|_\infty$$

$$\leq \left\| \sum_{k=1}^n \int_{t_{k-1}}^{t_k} \left(\frac{1}{\lceil \gamma \rceil!} \max_{0 \leq t \leq t_n} |f^{(\gamma)}(s)| (t_k - s)^\gamma \right) K(t_n - s)\, ds \right\|_\infty$$

$$\leq \frac{1}{\lceil \gamma \rceil!} \max_{0 \leq t \leq t_n} |f^{(\gamma)}(s)| \tau^\gamma \left\| \sum_{k=1}^n \int_{t_{k-1}}^{t_k} |K(t_n - s)|\, ds \right\|_\infty$$

$$= \frac{1}{\lceil \gamma \rceil!} \max_{0 \leq t \leq t_n} |f^{(\gamma)}(s)| \tau^\gamma \left\| \int_0^{t_n} |K(t_n - s)|\, ds \right\|_\infty$$

$$\leq C\tau^\gamma,$$

where $C = \dfrac{1}{\lceil \gamma \rceil!} \left\| \int_0^{t_n} |K(t_n - s)|\, ds \right\|_\infty = \dfrac{1}{\lceil \gamma \rceil!} \|K\|_{L^1[0,T]} < \infty.$ $\qquad \square$

For the fractional order regularity assumption, we have the following convergence rate results.

Theorem 3.3.7. *Let $0 \leq s \leq t_n$ for any prescribed $t_n \in [0, T]$. Let $K \in L^1[0, T]$ be positive and nonincreasing on $[0, T]$ and let $\tau > 0$. Let $f(s) \in C^\gamma[0, T]$ satisfy the stable scheme (49) up for any $\gamma \in (0, 5) - \{1, 2, 3, 4\}$, where γ is the order of approximation. Let $\gamma = n + \alpha$, where $n = 0, 1, 2, 3, 4$ and $0 < \alpha < 1$. Then, for some $C > 0$,*

$$\left\| \int_0^{t_n} f(s) K(t_n - s)\, ds - \sum_{k=0}^n \tilde{w}_k^\gamma f(t_k) \right\|_\infty \leq C \max\left(\tau^\gamma, \tau^{n+1} \right). \tag{55}$$

Proof. By fixing $\gamma = n + \alpha$ where $\gamma \in (0, 5) - \{1, 2, 3, 4\}$ and $0 < \alpha < 1$, we have for some $C_1 > 0$,

$$\left\| \int_0^{t_n} f(s) K(t_n - s)\, ds - \sum_{k=1}^n \tilde{w}_k^\gamma f(t_k) \right\|_\infty$$

$$= \left\| \sum_{k=1}^n \int_{t_{k-1}}^{t_k} \left(f(s) - \sum_{j=0}^{\lceil \gamma \rceil - 1} c_j^k(s) f(t_{k-j}) \right) K(t_n - s)\, ds \right\|_\infty$$

$$\leq C \max\left(\tau^\gamma, \tau^{n+1} \right) \left\| \sum_{k=1}^n \int_{t_{k-1}}^{t_k} K(t_n - s)\, ds \right\|_\infty$$

$$= C \max\left(\tau^\gamma, \tau^{n+1} \right) \left\| \int_0^{t_n} |K(t_n - s)|\, ds \right\|_\infty$$

$$\leq C \|K\|_{L^1[0,T]} \max\left(\tau^\gamma, \tau^{n+1} \right),$$

where $\|K\|_{L^1[0,T]} < \infty.$ $\qquad \square$

We present an example demonstrating that the kernel K improves this estimate accordingly.

Example 3.3.8. *Let $K(t) = t^{\alpha-1}$ for $0 < \alpha < 1$ and consider an order α approximation to $f(s)$ from the scheme* (49). *Then, we define*

$$
\begin{aligned}
|R_n| &:= \int_0^{t_n} (t_n - s)^{\alpha-1} |f(s) - f(t_k)| \, ds \\
&= \sum_{k=1}^{n} \int_{t_{k-1}}^{t_k} \left| (s - t_{k-1})^\alpha - \tau^\alpha + O\left({}_0^C D_t^{2\alpha} f \right) \right| (t_n - s)^{\alpha-1} \, ds \\
&\leq \sum_{k=1}^{n} \int_{t_{k-1}}^{t_k} \tau^\alpha (t_n - s)^{\alpha-1} \, ds \\
&\leq \frac{\tau^\alpha}{\alpha} \max_{1 \leq k \leq n} \tau^\alpha \\
&= C\tau^{2\alpha},
\end{aligned}
$$

which is attained under a uniform mesh size. However, if $2\alpha > 1$, we obtain the secondary estimate of $C\tau$, since then it is the maximum of that and $C\tau^{2\alpha}$.

3.4 NUMERICAL EXAMPLES

Our first example is a Volterra equation of the second kind with kernel $K(t) = t^{\alpha-1}$

$$
u(t) = f(t) + \int_0^t u(s)(t-s)^{\alpha-1} \, ds \tag{56}
$$

$$
u(0) = 0, \quad \forall \, t \in [0, T], \tag{57}
$$

where we consider the exact solution $u(t) = t^{6+\alpha} - t^{9/2}$. We define N to be the number of intervals in a uniform partition of the time domain $[0, T]$, $E_{3,\infty}(N)$ to be the maximum error attained over the total mesh for a third order accurate scheme, and $\text{rate}_3 = \log_2 \left(\frac{E_{3,\infty}(N/2)}{E_{3,\infty}(N)} \right)$. Analogously, we will define $E_{4,\infty}(N)$, $E_{\alpha,\infty}(N)$, rate_4, and rate_α for the fourth-order accurate and α-order accurate schemes. We will take $\alpha = 0.1, 0.4, 0.5, 0.7, 0.9$ in this example. The numerical results are as follows.

Table 4: Numerical Error for $u(t) = t^{6+\alpha} - t^{9/2}$, T=1 using a third-order scheme

Numerical Error for $u(t) = t^{6+\alpha} - t^{9/2}$, T=1 using a third-order scheme			
α	N	$E_{3,\infty}(N)$	rate$_3$
0.1	10	0.0010	–
	20	0.0002	2.6369
	40	2.4729e–5	2.7585
	80	3.4911e–6	2.8245
	160	4.7969e–7	2.8635
0.4	10	0.1148	–
	20	0.0144	2.992
	40	0.0020	2.8689
	80	0.0003	2.9013
	160	3.4531e–5	2.9364
0.5	10	0.0049	–
	20	0.0008	2.6731
	40	0.0001	2.8254
	80	1.4432e–5	2.9052
	160	1.8719e–6	2.9468
0.7	10	0.0022	–
	20	0.0003	2.7754
	40	4.3309e–5	2.8883
	80	5.6279e–6	2.944
	160	7.1747e–7	2.9716
0.9	10	0.0012	–
	20	0.0002	2.8067
	40	2.2852e–5	2.905
	80	2.9506e–6	2.9532
	160	3.7479e–7	2.9769

By applying the fourth order scheme to the first example, we have the following results.

Table 5: Numerical Error for $u(t) = t^{6+\alpha} - t^{9/2}$, T=1 using a fourth-order scheme

Numerical Error for $u(t) = t^{6+\alpha} - t^{9/2}$, T=1 using a fourth-order scheme			
α	N	$E_{4,\infty}(N)$	rate$_4$
0.1	10	0.0003	–
	20	2.2041e–5	3.6373
	40	1.6168e–6	3.769
	80	1.1313e–7	3.8371
	160	7.6929e–9	3.8783
0.4	10	0.0362	–
	20	0.0028	3.7128
	40	0.0002	3.7667
	80	1.3999e–5	3.8564
	160	9.2778e–7	3.9154
0.5	10	0.0021	–
	20	0.0002	3.5777
	40	1.2673e–5	3.7898
	80	8.537e–7	3.8919
	160	5.5542e–8	3.9421
0.7	10	0.0008	–
	20	6.2265e–5	3.691
	40	4.3148e–6	3.8511
	80	2.8369e–7	3.9269
	160	1.822e–8	3.9607
0.9	10	0.0004	–
	20	3.417e–5	3.7087
	40	2.3549e–6	3.859
	80	1.5441e–7	3.9308
	160	9.8935e–9	3.9642

When we have $\alpha = 0.25$, we have spurious and large blowup for small values of N, but as $N \to \infty$, we still exhibit the appropriate order of convergence, and hence still preserve the stability condition. For example, using the fourth order scheme for the second example, with $\alpha = 0.25$, we have the following rate of convergence for up to $N = 10240$:

Table 6: Numerical blowup for $u(t) = t^6$, $\alpha = 0.25$, T=1 using a fourth order scheme

Numerical rate for $u(t) = t^6$, T=1 using a fourth order scheme		
α	N	rate$_4$
0.25	10	$-$
	20	-9.1682
	40	-53.279
	80	-300.81
	160	127.59
	320	11.223
	640	4.3639
	1280	3.8026
	2560	3.8409
	5120	3.8947
	10240	4.223

Another consequence of the α-order accurate scheme is that we can also numerically approximate $u(t)$ when the exact function is not known. Consider equation (56) where $f(t) = t^{2\alpha}$ and $u(t)$ is unknown. Since the exact solution is not known explicitly, we instead compute the error using the two mesh principle as outlined in [46] and the references therein. Given a uniform time mesh, we define u^n to be the numerical approximation to u at time $t = t_n$ for N total grid points, and z^n to be the numerical approximation to u at time $t = t_n$ for 2N total grid points. Then, the maximum error considered between the two meshes is computed by $E_{\alpha,\infty}(N) = \max_{1 \le n \le N} |u^n - z^{2n}|$. We then define the rate of convergence in this case by

$$rate_\alpha = \log_2 \left(\frac{E_{\alpha,\infty}(N/2)}{E_{\alpha,\infty}(N)} \right).$$

When $\alpha = 0.05, 0.25, 0.5, 0.75, 0.95$, we have the following numerical results.

Table 7: Numerical Error for (56), $f(t) = t^{2\alpha}$ using an α-order scheme, u unknown

Numerical Error for (56), $f(t) = t^{2\alpha}$ using an α-order scheme, u unknown			
α	N	$E_{\alpha,\infty}(N)$	rate$_\alpha$
0.05	10	–	–
	20	5.0445e–5	–
	40	4.8623e–5	0.0531
	80	4.6863e–5	0.0532
	160	4.5163e–5	0.0533
0.25	10	–	–
	20	0.0025	–
	40	0.0019	0.3858
	80	0.0014	0.4054
	160	0.0011	0.4263
0.5	10	–	–
	20	0.0053	–
	40	0.0029	0.8886
	80	0.0015	0.9193
	160	0.0008	0.9422
0.75	10	–	–
	20	0.0100	–
	40	0.0052	0.9566
	80	0.0026	0.9753
	160	0.0013	0.9859
0.95	10	–	–
	20	0.0126	–
	40	0.0064	0.9797
	80	0.0032	0.9893
	160	0.0016	0.9944

Our second example is the Volterra equation of the second kind that is motivated by the findings in [56] and [8]. This particular equation is obtained by applying the Laplace transform to equation (1.2) of [56] to obtain:

$$u(x,t) = \phi(x) + \int_0^t \left(g(x,s) + \frac{\partial^2 u}{\partial x^2}(x,s) \right) \frac{(t-s)^{\alpha-1}}{\Gamma(\alpha)} \, ds \tag{58}$$

$$u(x,0) = \phi(x), \quad u(t,0) = u(t,1) = 0 \tag{59}$$

on the interval $x \in [0,1]$, $t \in [0,1]$, which has the initial condition $\phi(x) = 0$ and the exact solution $u(x,t) = \sin(\pi x)t^{1-\alpha}$. We apply a fixed fourth order Laplacian operator in space as in [56] and the α order scheme presented in Section 3 to analyze the problem. By fixing $M = 25$ space steps and using $\alpha = 0.05, 0.25, 0.5, 0.75, 0.75, 0.95$, we have the following numerical results.

Table 8: Numerical Error for $u(x,t) = \sin(\pi x)t^{1-\alpha}$, using an α-order scheme

Numerical Error for $u(x,t) = \sin(\pi x)t^{1-\alpha}$, using an α-order scheme			
α	N	$E_{\alpha,\infty}(N)$	rate$_\alpha$
0.05	10	0.0078	–
	20	0.0046	0.7578
	40	0.0026	0.8156
	80	0.0015	0.8490
	160	0.0008	0.8713
0.25	10	0.0226	–
	20	0.0132	0.7730
	40	0.0077	0.7767
	80	0.0045	0.7806
	160	0.0026	0.7856
0.5	10	0.0385	–
	20	0.0249	0.6265
	40	0.0158	0.6618
	80	0.0097	0.7017
	160	0.0058	0.7443
0.75	10	0.1757	–
	20	0.1197	0.5537
	40	0.0763	0.6497
	80	0.0456	0.7426
	160	0.0258	0.8219
0.95	10	0.4118	–
	20	0.2767	0.5735
	40	0.1683	0.7172
	80	0.0948	0.8284
	160	0.0507	0.9025

Of particular interest is the cases where $\alpha \geq 1/2$, which validate the findings in Example 3.8. By further applying a second order scheme, consistent with the L1-method presented in [56], we obtain a better rate of convergence under an equivalent assumption of $u(x,t) \in C^2([0,T]; C^6([0,1]))$. By letting $u(x,t) = \sin(\pi x)t^2$, fixing $M = 25$ space steps and using $\alpha = 0.05, 0.25, 0.5, 0.75, 0.75, 0.95$, we have the following numerical results.

Table 9: Numerical Error for $u(x,t) = \sin(\pi x)t^2$, using a second-order scheme

Numerical Error for $u(x,t) = \sin(\pi x)t^2$, using a second-order scheme			
α	N	$E_{2,\infty}(N)$	rate$_2$
0.05	10	0.0003	–
	20	9.6628e–5	1.7965
	40	2.6866e–5	1.8467
	80	7.3283e–6	1.8742
	160	1.9731e–6	1.893
0.25	10	0.0011	–
	20	0.0003	1.822
	40	7.912e–5	1.9255
	80	2.0521e–5	1.9469
	160	5.2743e–6	1.9601
0.5	10	0.0014	–
	20	0.0004	1.9458
	40	9.5596e–5	1.9746
	80	2.4128e–5	1.9862
	160	6.0645e–6	1.9922
0.75	10	0.0016	–
	20	0.0004	1.9777
	40	0.0001	1.992
	80	2.5174e–5	1.9968
	160	6.2976e–6	1.9991
0.95	10	0.0016	–
	20	0.0004	1.9951
	40	0.0001	1.9984
	80	2.5856e–5	1.9995
	160	6.4628e–6	2.0003

We further remark that the scheme does not provide a rate of convergence beyond the regularity assumption of the scheme. That is, given a function $u(x,t) \in C^{2+\alpha}([0,T]; C^6([0,1]))$ and using a second-order in time approximation, we will only exhibit a second-order rate of convergence. Consider the function $u(x,t) = \sin(\pi x)t^{2+\alpha}$, fixing $M = 25$ space steps and using $\alpha = 0.05, 0.25, 0.5, 0.75, 0.75, 0.95$, we have the following numerical results.

Table 10: Numerical Error for $u(x,t) = \sin(\pi x)t^{2+\alpha}$, using a second-order scheme, demonstating regularity barrier

Numerical Error for $u(x,t) = \sin(\pi x)t^{2+\alpha}$, using a second-order scheme			
α	N	$E_{2,\infty}(N)$	rate$_2$
0.05	10	0.0004	–
	20	0.0001	1.8014
	40	2.8677e–5	1.8482
	80	7.822e–6	1.8743
	160	2.1069e–6	1.8924
0.25	10	0.0015	–
	20	0.0004	1.822
	40	0.0001e–5	1.9255
	80	2.0521e–5	1.9469
	160	5.2743e–6	1.9601
0.5	10	0.0014	–
	20	0.0004	1.9458
	40	9.5596e–5	1.9746
	80	2.4128e–5	1.9862
	160	6.0645e–6	1.9922
0.75	10	0.0016	–
	20	0.0004	1.9777
	40	0.0001	1.992
	80	2.5174e–5	1.9968
	160	6.2976e–6	1.9991
0.95	10	0.0016	–
	20	0.0004	1.9951
	40	0.0001	1.9984
	80	2.5856e–5	1.9995
	160	6.4628e–6	2.0003

CHAPTER 4

EXTENSIONS OF THE FINITE DIFFERENCE SCHEMES UNDER A

FOURIER TRANSFORM

We present a treatment of a time-fractional diffusion equation by using Fourier transform in the spatial variable and the Laplace transform in the time variable. The resulting equation allows us to consider a wider class of functions and allows for the relaxation of regularity assumptions on the spatial variable. When applying the Fourier transform to a diffuison equation, a Fredholm integral equation with a convolution integral kernel is formed. We apply a finite difference scheme in the transformed space variable and can consider functions $u(x,t) \in C^\alpha([0,T]; C^\gamma[\Omega]), 0 < \gamma \leq 2$, with a first order rate of convergence independent on the choice of γ, due to the integral kernel. By applying a fractional-order scheme to the time variable and trigonometric interpolation to the space variable, we can ultimately functions $u(x,t) \in C^\alpha\left([0,T]; C_{2\pi}^{m,\beta}[\Omega]\right)$ with a resulting order of convergence $O\left(N^{-\alpha} + \frac{ln(M)}{M^{m+\beta}}\right)$, where M is the number of partitions in the space variable, and N is the number of partitions in the time variable. By strengthening the regularity assumption to instead $u(x,t) \in C^\alpha\left([0,T]; C^\infty[\Omega]\right)$, we obtain a resulting order $O(\tau^\alpha + e^{-Ms(u)})$. We then present one numerical examples which demonstrates these results in the space variable for the difference scheme.

4.1 INTRODUCTION

We motivate our discussion based on the findings in [8] and [56], where the one-dimensional time-fractional diffusion equation with initial and boundary conditions

$$\mathcal{D}_t^\alpha u(\mathbf{x},t) = \frac{\partial^2}{\partial x^2} u(\mathbf{x},t) + f(\mathbf{x},t), \ \mathbf{x} \in [0,1], \ t \in [0,T], \tag{60}$$

$$u(x,0) = \phi(x), u(0,t) = u(1,t) = 0, \tag{61}$$

with $\alpha \in (0,1)$ order Caputo fractional time derivative defined by

$$\mathcal{D}_t^\alpha u(\mathbf{x},t) = \frac{1}{\Gamma(1-\alpha)} \int_0^t \frac{\partial u(\mathbf{x},s)}{\partial s} (t-s)^{-\alpha} \, ds,$$

where $\Gamma(x) = \int_0^\infty e^{-t} t^{x-1} \, dt$. A numerical scheme was derived in [56] using the L1-method to treat the fractional time derivative term, and a fourth-order spatial discretization was used

to treat the Laplacian operator. A parallel to the L1-method was derived in [8] by utilizing the Laplace transform to turn the time-fractional derivative operator into a time-fractional convolution integral by use of convolution theory. The advantage of this method was in the regularity assumptions used on the objective function $u(x,t)$, and the numerical convergence rate was optimal under lesser regularity assumptions. We wish to use the Fourier transform and its properties (c.f [7], [10], [14], and [19]) on (60) to obtain similar results, and ultimately provide exponential convergence results by utilizing trigonometric interpolation in the spatial variable for real-analytic functions. We define the Fourier transform by

$$\mathcal{F}\left(f(x);\omega\right) = \int_{-\infty}^{\infty} f(x)e^{-2\pi ix\omega}\,dx$$

and the Inverse Fourier transform by

$$\mathcal{F}^{-1}\left(\hat{f}(\omega);x\right) = \int_{-\infty}^{\infty} \hat{f}(\omega)e^{2\pi ix\omega}\,d\omega.$$

The main propertiy used here is the derivative transform property, where

$$\mathcal{F}\left(\frac{d^n f(x)}{dx^n};\omega\right) = \int_{-\infty}^{\infty} \frac{d^n f(x)}{dx^n}e^{-2\pi ix\omega}\,dx$$
$$= (-2\pi i\omega)^n \mathcal{F}\left(f(x);\omega\right)$$

by repeated applications of integration by parts. The existence and uniqueness to a solution of (60) was studied in [8] based on the findings in [17]. We now state the result of applying the Fourier transform to (60).

Lemma 4.1.1. *Let $u(x,t)$ be the unique solution of* (60) *with compact support on $[0,T]\times\Omega$. Then, u(x,t) satisfies* (60) *if and only if it satisfies*

$$u(x,t) = \int_{\Omega} |x-\omega|\left(f(\omega,t) - \mathcal{D}_t^\alpha u(\omega,t)\right)\,d\omega \tag{62}$$

Proof. By applying the Fourier transform to both sides of (60), we have after defining

$$\hat{u}(\omega, t) = \mathcal{F}\left(u(x, t); \omega\right)$$

$$\mathcal{F}\left(\mathcal{D}_t^\alpha u(\mathbf{x}, t); \omega\right) = \mathcal{F}\left(\frac{\partial^2}{\partial x^2} u(\mathbf{x}, t) + f(\mathbf{x}, t); \omega\right)$$

$$\mathcal{D}_t^\alpha \hat{u}(\omega, t) = (-i\omega)^2 \hat{u}(\omega, t) + \hat{f}(\omega, t)$$

$$\mathcal{D}_t^\alpha \hat{u}(\omega, t) = -\omega^2 \hat{u}(\omega, t) + \hat{f}(\omega, t)$$

$$\hat{u}(\omega, t) = \frac{1}{\omega^2}\left(\hat{f}(\omega, t) - \mathcal{D}_t^\alpha \hat{u}(\omega, t)\right)$$

$$\mathcal{F}^{-1}\left(\hat{u}(\omega, t); x\right) = \mathcal{F}^{-1}\left(\frac{1}{\omega^2}\left(\hat{f}(\omega, t) - \mathcal{D}_t^\alpha \hat{u}(\omega, t)\right); x\right)$$

$$u(x, t) = \mathcal{F}^{-1}\left(\frac{1}{\omega^2}; x\right) * \mathcal{F}^{-1}\left(\hat{f}(\omega, t) - \mathcal{D}_t^\alpha \hat{u}(\omega, t); x\right)$$

$$u(x, t) = \int_{-\infty}^{\infty} (x - \omega) sgn(x - \omega)\left(\mathcal{D}_t^\alpha u(\omega, t) - f(\omega, t)\right) d\omega$$

$$= \int_{-\infty}^{\infty} |x - \omega|\left(\mathcal{D}_t^\alpha u(\omega, t) - f(\omega, t)\right) d\omega.$$

Finally, since u is defined only to have compact support, then

$$u(x, t) = \int_\Omega |x - \omega|\left(\mathcal{D}_t^\alpha u(\omega, t) - f(\omega, t)\right) d\omega.$$

Since the steps are reversible under the Fourier transform, the proof is complete. $\qquad\square$

The result is a Fredholm integral equation (c.f [51], [25]) in the space variable, and a fractional differential equation in the time variable.

Remark 4.1.2. *We remark that the integral kernel $K(x) = |x|$ satisfies $K \in L^1(\Omega)$ provided that $\mu(\Omega) < \infty$, where μ denotes the usual Lebesgue measure of a set. Further, $K(x) = |x|$ is not differentiable at $x = 0$, hence $K(x - \omega) = |x - \omega|$ is not differentiable along the diagonal line $x = \omega$, and by extension,*

$$\int_\Omega K(x - \omega)\, d\omega = \int_\Omega |x - \omega|\, d\omega = \left.\frac{|x - \omega|^2}{2}\right|_\Omega$$

is also not differentiable along the lines of the endpoints of the interval of integration $x = x_0$ and $x = x_f$ where $\Omega = [x_0, x_f] \subset \mathbb{R}^1$. Moreover, along any subinterval of integration which arises by discretizing the integral using the finite difference method outlined in Chapters 1 and 2 the integral

$$\int_{x_{j-1}}^{x_j} K(x_j - \omega)\, d\omega = \int_{x_{j-1}}^{x_j} |x_j - \omega|\, d\omega = \left.\frac{|x_j - \omega|^2}{2}\right|_{x_{j-1}}^{x_j}$$

is not differentiable on the endpoint of each subinterval of integration on the lines $x = x_j$ where $x_0 < x_1 < x_2 < ... < x_f$, for $j = 1, 2, ..., M$, where $x_f = x_M$.

4.2 SPATIAL DISCRETIZATION AND TRIGONOMETRIC INTERPOLATION

Let $x_m = m\pi/M$, $m = 1, 2, ..., 2M - 1$ be the uniform partition of the space variable. We now present two discretizations in the space variable for (62), using a finite difference approach and a trigonometric interpolation approach. Each method has unique advantages due to the integral term combined with the regularity assumptions. The finite difference approach will construct a scheme that obtains optimal order of convergence for a first-order approximation and is absolutely stable, which is not guaranteed under a first-order discretization of the problem in fully-differential form. For diffusion and sub-diffusion problems that assume less regularity in the space variable than the usual $u \in C_{2\pi}^{m,\beta}[0, 1]$, we can use a scheme with an appropriate regularity assumption and still obtain optimal convergence.

4.2.1 FINITE DIFFERENCE APPROACH

The finite difference method outlined in the previous chapter can be applied to discretize the integral

$$\int_\Omega |x - \omega| g(\omega) \, d\omega$$

under the same considerations. Before constructing the scheme, we remark that the integral kernel $K(x) = |x|$ is an increasing function and is not differentiable on the diagonal line $x = w$ in convolution form. The finite difference method was proved to be stable and convergent for any $K \in L^1[\Omega]$ for up to second-order accurate schemes. Therefore, we will apply the second order finite difference scheme to provide optimal convergence for the given regularity. We define $h = \pi/M$ for convenience. The stable second-order approximation is defined by

$$c_0^k = 1 - \frac{x_m - \omega}{h}, \ c_1^k = \frac{x_m - \omega}{h},$$
$$g(\omega) = c_0^k g(x_m) + c_1^k g(x_{m-1}) + O(h^2).$$

The semi-discrete form of the problem reads for each $m = 1, 2, ..., M$

$$u(x_m, t) = \int_\Omega |x_m - \omega| \left(\mathcal{D}_t^\alpha \left(c_0^m u(x_m, t) + c_1^m u(x_{m-1}, t) + O(h^2) \right) - f(\omega, t) \right) \, d\omega,$$

$$\approx \sum_{i=1}^M \int_{x_{i-1}}^{x_i} |x_m - \omega| \left(\mathcal{D}_t^\alpha \left(c_0^i u(x_i, t) + c_1^i u(x_{i-1}, t) \right) - f(\omega, t) \right) \, d\omega. \tag{63}$$

There are two suitable approaches to discretizing the problem in the time variable. On the one hand, we may directly apply the L1 method as outlined in [56]. Given $0 = t_0 < t_1 <$

$\ldots < t_n$, $t_k - t_{k-1} = \tau_k$ for all $k = 1, 2, \ldots, n$ and the local truncation error r^n, we recall the traditional L1 method approximation to the Caputo fractional derivative:

$$\mathcal{D}_t^\alpha u(\mathbf{x}, t_n) = \frac{1}{\Gamma(1-\alpha)} \sum_{k=1}^n \frac{u(\mathbf{x}, t_k) - u(\mathbf{x}, t_{k-1})}{t_k - t_{k-1}} \int_{t_{k-1}}^{t_k} (t_n - s)^{-\alpha} \, ds + r^n.$$

$$\mathcal{D}_t^\alpha u(\mathbf{x}, t_n) \approx \frac{1}{\Gamma(1-\alpha)} \sum_{k=1}^n \frac{u(\mathbf{x}, t_k) - u(\mathbf{x}, t_{k-1})}{t_k - t_{k-1}} \int_{t_{k-1}}^{t_k} (t_n - s)^{-\alpha} \, ds. \tag{64}$$

From [56] and many others before, it is shown that $r^n = O(\tau^{2-\alpha})$ for a uniform mesh $\tau_k = \tau$. Further, this method requires the function $u \in C^2([0, T]; C^2(\Omega))$, which is a much stronger regularity requirement than necessary. Still, by applying the approximation (64) to the Caputo time-fractional derivative term in (63), we obtain:

$$u(x_m, t_n) \approx \int_\Omega |x_m - \omega| \left(-f(\omega, t) + \frac{1}{\Gamma(1-\alpha)} \sum_{k=1}^n \frac{a_n^k c_0^k \left(u(x_m, t_k) - u(x_m, t_{k-1}) \right)}{t_k - t_{k-1}} \right.$$
$$\left. + \frac{a_n^k c_1^k \left(u(x_{m-1}, t_k) - u(x_{m-1}, t_{k-1}) \right)}{t_k - t_{k-1}} \right) d\omega, \tag{65}$$

which is to be solved for each $m = 1, 2, \ldots, M$, $n = 1, 2, \ldots, N$. We remark that under this construction, now we can assume exact regularity in the space variable, hence here we can assume $u \in C^2([0, T]; C^2[\Omega])$ at the cost of assuming more regularity in the time variable. This tradeoff can be further mitigated by taking a Laplace transform in the time variable in addition to the Fourier transform. We remark that the order of the transforms is irrelevant.

Lemma 4.2.1. *Let $u(x, t)$ be the unique solution of* (60) *with compact support on $[0, T] \times \Omega$. Then, $u(x,t)$ satisfies* (60) *if and only if it satisfies*

$$I^\alpha(u(x, t); s) = \int_\Omega |x - \omega| \left(u(\omega, t) - I^\alpha(f(\omega, t); s) \right) d\omega, \tag{66}$$

$$I^\alpha(u(x, t); s) = \int_0^t \frac{(t - s)^{\alpha-1}}{\Gamma(\alpha)} u(x, s) \, ds.$$

For the Fourier Transform formulation, the approximation schemes and the theory therein still hold by rewriting the integral term as a sum of two Volterra integrals in the following way:

$$u(x) + \int_\Omega |x - \omega| u(\omega) \, d\omega = F(x), \quad \Omega = [a, b]$$

$$u(x) + \int_a^x (x - \omega) u(\omega) \, d\omega + \int_x^b (\omega - x) u(\omega) \, d\omega = F(x),$$

$$F(x) = \int_\Omega |x - \omega| f(\omega) \, d\omega,$$

where both integral kernels are positive and are in L^1 for finite intervals of integration. However, since the integral kernel $K(x) = |x|$ is not differentiable at the origin, we find that the rate of convergence to the approximation to $u(x, t)$ is limited by the integral kernel in this case. That is, the second-order approximation to the Fredholm integral equation

$$u(x) + \int_\Omega |x - \omega| u(\omega)\, d\omega = F(x)$$

$$F(x) = \int_\Omega |x - \omega| f(\omega)\, d\omega,$$

where $u \in C^2[\Omega]$ is obtained by applying the Fourier transform to the diffusion equation with compact support defined on a compact interval $\Omega \subset \mathbb{R}^1$

$$u(x) + u_{xx}(x) = f(x), \quad x \in \Omega$$

$$u(x) = 0, \quad x \notin \Omega$$

only attains a first-order rate of convergence $O(M^{-1})$. We juxtapose the first-order and $\alpha-$order accurate schemes which require less regularity, $u \in C^1[\Omega]$ for the first-order accurate scheme and $u \in C^\alpha[\Omega]$ for the $\alpha-$order accurate scheme, both of which also attain a first-order rate of convergence $O(M^{-1})$.

4.2.2 TRIGONOMETRIC INTERPOLATION

We recall the definition of the trigonometric polynomial defined in [26]

$$u(x) = \frac{\alpha_0}{2} + \sum_{k=1}^{n} [\alpha_k \cos(kx) + \beta_k \sin(kx)], \tag{67}$$

subject to the interpolation property $u(x_m) = g_m$, $m = 1, 2, ..., 2M - 1$. Each coefficient is given by

$$\alpha_k = \frac{1}{M} \sum_{j=0}^{2M-1} g_m \cos kx_m, \quad k = 0, ..., n, \tag{68}$$

$$\beta_k = \frac{1}{M} \sum_{j=0}^{2M-1} g_m \sin kx_m, \quad k = 1, ..., n - 1. \tag{69}$$

Define the trigonometric interpolation operator, P_M, for M equidistant interpolation points by the sum of the Lagrange basis functions (c.f (11.13) of [26])

$$P_M(g) = \sum_{j=0}^{2M-1} |L_j(x)| \tag{70}$$

$$L_j(x) = \frac{1}{2M} \left\{ 1 + 2 \sum_{k=1}^{M-1} \cos k(x - x_j) + \cos M(x - x_j) \right\} \tag{71}$$

for $x \in [0, 2\pi]$ and $j = 0, ..., 2M - 1$. Theorem 11.4 and Lemma 11.5 of [26] provide basic stability estimates for the trigonometric interpolation operator P_n, which we employ in this paper.

Theorem. *(11.4 of [26]) For $M \geq 2$, the trigonometric interpolation operator with $2M$ equidistant interpolation points has norm*

$$\|P_M\|_\infty < 3 + \frac{2}{\pi} \ln(2M).$$

Lemma. *(11.5 of [26]) The trigonometric interpolation operator satisfies*

$$\|P_M u\|_2 \leq \sqrt{3\pi} \, \|u\|_\infty$$

for all $M \in \mathbb{N}$ and all continuous 2π-periodic functions u.

As a caveat, the estimate from Theorem 11.4 of [26] implies directly that $\|P_M\|_\infty \to \infty$ as $n \to \infty$. We denote the space of 2π-periodic Hölder continuous functions by $C_{2\pi}^{0,\alpha}$, where $0 < \alpha \leq 1$. Analogously, we define the space of 2π-periodic and m-times Hölder continuously differentiable functions by $C_{2\pi}^{m,\alpha}$, equipped with the norm

$$\|g\|_{m,\alpha} = \|u\|_\infty + \left\|u^{(m)}\right\|_{0,\alpha}$$

In its semi-discrete form, for $m = 1, 2, ..., 2M - 1$, the semi-discrete scheme reads after applying the trigonometric interpolation operator P_M to both sides

$$P_M u(x, t) = \int_\Omega |x - \omega| \left(P_M f(\omega, t) - P_M \mathcal{D}_t^\alpha u(\omega, t)\right) d\omega.$$

When evaluated at each $x_m \in [0, 1]$, $m = 1, 2, ..., 2M - 1$, we have

$$P_M u(x_j, t) = \int_0^1 |x_j - \omega| \left(f(\omega, t) - P_M \mathcal{D}_t^\alpha u(\omega, t)\right) d\omega. \tag{72}$$

The following theorem proves numerical convergence for the discrete equation (72), which follows from the steps outlined in Theorem 11.6 of [26].

Theorem 4.2.2. *Let $m \in \mathbb{N} \cup \{0\}$ and $0 < \beta \leq 1$. Then for the semi-discrete approximate equation (72), we have*

$$\|P_M u - u\|_{L^\infty[0,1]} \leq C \frac{\ln(M)}{M^{m+\beta}} \|u\|_{m,\beta},$$

for $u \in C_{2\pi}^{m,\beta}[0, 1]$ and for some constant C dependent on m and β.

Proof.

$$\|P_M u - u\|_{L^\infty[0,1]} = \left\|\int_0^1 |x_j - \omega| \left(P_M \mathcal{D}_t^\alpha u(\omega, t) - \mathcal{D}_t^\alpha u(\omega, t)\right) d\omega.\right\|_\infty.$$

Let p_M be the best approximation of u with respect to the trigonometric polynomials of the form (67) and the maximum norm. Then, by Jackson's theorem (c.f [3]), there exists some $c > 0$ independent of u such that

$$\|p_M - u\|_{L^\infty[0,1]} \le \frac{c}{M^{m+\beta}} \|u\|_{m,\beta}.$$

Next, by writing

$$P_M u - u = P_M(u - p_M) - (u - p_M),$$

we obtain

$$
\begin{aligned}
\|P_M u - u\|_{L^\infty[0,1]} &= \|x_j - \omega\|_{L^1[0,1]} \|P_M(u - p_M) - (u - p_M)\|_{L^\infty[0,1]} \\
&\le \frac{1}{2} \|P_M\|_\infty \|u - p_M\|_{L^\infty[0,1]} + \frac{1}{2} \|u - p_M\|_{L^\infty[0,1]} \\
&= \frac{1}{2}(1 + \|P_M\|_\infty) \|u - p_M\|_{L^\infty[0,1]} \\
&\le (2 + \frac{1}{\pi} \ln(2M)) \frac{c}{M^{m+\beta}} \|u\|_{m,\beta} \\
&\le C \frac{\ln(M)}{M^{m+\beta}} \|u\|_{m,\beta},
\end{aligned}
$$

where $C = \left(2 + \frac{\ln(2)}{\pi}\right) K.$ $\qquad\square$

By further restricting the regularity assumption to have u be a Real-analytic and 2π-periodic function, we obtain exponential convergence with the following results. The following theorem is a direct analogue to Theorem 11.7 of [26].

Theorem 4.2.3. *Let $u : \mathbb{R} \times [0, T] \to \mathbb{R}^2$ be analytic and 2π-periodic. Then there exists a strip $D = \mathbb{R} \times (-s, s) \subset \mathbb{C}$ with $s > 0$ such that u can be extended to a holomorphic and 2π-periodic bounded function $u : D \times [0, T] \to \mathbb{C} \times \mathbb{R}$. Then the error for the trigonometric interpolation can be estimated by*

$$\|P_M u - u\|_\infty \le C \frac{\coth(\frac{s}{2})}{2 \sinh(Ms)}, \tag{73}$$

where C is the bound for the holomorphic function u on $D \times [0, T]$.

Proof. Let $0 < \sigma < s$ be arbitrary. Utilizing the construction outlined in Theorem 11.7 of [26], we obtain the representation

$$u(x,t) - (P_M u)(x,t) = \frac{1}{2\pi} \sin(Mt) \Re \left\{ \int_{i\sigma}^{i\sigma+2\pi} \frac{i \cot\left(\dfrac{\omega - x}{2}\right)}{\sin(M\omega)} u(\omega,t) \, d\omega \right\}$$

Next, for $\Im\omega = \sigma$, we have the inequalities

$$|\sin(M\omega)| \geq \sinh(M\sigma) \quad \text{and} \quad |\cot(\omega/2)| \leq \coth(\sigma/2).$$

Utilizing the above inequalities and the results in Theorem 4.2.2, we obtain the result after sending $\sigma \to s$. $\qquad\square$

Thus, when the objective function is analytic in the space variable, we can obtain exponential order of convergence using trigonometric interpolation.

4.2.3 NUMERICAL EXAMPLE

As a proof of concept, we will consider a basic diffusion equation with varying regularity requirements to demonstrate the findings of the finite difference schemes when applied to the Fourier transform. Consider the test diffusion equation

$$u(x) + u_{xx}(x) = f(x), \quad x \in \Omega$$
$$u(x) = 0, \quad x \notin \Omega,$$

which can be Fourier Transformed to yield the Fredholm integral equation

$$u(x) + \int_{\Omega} |x - \omega| u(\omega) \, d\omega = F(x) \tag{74}$$
$$F(x) = \int_{\Omega} |x - \omega| f(\omega) \, d\omega.$$

The first-order approximation to the above Fredholm integral equation, as outlined in Chapter 2, is

$$u(x_m) + \sum_{j=1}^{M} (u(x_m) + O(\Delta x)) \int_{x_{m-1}}^{x_m} |x_m - \omega| \, d\omega = F(x_m), \quad x \in [x_0, x_f]$$
$$F(x) = \int_{\Omega} |x - \omega| f(\omega) \, d\omega,$$

which is equivalent to the α order approximation, where $\Delta x = \dfrac{x_f - x_0}{M}$ for a uniform partition of the interval Ω, which is to be solved for each $m = 1, 2, ..., M$. By contrast, the second order approximation, using the methods and definitions outlined in Chapter 2, is

$$u(x_m) + \sum_{j=1}^{M} (u(x_m) + O(\Delta x)) \int_{x_{m-1}}^{x_m} |x_m - \omega|(c_0^m(\omega) + c_1^{m-1}(\omega))\, d\omega = F(x_m)$$

$$F(x) = \int_{\Omega} |x - \omega| f(\omega)\, d\omega, \quad x \in [x_0, x_f].$$

To address the lack of data at the node x_{-1} we supplement the exact data at that node in each approximation $u(x_0) = u_0$. Consider the test function $u(x) = x^\alpha$, $\alpha > 0$, $x \geq 0$, which has the forcing function

$$F(x) = x^\alpha + \left(\frac{2}{\alpha + 1} - \frac{2}{\alpha + 2} \right) x^{\alpha+2} + \frac{1}{\alpha + 2} \left(x_f^{\alpha+2} + x_0^{\alpha+2} \right) - \frac{x}{\alpha + 1} (x_f^{\alpha+1} + x_0^{\alpha+1}).$$

The regularity requirement for the choice of $u(x) = x^\alpha$ satisfies $u \in C^\alpha[\Omega]$, where $\alpha > 0$. By letting $\Omega = [0, 1]$, $M = 10, 20, 40, 80, 160$ space steps, and using $\alpha = 0.05, 0.25, 0.5, 0.75, 0.95$, we have the following numerical results for the first and second-order schemes.

Table 11: Numerical Error for $u(x) = x^\alpha$, using a first-order scheme

Numerical Error for $u(x) = x^\alpha$, using a first-order scheme			
α	M	$E_{\alpha,\infty}(N)$	rate$_\alpha$
0.05	10	0.1203	−
	20	0.0585	1.0396
	40	0.0288	1.021
	80	0.0143	1.0126
	160	0.0071	1.0085
0.25	10	0.1034	−
	20	0.0498	1.0528
	40	0.0244	1.0298
	80	0.0120	1.0184
	160	0.0060	1.0123
0.5	10	0.0910	−
	20	0.0438	1.0549
	40	0.0215	1.0284
	80	0.0106	1.0154
	160	0.0053	1.0087
0.75	10	0.0834	−
	20	0.0402	1.0539
	40	0.0197	1.0262
	80	0.0098	1.0131
	160	0.0049	1.0067
0.95	10	0.0791	−
	20	0.0381	1.0535
	40	0.0187	1.0255
	80	0.0093	1.0125
	160	0.0023	1.0062

For the second order scheme, note that the rate of convergence similar, while the maximum error is higher than using the first-order scheme.

Table 12: Numerical Error for $u(x) = x^\alpha$, using a second-order scheme

Numerical Error for $u(x) = x^\alpha$, using a second-order scheme			
α	M	$E_{2,\infty}(N)$	rate$_2$
0.05	10	0.2053	–
	20	0.1014	1.0178
	40	0.0503	1.0107
	80	0.0251	1.0058
	160	0.0125	1.003
0.25	10	0.2313	–
	20	0.1053	1.0174
	40	0.0523	1.0108
	80	0.0260	1.0058
	160	0.0130	1.003
0.5	10	0.2242	–
	20	0.1110	1.0169
	40	0.0550	1.0107
	80	0.0274	1.0058
	160	0.0137	1.003
0.75	10	0.2368	–
	20	0.1171	1.0163
	40	0.0581	1.0106
	80	0.0289	1.0058
	160	0.0144	1.003
0.95	10	0.2480	–
	20	0.1226	1.0158
	40	0.0609	1.0104
	80	0.0303	1.0058
	160	0.0151	1.003

Both scenarios pose better-than-expected results, since $u \in C^\alpha[\Omega]$, where here $0 < \alpha < 1$. By [9], the order of convergence should be $O(\Delta x^\alpha)$. This suggests that the order of convergence cannot be superseded by the regularity of the Kernel function after integration. Finally, consider the test function $u(x) = |x|$, $\Omega = [-1, 1]$, using the first and second-order schemes. Note that now u is continuous but not differentiable at the origin. The numerical results for both schemes are as follows:

Table 13: Numerical Error for $u(x) = |x|$, using a first-order scheme

Numerical Error for $u(x) = |x|$, using a first-order scheme		
M	$E_{2,\infty}(N)$	rate$_2$
10	2.0784	–
20	0.2792	2.8962
40	0.1092	1.3542
80	0.0502	1.1208
160	0.0242	1.0526
320	0.0120	1.0246
640	0.0059	1.0119

Table 14: Numerical Error for $u(x) = |x|$, using a second-order scheme

Numerical Error for $u(x) = |x|$, using a second-order scheme		
M	$E_{2,\infty}(N)$	rate$_2$
10	15.79	–
20	1.2642	3.6427
40	0.4008	1.6572
80	0.1682	1.2532
160	0.0788	1.0935
320	0.0382	1.0443
640	0.0188	1.0216

For the second order scheme, note that the rate of convergence similar, while the maximum error is higher than using the first-order scheme. This effect is exaggerated when examining the test problem $u(x) = |x|$.

CHAPTER 5

APPLICATIONS TO GROUNDWATER FLOW

5.1 INTRODUCTION

We motivative this discussion based on the framework paper [1], which presents a time-fractional order derivative to model groundwater flow under Thiem's groundwater flow equation. The ODE form of Theim's groundwater flow equation is seen as

$$D_r r^\alpha \Phi(r) + \frac{1}{r}\Phi(r) = 0, \quad 1 < \alpha \le 2, \tag{75}$$

where r is the distance from the pump used in testing, $\Phi(r)$ measures the level of water as a function of distance, and subject to the initial condition $Q = 2\pi T D_r(\Phi(r_b))$, and

$$D_r^\alpha(f(r)) = \frac{1}{\Gamma(n-\alpha)}\frac{d^n}{dr^n}\int_0^r (r-s)^{n-\alpha-1}f(s)\,ds, \quad n-1 \le \alpha \le n \tag{76}$$

is the n-th order Caputo fractional derivative with parameter α. For the unsteady, momentary state equation, Theis [49] introduced an equation that derived a relationship between the flow of groundwater and the conduction of heat as

$$SD_t\Phi(r,t) = TD_{rr}\Phi(r,t) + \frac{1}{r}D_r\Phi(r,t). \tag{77}$$

In [1], a time-fractional version of (76) was presented by

$$\begin{cases} SD_t^\alpha\Phi(r,t) = TD_{rr}\Phi(r,t) + \dfrac{1}{r}D_r\Phi(r,t) \\ \Phi(r,0) = 0, \quad \lim_{r\to\infty}\Phi(r,t) = 0 \\ r \in (0,R], \quad t \in [0,T], \end{cases} \tag{78}$$

where now $Q = 2\pi T D_r(\Phi(r_b,t))$ is the discharge rate of the groundwater from the aquifer, T is the transmissivity of the aquifer, and r_b is the radius of the borehole. One of the main advantages of this formulation is the ability to include the variability of the medium which the groundwater flows through. Numerical comparison between equation (78) and experimental data from observation is presented in [1], showing that (78) accurately models the physical phenomena that is observed in reality. We seek to numerically compute (78) to provide an arbitrarily accurate prediction of the rate of change of water over time, through

various materials. One of the main obstacles in numerically discretizing (78) is the time-fractional derivative term, the shortcomings of which were initially presented in [56] and [8]. Namely, the usual L1-method, utilized in [56], only provides up to order $k^{1-\alpha}$ accuracy while requiring the function to lie in $C^2[0, T]$ in the time variable, where k is the time-step size. By utilizing the Laplace transform in [8], an equivalent equation was established with a fractional convolution integral instead of a fractional derivative term. Generalized schemes for this fractional convolution integral term were studied further in [9], which provided more accurate and stable schemes up to order γ accuracy for $\gamma < \eta$, $\eta > 6$ where the function is required to lie in $C^\gamma[0, T]$ in the time variable. To fully utilize the results in [9], we begin by applying the Laplace Transform to (78) to recover a fractional integral term. Existence and uniqueness of a solution to (78) was presented in [1] utilizing both transform methods and by utilizing the Boltzmann transformation, which we will use for the following lemma.

Lemma 5.1.1. *Let* $\Phi(r, t) \in C^1[0, T] \times C^2[0, R]$ *be the solution to* (78) *by*

$$\Phi(r, t) = \frac{Q}{4\pi T} \sum_{n=0}^{\infty} E_{\alpha, 1}\left(\frac{-S}{T}\lambda_n^2 t^\alpha J_0(\lambda_n r)\right), \tag{79}$$

where $E_{\alpha, 1}$ *is the Mittag-Leffler function* $E_{\alpha, 1} = \sum_{n=0}^{\infty} \dfrac{t^{n\alpha}}{\Gamma(n\alpha + 1)}$, λ_n *are the eigenvalues of the Sturm-Liouville spatial equation resultant from* (78), *and*

$$J_0(r) = \sum_{k=0}^{\infty} \frac{(-1)^k}{k!\Gamma(k+1)}\left(\frac{r}{2}\right)^{2k}$$

is the Bessel function of the first kind. Then, $\Phi(r, t)$ *satisfies equation* (78) *if and only if it satisfies*

$$\Phi(r, t) = \int_0^t \frac{(t-s)^{\alpha-1}}{\Gamma(\alpha)}\left(\frac{T}{S}D_{rr}\Phi(r, s) + \frac{1}{Sr}D_r\Phi(r, s)\right) ds. \tag{80}$$

Proof. We define the Laplace transform in the time variable as

$$\mathcal{L}(f(t); s) = \int_0^\infty f(t)e^{-st}\, dt \tag{81}$$

and we denote the Laplace transform of a function by $\mathcal{L}(f(t); s) = \hat{f}(s)$. Using the same technique as in Lemma 2.1 of [8] , we apply the Laplace transform to equation (78) to obtain

$$\mathcal{L}\left(SD_t^\alpha\Phi(r, t); s\right) = \mathcal{L}\left(TD_{rr}\Phi(r, t); s\right) + \mathcal{L}\left(\frac{1}{r}D_r\Phi(r, t); s\right), \tag{82}$$

which, after some algebra and applying the given initial condition, yields

$$s^{\alpha-1}\left(\hat{\Phi}(r,s)-\hat{\Phi}(r,0)\right)=\frac{T}{S}D_{rr}\hat{\Phi}(r,t)+\frac{1}{Sr}D_r\hat{\Phi}(r,t) \tag{83}$$

$$\Phi(\hat{r},s)=s^{-\alpha}\left(\frac{T}{S}D_{rr}\hat{\Phi}(r,t)+\frac{1}{Sr}D_r\hat{\Phi}(r,t)\right) \tag{84}$$

$$\Phi(r,t)=\int_0^t\frac{(t-s)^{\alpha-1}}{\Gamma(\alpha)}\left(\frac{T}{S}D_{rr}\Phi(r,s)+\frac{1}{Sr}D_r\Phi(r,s)\right)ds, \tag{85}$$

where the inverse Laplace transform was applied in the final step, which yields the result. $\square$

5.2 FULL DISCRETIZATION OF (85)

With the existence and uniqueness of a solution to equations (78) and (85), we now wish to provide a numerical scheme to the integral equation (85). We recall the results from [9] to present the stable discretization in the time variable for any level of regularity in the time variable. One of the key advantages of using the schemes presented in both [8] and [9] is the ability to have any level of regularity in the time variable, while providing the same order of convergence, which is not possible under the usual L1-method. We present Lemma 3.1 of [9] to discretize equation (85).

Lemma (3.1 of [9]). *Let $0 \leq s \leq t_n$ for any prescribed $t_n \in [0,T]$. Let γ denote the order of the desired approximation to the function $f(s)$, let $\phi(s) = f(s)K(t_n - s)$ such that $f(s) \in C^\gamma[0,T]$ and $K(t_n - \cdot) \in L^1[0,T]$. Then, for an order γ scheme, as described in Theorem 2.2 of [9], we have*

$$\int_0^{t_n}\phi(s)\,ds=\sum_{k=1}^n\sum_{j=0}^{\gamma-1}w_j^k f(t_{k-j})+O(\epsilon) \tag{86}$$

$$=\sum_{k=1}^n\tilde{w}_k^\gamma f(t_{k-j})+O(\epsilon), \tag{87}$$

where $\tilde{w}_k^\gamma$ is defined in Remark 3.2 of [9].

The scheme (86) was shown to be stable up to some order $\eta > 6$ and thus convergent, see Theorem 3.6 of [9]. We now present a spatial discretization of (85) to obtain a fully discretized PDE. Let M denote the number of partitions of the spatial mesh, and let Δr denote the size of the partition for a uniformly spaced mesh. For each $r_i \in (0,R]$, $i = 1,2,...,M$, we utilize a similar Taylor series expansion argument seen in [27] to equation (85) to define the

following discretizations:

$$D_{rr}\Phi(r_i) := \delta_{rr}\Phi(r_i) = \frac{\Phi(r_{i-1}) - 2\Phi(r_i) + \Phi(r_{i+1})}{\Delta r^2} + O(\Delta r^4), \tag{88}$$

$$D_r\Phi(r_i) := \delta_r\Phi(r_i) = \frac{\Phi(r_{i+1}) - \Phi(r_{i-1})}{\Delta r} + O(\Delta r^2). \tag{89}$$

By applying both discretizations to (85), the resulting approximation equation is

$$\Phi(r_i, t_n) = \sum_{k=1}^{n} \tilde{w}_k^\gamma \left(\frac{T}{S} \delta_{rr}\Phi(r, t_k) + \frac{1}{Sr_i} \delta_r\Phi(r, t_k) \right), \tag{90}$$

which is to be solved for each $r_i \in (0, R]$, $t_n \in [0, T]$. The consistency of the scheme (90) is immediate from the consistency of the scheme (86) and the discretizations (88) and (89). We present an alternative discretization under the assumption of axi-symmetric diffusion due to the lack of the point $r = 0$. This alternative model can model the phenomena of the fractional groundwater flow under a rather mild homogeneity assumption of the media of diffusion.

5.2.1 AXI-SYMMETRIC DIFFUSION AND DISCRETIZATION

Given the Volterra equation (85), we may consider the physical phenomenon where instead the following Neumann boundary conditions are imposed:

$$\begin{cases} SD_t^\alpha \Phi(r,t) = TD_{rr}\Phi(r,t) + \frac{1}{r}D_r\Phi(r,t) \\ \Phi(r,0) = 0, \quad \lim_{r\to\infty}\Phi(r,t) = 0, \quad \frac{\partial\Phi(0,t)}{\partial r} = 0 \\ r \in [0,R], \quad t \in [0,T], \end{cases} \tag{91}$$

which models the axi-symmetric diffusion of water from a cylindrical tube to a point r. This physical assumption more accurately models the injection of water into the ground, which can model groundwater flow accurately as well. Using the same Fourier Transform, we may arrive at the axi-symmetric parallel to (85) in

$$\Phi(r,t) = \int_0^t \frac{(t-s)^{\alpha-1}}{\Gamma(\alpha)} \left(\frac{T}{S}D_{rr}\Phi(r,s) + \frac{1}{Sr}D_r\Phi(r,s) \right) ds, \tag{92}$$

$$\Phi(r,0) = 0, \quad \lim_{r\to\infty}\Phi(r,t) = 0, \quad \frac{\partial\Phi(0,t)}{\partial r} = 0 \tag{93}$$

$$r \in [0,R], \quad t \in [0,T], \tag{94}$$

We present a numerical example illustrating the presence of axi-symmetric diffusion in this form, equivalently expressed by (90), with one extra consideration made for the point at

$r_i = 0$. Since there is a factor of $\dfrac{1}{r_i}$, we must consider a different PDE discretization at $r_i = 0$. Because of the Neumann boundary condition (98), we utilize L'Hospital's rule, as described in Section 3.5.6 of [27] to obtain

$$\lim_{r \to 0} \frac{1}{r} \frac{\partial \Phi}{\partial r} = \frac{\partial^2 \Phi}{\partial r^2}. \tag{95}$$

Hence, the Volterra equation (92) at $r = 0$ is instead

$$\Phi(r, t) = \frac{(1 + T)}{S\Gamma(\alpha)} \int_0^t (t - s)^{\alpha - 1} D_{rr} \Phi(r, s) \, ds \tag{96}$$

under axi-symmetric conditions. The resulting discretization under this assumption is the same except for $r_0 = 0$, which instead has the following discretization:

$$\Phi(r_0, t_n) = \frac{(1 + T)}{S\Gamma(\alpha)} \int_0^t (t - s)^{\alpha - 1} \delta_{rr} \Phi(r, s) \, ds \tag{97}$$

$$\Phi(r_0, t_n) \approx \frac{(1 + T)}{S\Gamma(\alpha)} \sum_{k=1}^n \tilde{w}_k^\gamma \frac{2\Phi(r_1, t_k) - 2\Phi(r_0, t_k)}{\Delta r^2} \tag{98}$$

where under axi-symmetry we may assume that $r_{-1} = r_1$ without loss of generality, due to symmetry over all angles.

CHAPTER 6

FURTHER APPLICATIONS TO NONLINEAR VOLTERRA INTEGRAL

EQUATIONS

6.1 INTRODUCTION

In their work [31], Lighthill presented a nonlinear Volterra integral equation describing the temperature distribution of the surface of a projectile moving through some laminar layer by

$$F(z)^4 = \frac{-1}{2\sqrt{z}} \int_0^z \frac{F'(s)}{(z^{3/2} - s^{3/2})^{1/3}} \, ds,$$
$$F(0) = 1 \quad F(t) \to 0, t \to \infty.$$

By applying an Abel type inversion, Franco et a.l in [15] rewrote the integral equation in an equivalent form:

$$F(z) = 1 - \frac{3\sqrt{3}}{2\pi} \int_0^z \frac{xF(x)^4}{(z^{3/2} - x^{3/2})^{2/3}} \, dx, \quad z \in [0, 1],$$

which, after some careful re-writing and transformation, was then rewritten in Diogo et al. [13] as

$$y(t) = 1 - \frac{3\sqrt{3}}{2\pi} \int_0^t \frac{s^{1/3}y(s)^4}{(t-s)^{2/3}} \, ds, \quad t \in [0, 1], \tag{99}$$

where now $y(t) = F(t^{2/3})$ and $K(t) = t^{-2/3}$. A generalization of this Abel-type nonlinear integral equation considers instead an integral kernel of $K(t) = t^{-\alpha}$, where $0 < \alpha < 1$, which results in the equation

$$y(t) = 1 - \frac{3\sqrt{3}}{2\pi} \int_0^t \frac{s^{1-\alpha}y(s)^4}{(t-s)^\alpha} \, ds, \quad t \in [0, 1], \, 0 < \alpha < 1. \tag{100}$$

The regularity of (100) was shown in Lemma 2.1 of [13] where $y \in C^{1,2/3}(\epsilon, 1]$, for $0 < \epsilon < R^{3/2}$ and $R \approx 0.106$. That is,

$$y(t) \in C^1[\epsilon, 1] \text{ and } |y'(t)| \leq C_y(t - \epsilon)^{-2/3}, \quad t \in (\epsilon, 1].$$

The Euler's method defined in [13] for the nonlinear integral equation (100) is as follows. For the numerical approximation to the solution of y of equation (100), the method for each $k = 1, 2, ..., N$ is

$$\begin{cases} y_0 & = 1 \\ y_k & = 1 - \dfrac{3\sqrt{3}}{2\pi} \displaystyle\sum_{j=0}^{k-1} \int_{t_j}^{t_{j+1}} \dfrac{ds}{(t_k - s)^{2/3}} t_j^{1/3} y_j^4, \quad k = 1, 2, ..., N \end{cases} \tag{101}$$

Our aim is to instead discretize equation (100) using a Taylor-series expansion of the nonlinear function $N(s, y(s)) = s^{1-\alpha} y(s)^4$ for $0 < \alpha < 1$ to solve the problem numerically over the domain $t \in [0.1]$. We define a uniform mesh of the domain $[0, T]$ by $t_k{}_{k=0}^N \in [0, T]$ for $N > 0$ such that $t_0 = 0$ and $t_K = T$. Further, we define $\tau = \tau_k = t_k - t_{k-1}$ to be the size of the partition of the mesh for each $k = 1, 2, ..., N$. We recall the definition of the Taylor series expansion for a nonlinear function $N(y(s))$ about the point $t = t_k \in [0, t_k]$:

$$N(y(t_k)) = N(y(t_k))$$

$$N(y(t_{k-1})) = N(y(t_k)) - \tau N'(y(t_k)) y'(t_k) + \frac{\tau^2}{2!} \left(N'(y(t_k)) y'(t_k) \right)' - O(\tau^3)$$

$$N(y(t_{k-2})) = N(y(t_k)) - 2\tau N'(y(t_k)) y'(t_k) + \frac{2\tau^2}{2!} \left(N'(y(t_k)) y'(t_k) \right)' - O(\tau^3)$$

$$...$$

$$N(y(t_0)) = N(y(t_k)) - k\tau N'(y(t_k)) y'(t_k) + \frac{k\tau^2}{2!} \left(N'(y(t_k)) y'(t_k) \right)' - O(\tau^k)$$

In other words, the implicit j-th order approximation the nonlinear function to $N(y(s))$ at the point $t_k \in [0, t_k]$ is found by solving the system of linear equations:

$$\sum_{i=0}^{j-1} c_i^k N(y(t_{k-i})) = N(y(s)) \tag{102}$$

$$= \sum_{i=0}^{j-1} \frac{(s - t_k)^i}{i!} (N(y(t_k)))^{(i)} + O((s - t_k)^j), \tag{103}$$

The regularity of the solution implies that we can investigate a first and second-order scheme under this construction. We remark that by instead considering the fractional Taylor series expansion, as detailed in [53], we can solve a similar system of equations to provide the optimal fractional-order accuracy from $y \in C^{1,2/3}(\epsilon, 1]$. In particular, the second order scheme will achieve the optimal order of convergence, which is consistent with the fractional Taylor series expansion. There are two potential methods to investigate.

6.2 METHOD 1: EXPLICIT SCHEME

One such method of analysis is to instead investigate the stability and convergence of the modified explicit Euler's method by

$$
\begin{cases}
y_0 & = 1 \\
y_k & = 1 - \dfrac{3\sqrt{3}}{2\pi} \displaystyle\sum_{j=1}^{k-1} \int_{t_{j-1}}^{t_j} \dfrac{s^{1/3}ds}{(t_k - s)^{2/3}} y_j^4, \quad k = 1, 2, ..., N,
\end{cases}
\tag{104}
$$

where the $s^{1/3}$ is not approximated in addition to y. A second order approximation to the scheme is thus defined:

$$
c_0^k = 1 - \frac{t_k - s}{\tau}, \; c_1^k = \frac{t_k - s}{\tau},
$$

$$
N(y(s)) = c_0^k N(y(t_k)) + c_1^k N(y(t_{k-1})) + O(\tau^2).
$$

6.3 METHOD 2: IMPLICIT SCHEME

When we solve the system of equations (102) for $j = 1$, we quickly find that $c_0^k = 1$, hence the numerical method to approximate the solution y of the equation (100) is

$$
\begin{cases}
y_0 & = 1 \\
y_k & = 1 - \dfrac{3\sqrt{3}}{2\pi} \displaystyle\sum_{j=1}^{k} \int_{t_{j-1}}^{t_j} \dfrac{ds}{(t_k - s)^{2/3}} t_j^{1/3} y_j^4, \quad k = 1, 2, ..., N.
\end{cases}
\tag{105}
$$

Similarly, we can define the second order approximation to the solution y of equation (100) by solving (102) for $j = 2$, which yields $c_0^k = 1 - \dfrac{t_k - s}{\tau}$, $c_1^k = \dfrac{t_k - s}{\tau}$. This results in the numerical method

$$
\begin{cases}
y_0 & = 1 \\
y_k & = 1 - \dfrac{3\sqrt{3}}{2\pi} \displaystyle\sum_{j=1}^{k} \int_{t_{j-1}}^{t_j} \dfrac{\left(c_0^k(s) y_j^4 t_j^{1/3} + c_1^k(s) y_{j-1}^4 t_{j-1}^{1/3} \right) ds}{(t_k - s)^{2/3}}, \quad k = 1, 2, ..., N.
\end{cases}
\tag{106}
$$

While this scheme closely resembles the previous ones, the difference is in the stability criterion and the implementation in the numerical examples. To implement the above schemes, we may rewrite the above in the following manner:

$$
\begin{cases}
y_0 = 1 \\
\dfrac{\sqrt{3}}{\pi} \gamma_j y_k^4 + y_k - \Gamma_k = 0, \quad k = 1, 2, ..., N,
\end{cases}
\tag{107}
$$

where γ_j, Γ_k are defined according to the order of approximation (c.f appendix B for a similar construction). This results in solving the quartic equation $ax^4 + dx + e = 0$ to implement the scheme. The generalized solution to the quartic equation $ax^4 + bx^3 + cx^2 + dx + e = 0$ was presented as an extension of Ferrari's method, using the works of [54]. Here, we find the solution of a quartic equation using:

$$x_{1,2} = \frac{-b}{4a} - S \pm \frac{1}{2}\sqrt{-4S^2 - 2p + \frac{q}{S}}$$

$$x_{3,4} = \frac{-b}{4a} + S \pm \frac{1}{2}\sqrt{-4S^2 - 2p - \frac{q}{S}},$$

$$p = \frac{8ac - 3b^2}{8a^2}$$

$$q = \frac{b^3 - 4abc + 8a^2d}{8a^3},$$

$$S = \frac{1}{2}\sqrt{\frac{-2}{3}p + \frac{1}{3a}\left(Q + \frac{\Delta_0}{Q}\right)}$$

$$Q = \sqrt[3]{\frac{\Delta_1 + \sqrt{\Delta_1^2 - 4\Delta_0^3}}{2}},$$

$$\Delta_0 = c^2 - 3bd + 12ae$$

$$\Delta_1 = 2c^3 - 9bcd + 27b^2e + 27ad^2 - 72ace.$$

In the implicit method (107), we have $a := \frac{\sqrt{3}}{\pi}\gamma_j$, $b = c = 0$, $d = 1$, $e = -\Gamma_k$, which simplifies some of the above to yield $p = 0$ and $q = \frac{8\pi}{\gamma_j\sqrt{3}} > 0$. Further, we immediately note that then $\Delta_0 = \frac{-12\gamma_j\Gamma_k\sqrt{3}}{\pi} < 0$ and $\Delta_1 = \frac{27\sqrt{3}\gamma_j}{\pi} > 0$, hence $Q > 0$. By combining

the above, we arrive at

$$
\begin{aligned}
S &= \frac{1}{2}\sqrt{\frac{-2}{3}p + \frac{1}{3a}\left(Q + \frac{\Delta_0}{Q}\right)} \\
&= \frac{1}{2}\sqrt{\frac{\pi}{3\gamma_j\sqrt{3}}\left(Q + \frac{\Delta_0}{Q}\right)} \\
&= \frac{1}{2}\sqrt{\frac{\pi}{3\gamma_j\sqrt{3}}\left(Q - \frac{12\gamma_j\Gamma_k\sqrt{3}}{\pi Q}\right)} \\
&= \frac{1}{2}\sqrt{\frac{\pi}{3\gamma_j\sqrt{3}}\left(\sqrt[3]{\frac{\Delta_1 + \sqrt{\Delta_1^2 - 4\Delta_0^3}}{2}} - \frac{12\gamma_j\Gamma_k\sqrt{3}}{\pi\sqrt[3]{\frac{\Delta_1 + \sqrt{\Delta_1^2 - 4\Delta_0^3}}{2}}}\right)},
\end{aligned}
$$

$$(108)$$

which can be analyzed *a priori* to select the numerical solution of u to accurately approximate the exact solution. Since this method relies strongly on knowing the exact solution at all times, this method is not always practical. We conjecture that the implicit scheme would be more practical by restricting the space of functions considered to be purely positive or negative to help accommodate this scheme, but this can be overcome by simply choosing the explicit scheme. Further, with the explicit scheme, one can also apply the stable first-order approximation to equation (100) to fully satisfy the regularity requirement that $y \in C^{1,2/3}(\epsilon, 1]$.

CHAPTER 7

CONCLUDING REMARKS

Fractional derivatives and fractional partial differential equations play a major role in generalizing physical phenomena to accommodate a wide array of media. Their presence demands special attention to their solutions, as well as their numerical treatment, to be able to properly implement and further investigate these phenomena. It is therefore pivotal that these problems require exact regularity and exhibit an optimal rate of convergence to best model these problems.

When written in differential form, classical discretizations often over-assume regularity for the solution to the underlying fractional partial differential equation as in [43] and [44]. This doubly penalizes any numerical discretization twofold, from restricting the class of admissible functions to model as well as from limiting the rate of convergence negatively based on the integral kernel on the fractional derivative term. These penalties automatically severely limits the practicality of modeling the differential equation in differential form. The use of the Laplace Transform is a natural choice to preserve the fractional derivative and the underlying structure of the problem, while posing the previously-troublesome fractional derivative term as a convolution integral instead. Other integral transformations with a convolution property and a derivative-resolving property are natural choices to resolve such issues.

Previous methods of discretization, such as the L1-method and other fast solvers of a similar nature as in [22], [23], [29], [32], and [56], exhibit such issues despite their accomplishments. While some of these issues are shored up using non-uniform and quasi-uniform time-meshes in their discretization, the regularity issue still persists and cannot be as easily shirked. More recent works pose the problem in a weak formulation by integrating the problem over a suitable time domain, but ultimately, the rate of convergence issue prevails instead. This dichotomy of a trade-off of rate of convergence versus regularity in differential formulation lends to the richness of problems that arise naturally here, as noted in [45].

This work sets out establishing the equivalency of the time-fractional diffusion equation and its equivalent Volterra integral equation by a routine application of the Laplace transform, which is then solved for the time-fractional diffusion term. By inverting the Laplace transform, a convolution integral term arises from the Laplacian term and the forcing function, which is unique to this formulation. This isometric transform preserves the regularity

requirement in both variables, while writing the equation as a full integral equation with a Laplacian term. Two schemes are derived in Chapter 2 that naturally take advantage of this new formulation, which better conform to the regularity requirements of the underlying equation. The α-order accurate scheme required $u(t) \in C^\alpha[0, T]$, the minimal regularity requirement for the underlying equation, and the midpoint scheme required a modest increase in regularity in assuming $u(t) \in C^1[0, T]$. In the numerical experiments presented, the spacial regularity assumed was $u(x) \in C^6([0, 1])$, yet this regularity assumption was only made to match the results in the literature [56]. In the time variable discretization, this ultimately led to the superconvergence in the case of the midpoint scheme with a rate of convergence resembling $O(\tau^{1+\alpha})$. While the superconvergence property is appreciated, it was not immediate from the discretization if this could be further improved upon, or if there were more schemes that could be derived analogously.

Chapter 3 investigates the unanswered questions that arise from the end of chapter 2, where then the question of optimal schemes is better answered. Ultimately, the midpoint and the α-order accurate scheme are not the only optimal schemes, which led to the derivation of the γ-order accurate scheme, with regularity assumption $u(t) \in C^\gamma[0, T]$, where now $0 < \gamma \leq 5$. The Taylor series and fractional Taylor series expansion approach outlined in Chapter 2 generalized naturally to develop these new schemes. While the Taylor series expansion theory suggested that any order of approximation can be achieved in this manner, the stability of the scheme ultimately serves as a barrier for the level of approximation. One key result links the results in [2] for quadrature methods to establish general stability provided the integral kernel $K \in L^1[0, T]$ is positive. In particular, the assumption that K is nonincreasing is only mandatory for second-order approximations and above. This suggests that other integral transforms are not only viable, but sensible depending on the underlying equations.

Chapter 4 demonstrates the use of the Fourier transform under a similar construction when applied to traditional diffusion equations. With the results from chapter 3, stable and convergent schemes can be applied to the Fourier transform equivalent of a diffusion equation, which resulted in a Fredholm integral equation with integral kernel $K(x) = |x|$. This natural extension is examined numerically with minimal regularity assumed, while attaining positive results for the first-order scheme. For higher levels of regularity assumed, the use of trigonometric interpolation can be utilized instead to discretize the problem akin to [26]. Once again these results generalize nicely beyond a standard diffusion equation, due to the use of the Fourier transform and by reforming the differential equation as a convolution

integral equation.

Chapter 5 and chapter 6 illustrate these same ideas in two separate physical applications. Chapter 5 investigates a similar time-fractional partial differential equation arising from groundwater flow mechanics as in [1] and [49]. The polar equation setting is natural when considering axial symmetry to model quasi-uniform distribution of groundwater from an aquifer at a central location. The presence of a time-fractional derivative in a polar diffusion equation lends naturally to a Laplace transform, which is provided with a discrete scheme to satisfy all physical conditions. By contrast, chapter 6 instead investigates temperature distribution of the surface of a projectile moving through laminar flow as in [13], [15], and [31]. Featured here is a nonlinear Volterra integral equation, which two suitable methods of discretization are presented based on the findings in previous chapters.

REFERENCES

[1] A. Atangana, N. Bildik, *The Use of Fractional Order Derivative to Predict the Groundwater Flow*, Hindawi (2013).

[2] C. Baker, M. Derakhshan, *Convergence and stability of quadrature methods applied to Volterra equations with delay*, IMA J. Num. Anal. 13 (1993), pp. 67-91.

[3] R. Bojanic, R. DeVore, *A proof of Jackson's theorem*, Bull. Amer. Math. Soc., 75 (1969), pp.364-367

[4] J. Bouchard, A. Georges,*Anomalous diffusion in disordered media: Statistical mechanisms, models, and physical applications*, Phys. Rep 195 (1990), pp. 127-293.

[5] H. Brunner, *Collocation Methods for Volterra Integral and Related Functional Equations*, Cambridge University Press, Cambridge, 2004.

[6] J. Conway, *Functions of One Complex Variable*, Springer-Verlag, New York, 1978.

[7] B. Davies, *Integral Transforms and their Applications*, Springer-Verlag, New York, 2002.

[8] W. Davis, R. Noren, K. Shi, *A C^α Finite Difference Method for the Caputo Time-Fractional Diffusion Equation*, Numer. Methods Partial Differential Equations 37 (2021), https://doi.org/10.1002/num.22686.

[9] W. Davis, R. Noren, *Stable and Convergent Difference Schemes for Weakly Singular Convolution Integrals*, Submitted to J. Integral Eqautions Appl. Jan 2021, accepted Mar 30, 2021.

[10] L. Debnath, *Integral Transforms and Their Applications*, CRC Press, Boca Roton, 1995.

[11] K. Diethelm, N.J. Ford, A.D. Freed, *Detailed Error Analysis for a Fractional Adams Method*, Numer. Algorithms 36 (2004), pp. 3152.

[12] K. Diethelm, *The Mean Value Theorems and a Nagumo-Type Uniqueness Theorem for Caputo's Fractional Calculus*, Fract. Calc. Appl. Anal. 20 (2017), pp. 1567-1570.

[13] T. Diogo, P. Lima, M. Rebelo, *Numerical Solution of a Nonlinear Abel Type Volterra Integral Equation*, Commun. Pure Appl. Anal. 5 (2006), pp. 277-288.

[14] D. Duffy, *Transform Methods for Solving Partial Differential Equations*, CRC Press, Boca Roton, 1994.

[15] N.B.Franco, S.McKee, J.Dixon, *A numerical solution of Lighthill's equation for the surface temperature distribution of a projectile*, Mat. Aplic. Comp. 12 (1983), 257-271.

[16] A. Friedman, M. Shinbrot, *Integral Equations in Banach Space*, Trans. Amer. Math. Soc. 126 (1967), pp. 131-179.

[17] A. Friedman, *Monotonicity of Solutions of Volterra Integral Equations in Banach Space*, Trans. Amer. Math. Soc. 138 (1969), pp. 129-148.

[18] R. Gorenflo, F. Mainardi, D. Moretti, P. Paradisi, *Time Fractional Diffusion: A Discrete Random Walk Approach*, Nonlinear Dyn 29 (2002), pp. 129-143.

[19] R. Haberman, *Applied Partial Differential Equations with Fourier Series and Boundary Value Problems*, Pearson Education, 2013.

[20] E. Hairer, S. P. Nørsett, G. Wanner, *Solving ordinary differential equations I: Nonstiff problems (2nd ed.)*, Berlin: Springer Verlag (1993).

[21] A. Iserles, *A First Course in the Numerical Analysis of Differential Equations*, Cambridge University Press, 1996.

[22] B. Jin, R. Lazarov, Z. Zhou, *An analysis of the l1 scheme for the subdiffusion equation with nonsmooth data*, IMA J. Numer. Anal. 36 (2016), pp.197-221.

[23] B. Jin, R. Lazarov, Z. Zhou, *Two Fully Discrete Schemes for Fractional Diffusion and Diffusion Equations with Nonsmooth Data*, SIAM J. Sci. Comput. 38 (2016), pp.A146-A170.

[24] Y. Katznelson, *An Introduction to Harmonic Analysis*, Cambridge University Press, Cambridge, 1968.

[25] J. Kondo, *Integral Equations*, Oxford Applied Mathematics and Computing Series, 1991.

[26] R. Kress, *Linear Integral Equations, Third Edition*, Appl. Math. Sci., Springer, 82, 2014.

[27] H. Langtangen, S. Linge, *Finite Difference Computing with PDEs - A Modern Software Approach*, Springer, 2017, pp.251-253.

[28] J. Levin, *Nonlinearly Perturbed Volterra Equations*, Tohoku Math. J. 32 (1980), pp. 317-335.

[29] H. Liao, D. Li, J. Zhang, *Sharp error estimate of the nonuniform L1 formula for linear reaction-subdiffusion equations*, SIAM J. Numer. Anal 56 (2018), pp. 1112-1133.

[30] C. Li, Q. Yi, A. Chen, *Finite difference methods with non-uniform meshes for nonlinear fractional differential equations*, J. Comput. Phys. 316 (2016), pp.614-631.

[31] J. Lighthill, *Contributions to the Theory of the Heat Transfer through a Laminar Boundary Layer*, Proc. Roy. Soc. London 202A (1950), pp.359-377.

[32] Y. Lin, C. Xu, *Finite Difference/ Spectral Approximations for the Time-Fractional Diffusion Equation*, J. Comput. Phys. 225 (2007), pp. 1533-1552.

[33] X. Lin, M. Ng, *A fast solver for multidimensional time-space fractional diffusion equation with variable coefficients*, Comput. Math. Appl. 78 (2019), pp. 1477-1489.

[34] Y. Liu, J. Roberts, Y. Yan, *A note on finite difference methods for nonlinear fractional differential equations with non-uniform meshes*, Int. J. Comput. Math 95 (2018) pp.1151-1169.

[35] Y. Liu, J. Roberts, Y. Yan, *Detailed error analysis for a fractional Adams method with graded meshes*, Numer. Algor. 78 (2018), pp.1195-1216.

[36] C. Lubich, *Convolution quadrature and discretized operational calculus I.*, Numer. Math, 52 (1988), 129-145.

[37] C. Lubich, *Convolution quadrature and discretized operational calculus II.*, Numer. Math, 52 (1988), 413-425.

[38] C. Lubich, *On convolution quadrature and Hille-Phillips operational calculus*, Appl. Numer. Math, 9 (1992), 187-199.

[39] Y. Luchko, *Maximum principle for the generalized time-fractional diffusion equation*, J. Math. Anal. Appl 351 (2009), p.218-223.

[40] Y. Luchko, *Initial-boundary-value problems for the one-dimensional time-fractional diffusion equation*, Fract. Calc. Appl. Anal. 15 (2012) p. 141-160.

[41] J. Ma, H. Lu, *On the Convolution Quadrature Rule for Integral Transforms with Oscillatory Bessel Kernels*, Symmetry 10 (2018), pp. 239-254.

[42] R. Metzler, J. Klafter, *The Random Walk's Guide to Anomalous Diffusion: A Fractional Dynamics Approach*, Phys. Rep 339 (2000), pp. 1-77.

[43] K. Oldham, J. Spanier, *The Fractional Calculus*, Academic Press, New York, 1974.

[44] I. Podlubny, *Fractional Differential Equations*, Academic Press, New York, 1999.

[45] M. Stynes, *Too much regularity may force too much uniqueness*, Fract. Calc. Appl. Anal. 19 (2016), pp. 1554-1561.

[46] M. Stynes, E. O'Riordan, J.L. Gracia, *Error Analysis of a Finite Difference Method on Graded Meshes for a Time-Fractional Diffusion Equation*, SIAM J. Numer. Anal. 55 (2017), pp. 1057-1079.

[47] Z. Sun, X. Wu, *A Fully Discrete Difference Scheme for the Fractional Diffusion-Wave System*, Appl. Numer. Math. 56 (2006), pp. 193-209.

[48] E. Süli, D. Mayers , *An Introduction to Numerical Analysis*, Cambridge University Press, (2003).

[49] C.V. Theis, *The relation between the lowering of the piezometric surface and the rate and duration of discharge of a well using ground-water storage*, Transactions, American Geophysical Union, 16 (1935), pp. 519-524.

[50] L. Trefethen, D. Bau, *Numerical Linear Algebra*, SIAM, 1997.

[51] F.G. Tricomi, *Integral Equations*, Dover, 1985.

[52] L. Turner, *Inverse of the Vandermonde Matrix with Applications*, National Aeronautics and Space Administration, 1966, 129-04-06-02-22.

[53] D. Usero, *Fractional Taylor Series for Caputo Fractional Derivatives. Construction of Numerical Schemes*, Elsevier Preprint, 2008.

[54] M. Yacoub, G. Fraidenraich, *A solution to the quartic equation*, Math. Gaz. 96 (2012), pp. 271-275.

[55] Y. Yan, M. Kahn, N. Ford, *An analysis of the modified L1 scheme for time-fractional partial differential equations with nonsmooth data* SIAM J. Numer. Anal 56 (2018), pp.210-227.

[56] Y. Zhang, Z. Sun, H. Liao, *Finite difference methods for the time fractional diffusion equation on non-uniform meshes*, J. Comput. Phys. 265 (2014), pp. 195-210.

APPENDIX A

EXISTENCE AND UNIQUENESS OF A SOLUTION TO (2)

Consider the Hilbert space $L^2(0,1)$ and let $\sigma(A)$ denote the spectrum of the operator $A = -\dfrac{\partial^2}{\partial x^2}$ which is a strictly positive self-adjoint operator on the dense subspace $H_0^2(0,1)$. The operator valued equation $(\lambda I - A)(X) = 0$ has the solution

$$
\begin{aligned}
(\lambda I - A)(X) = (\lambda X - A(X)) &= 0 \\
&= X'' + \lambda X = 0 \\
&\Rightarrow X_\lambda(x) = \sin(\sqrt{\lambda}x), \text{ with Eigenvalues } \lambda_n = (n\pi)^2.
\end{aligned}
$$

Now, let

$$
\delta_A = \inf_{y \neq 0, \, y \in H_0^2((0,1))} \frac{(Ay, y)}{(y, y)} = \pi^2.
$$

It is easy to see that $a_{1-\alpha}(t) = \dfrac{t^{\alpha-1}}{\Gamma(\alpha)}$ is positive, decreasing on $(0, \infty)$, and $a_{1-\alpha} \in C(0, \infty) \cap L^1(0,1)$. Therefore, we may apply Theorem 4.1 from [17] to see that the operator S(t) defined as

$$
S(t)x_0 = \int_{\delta_A}^{\infty} S_\lambda(t) dE_\lambda x_0 \quad (x_0 \in L^2(0,1)),
$$

is the fundamental solution of (2), as defined in [17]. Here, $S_\lambda = S_\lambda(t)$ is the solution of the scalar equation

$$
S_\lambda(t) = 1 - \lambda \int_s^t a_{1-\alpha}(t - \tau) S_\lambda(\tau) \, d\tau, \tag{109}
$$

and E_λ is the resolution of the identity for A and because the operator-valued function $S = S(t)$ is a fundamental solution,
$S \in L^1\left((0, T]; \mathcal{B}\left(L^2(0,1)\right)\right)$, and for almost all $t \in [0, T]$

$$
S(t) = I - A \int_0^t a_{1-\alpha}(t - \tau) S(\tau) \, d\tau
$$

where $\mathcal{B}\left(L^2(0,1)\right)$ is the space of all bounded linear operators of $L^2(0,1)$ and I is the identity operator. If $\phi(x) = \sum_{n=1}^{\infty} a_n \sin(n\pi x) \in H_0^2(0,1)$ then $\sum_{n=1}^{\infty} |a_n|^2 n^2 < \infty$, and

$$
\begin{aligned}
A\phi(x) &= \int_{\delta_A}^{\infty} \lambda dE_\lambda \phi(x) \\
&= \sum_{n=1}^{\infty} \lambda_n a_n \sin(n\pi x) \\
&= \sum_{n=1}^{\infty} (\pi n)^2 a_n \sin(n\pi x).
\end{aligned}
$$

Let $\hat{a}_{1-\alpha}(s) = \mathcal{L}(a_{1-\alpha}(t))$. Define $g(s) = s\hat{a}_{1-\alpha}(s) = s(s^{-\alpha}) = s^{1-\alpha}$. We may calculate S_λ using the following from [17]:

$$
\begin{aligned}
S_\lambda &= \mathcal{L}^{-1}\left(\frac{1}{s + \lambda g(s)}\right) = \mathcal{L}^{-1}\left(\frac{1}{s + \lambda s^{1-\alpha}}\right) \\
&= \mathcal{L}^{-1}\left(\frac{s^{-1}}{1 + \lambda s^{-\alpha}}\right) = E_\beta(-\lambda t^\alpha),
\end{aligned}
$$

where E_β is the well known Mittag-Leffler function,

$E_\beta(z) = \sum_{n=0}^{\infty} \frac{z^n}{\Gamma(1 + n\beta)}$, see Theorem 6.1.1 of [5] for more details. Now, from the above calculations,

$$
\begin{aligned}
S(t)\phi(x) = \int_{\delta_a}^{\infty} S_\lambda(t) dE_\lambda \phi(x) &= \sum_{n=1}^{\infty} S_{\lambda n}(t) a_n \sin(n\pi x) \\
&= \sum_{n=1}^{\infty} \sum_{m=0}^{\infty} \left[\frac{(-\lambda_n t^\alpha)^m}{\Gamma(m\alpha + 1)}\right] a_n \sin(n\pi x) \\
&= \sum_{n=1}^{\infty} a_n \sin(n\pi x) \sum_{m=0}^{\infty} \left[\frac{(-\lambda_n t^\alpha)^m}{\Gamma(m\alpha + 1)}\right]. \quad (110)
\end{aligned}
$$

Then

$$
u(x,t) = S(t)\phi(x) + (S * f)(x,t)
$$

is, in closed form, the unique solution of (2), ensured by Theorem A.

APPENDIX B

NUMERICAL IMPLEMENTATION

From chapter 2, for a Volterra integral equation of the second kind

$$u(t) = f(t) + \int_0^t K(t,s)u(s)\,ds,$$

consider the numerical approximation $\tilde{u}$ of order γ to the integral equation at the time $t = t_n$

$$\tilde{u}(t_n) = f(t_n) + \sum_{k=1}^{n} \sum_{j=0}^{\lceil\gamma\rceil-1} \tilde{u}(t_{k-j}) \int_{t_{k-1}}^{t_k} c_j^k(s) K(t_n - s)\,ds, \tag{111}$$

where $0 < \gamma \le 5$, which is solved for each $n = 1, 2, ..., N$. We assume that the initial value $u(t_0) = u_0$. For simplicity, for the first $\lceil\gamma\rceil$ time values we use the exact value $\tilde{u}(t_x) = u(t_x)$, $x = 0, 1, ..., \lceil\gamma\rceil$ to begin iterating. The approximation can be rewritten as an implicit scheme:

$$\tilde{u}(t_n) = f(t_n) + \sum_{k=1}^{n-1} \sum_{j=0}^{\lceil\gamma\rceil-1} \tilde{u}(t_{k-j}) \int_{t_{k-1}}^{t_k} c_j^k(s) K(t_n - s)\,ds$$

$$+ \sum_{j=0}^{\lceil\gamma\rceil-1} \tilde{u}(t_{n-j}) \int_{t_{n-1}}^{t_n} c_j^n(s) K(t_n - s)\,ds$$

$$\tilde{u}(t_n) = f(t_n) + \sum_{k=1}^{n-1} \sum_{j=0}^{\lceil\gamma\rceil-1} \tilde{u}(t_{k-j}) \int_{t_{k-1}}^{t_k} c_j^k(s) K(t_n - s)\,ds$$

$$+ \sum_{j=1}^{\lceil\gamma\rceil-1} \tilde{u}(t_{n-j}) \int_{t_{n-1}}^{t_n} c_j^n(s) K(t_n - s)\,ds + \tilde{u}(t_n) \int_{t_{n-1}}^{t_n} c_0^n(s) K(t_n - s)\,ds$$

$$\tilde{u}(t_n)\left(1 - \int_{t_{n-1}}^{t_n} c_0^n(s) K(t_n - s)\,ds\right) = f(t_n) + \sum_{j=1}^{\lceil\gamma\rceil-1} \tilde{u}(t_{n-j}) \int_{t_{n-1}}^{t_n} c_j^n(s) K(t_n - s)\,ds$$

$$+ \sum_{k=1}^{n-1} \sum_{j=0}^{\lceil\gamma\rceil-1} \tilde{u}(t_{k-j}) \int_{t_{k-1}}^{t_k} c_j^k(s) K(t_n - s)\,ds,$$

where then the left hand side is entirely dependent on the data from previous steps on the right hand side. In general, $f(t)$ is known for all t, so then the approximation scheme requires

solving

$$\tilde{u}(t_n) = \left(1 - \int_{t_{n-1}}^{t_n} c_0^n(s)K(t_n - s)\,ds\right)^{-1}\left[f(t_n) + \sum_{j=1}^{\lceil\gamma\rceil-1}\tilde{u}(t_{n-j})\int_{t_{n-1}}^{t_n} c_j^n(s)K(t_n - s)\,ds\right.$$

$$\left. + \sum_{k=1}^{n-1}\sum_{j=0}^{\lceil\gamma\rceil-1}\tilde{u}(t_{k-j})\int_{t_{k-1}}^{t_k} c_j^k(s)K(t_n - s)\,ds\right],$$

which is to be solved for each $n = 1, 2, ..., N$, provided that the invertibility criterion

$$1 - \int_{t_{n-1}}^{t_n} c_0^n(s)K(t_n - s)\,ds \neq 1$$

is satisfied. In the 1-dimensional case above, the implementation is a direct time-marching algorithm with the known data on the right-hand side, where the data $\tilde{u}(t_n)$ is stored for each n to compute the memory term from previous time steps.

The 2-dimensional case requires additional treatment depending on the numerical scheme implemented in the other variable. In chapter 1, the α-order approximate problem considered is

$$\begin{cases} \mathcal{H}_h u_i^n = \mathcal{H}_h\phi(x_i) + \mathcal{H}_h f_{1-\alpha}(x_i, t_n) + \sum_{k=1}^{n}\dfrac{a_k^n}{h^2}\left[u_{i+1}^k - 2u_i^k + u_{i-1}^k\right] \\ \\ u_i^0 = 0, \quad u_0^n = u_M^n = 0, \end{cases}$$

which is solved for each $n = 1, 2, ..., N$, and each $i = 1, 2, ..., M$. By recalling the definition of the $\mathcal{H}_h$ operator, we have

$$\begin{cases} \dfrac{u_{i-1}^n + 10u_i^n + u_{i+1}^n}{12} = \dfrac{\phi_{i-1} + 10\phi_i + \phi_{i+1} + f_{1-\alpha,i-1}^n + 10f_{1-\alpha,i}^n + f_{1-\alpha,i+1}^n}{12} \\ \qquad\qquad\qquad\qquad\qquad + \sum_{k=1}^{n}\dfrac{a_k^n}{h^2}\left[u_{i+1}^k - 2u_i^k + u_{i-1}^k\right] \\ \\ u_i^0 = 0, \quad u_0^n = u_M^n = 0. \end{cases}$$

We wish to rewrite the above in order to solve for each of the values of u at the time $t = t_n$. To do so, we group all of the u^n terms on one side as before. By omitting initial and boundary conditions in the arithmetic, we obtain

$$\frac{u_{i-1}^n + 10u_i^n + u_{i+1}^n}{12} = \frac{\phi_{i-1} + 10\phi_i + \phi_{i+1} + f_{1-\alpha,i-1}^n + 10f_{1-\alpha,i}^n + f_{1-\alpha,i+1}^n}{12}$$

$$+ \sum_{k=1}^{n-1}\frac{a_k^n}{h^2}\left[u_{i+1}^k - 2u_i^k + u_{i-1}^k\right] + \frac{a_n^n}{h^2}\left[u_{i+1}^n - 2u_i^n + u_{i-1}^n\right]$$

$$\frac{u_{i-1}^n + 10u_i^n + u_{i+1}^n}{12} - \frac{a_n^n}{h^2}\left[u_{i+1}^n - 2u_i^n + u_{i-1}^n\right] = R.H.S.$$

We can re-cast the above as a matrix equation, where then we can solve for each $i = 1, 2, ..., M$ simultaneously from

$$
\begin{bmatrix}
\frac{10}{12} + \frac{2a_n^n}{h^2} & \frac{1}{12} - \frac{a_n^n}{h^2} & 0 & 0 & \ldots & 0 \\
\frac{1}{12} - \frac{a_n^n}{h^2} & \frac{10}{12} + \frac{2a_n^n}{h^2} & \frac{1}{12} - \frac{a_n^n}{h^2} & 0 & \ldots & 0 \\
0 & \frac{1}{12} - \frac{a_n^n}{h^2} & \frac{10}{12} + \frac{2a_n^n}{h^2} & \frac{1}{12} - \frac{a_n^n}{h^2} & \ldots & 0 \\
& & \ldots & & & \\
0 & 0 & 0 & 0 & \ldots & \frac{10}{12} + \frac{2a_n^n}{h^2}
\end{bmatrix}
\begin{bmatrix}
u_0^n \\
u_1^n \\
u_2^n \\
\ldots \\
u_M^n
\end{bmatrix}
= R.H.S.
$$

Namely, by defining the tridiagonal matrix for the α-order approximation (11)

$$
\mathbf{I}_\alpha^* =
\begin{bmatrix}
\frac{10}{12} + \frac{2a_n^n}{h^2} & \frac{1}{12} - \frac{a_n^n}{h^2} & 0 & 0 & \ldots & 0 \\
\frac{1}{12} - \frac{a_n^n}{h^2} & \frac{10}{12} + \frac{2a_n^n}{h^2} & \frac{1}{12} - \frac{a_n^n}{h^2} & 0 & \ldots & 0 \\
0 & \frac{1}{12} - \frac{a_n^n}{h^2} & \frac{10}{12} + \frac{2a_n^n}{h^2} & \frac{1}{12} - \frac{a_n^n}{h^2} & \ldots & 0 \\
& & \ldots & & & \\
0 & 0 & 0 & 0 & \ldots & \frac{10}{12} + \frac{2a_n^n}{h^2}
\end{bmatrix},
$$

where we solve for the vector $\{u_i^n\}_{i=0,1,...,M}$ by inverting the matrix $\mathbf{I}_\alpha^*$. We remark that here, none of the main diagonal entries are never 0, thus the determinant of the matrix is non-zero, thus can be inverted. Further, the entries of $\mathbf{I}_\alpha^*$ are entirely dependent on τ and h, which suggests that the condition number of $\mathbf{I}_\alpha^*$ is fixed over each time step. The full implementation of the scheme is achieved by re-casting the right hand side as a vector also, where we use the known data from all previous time steps u_i^{n-1} and the known initial and

forcing functions to obtain

$$R.H.S = \begin{bmatrix} \dfrac{10\phi_0 + \phi_1 + 10f_{1-\alpha,0} + f_{1-\alpha,1}}{12} + \displaystyle\sum_{k=1}^{n-1} a_k^n \dfrac{-2u_0^k + u_1^k}{h^2} \\[2em] \dfrac{\phi_0 + 10\phi_1 + \phi_2 + f_{1-\alpha,0} + 10f_{1-\alpha,1} + f_{1-\alpha,2}}{12} + \displaystyle\sum_{k=1}^{n-1} a_k^n \dfrac{u_0^k - 2u_1^k + u_2^k}{h^2} \\[2em] \dfrac{\phi_1 + 10\phi_2 + \phi_3 + f_{1-\alpha,1} + 10f_{1-\alpha,2} + f_{1-\alpha,3}}{12} + \displaystyle\sum_{k=1}^{n-1} a_k^n \dfrac{u_1^k - 2u_2^k + u_3^k}{h^2} \\[1em] ... \\ \dfrac{\phi_{M-1} + 10\phi_M + f_{1-\alpha,M-1} + 10f_{1-\alpha,M}}{12} + \displaystyle\sum_{k=1}^{n-1} a_k^n \dfrac{u_{M-1}^k - 2u_M^k}{h^2} \end{bmatrix}.$$

The full numerical implementation reads:

$$\begin{bmatrix} u_0^n \\ u_1^n \\ u_2^n \\ ... \\ u_M^n \end{bmatrix} = \mathbf{I}_\alpha^{*-1} \begin{bmatrix} \dfrac{10\phi_0 + \phi_1 + 10f_{1-\alpha,0} + f_{1-\alpha,1}}{12} + \displaystyle\sum_{k=1}^{n-1} a_k^n \dfrac{-2u_0^k + u_1^k}{h^2} \\[2em] \dfrac{\phi_0 + 10\phi_1 + \phi_2 + f_{1-\alpha,0} + 10f_{1-\alpha,1} + f_{1-\alpha,2}}{12} + \displaystyle\sum_{k=1}^{n-1} a_k^n \dfrac{u_0^k - 2u_1^k + u_2^k}{h^2} \\[2em] \dfrac{\phi_1 + 10\phi_2 + \phi_3 + f_{1-\alpha,1} + 10f_{1-\alpha,2} + f_{1-\alpha,3}}{12} + \displaystyle\sum_{k=1}^{n-1} a_k^n \dfrac{u_1^k - 2u_2^k + u_3^k}{h^2} \\[1em] ... \\ \dfrac{\phi_{M-1} + 10\phi_M + f_{1-\alpha,M-1} + 10f_{1-\alpha,M}}{12} + \displaystyle\sum_{k=1}^{n-1} a_k^n \dfrac{u_{M-1}^k - 2u_M^k}{h^2} \end{bmatrix},$$

which is solved for each n. In a similar manner, for the midpoint scheme derived in Chapter

2, we can rewrite the approximation scheme (15) in a matrix equation by

$$
\begin{bmatrix} u_0^n \\ u_1^n \\ u_2^n \\ \dots \\ u_M^n \end{bmatrix} = \mathbf{I_2^{*}}^{-1} \begin{bmatrix} \dfrac{10\phi_0 + \phi_1 + 10f_{1-\alpha,0} + f_{1-\alpha,1}}{12} + \displaystyle\sum_{k=1}^{n-1} a_k^n \dfrac{-2u_0^k + u_1^k}{h^2} \\[2ex] \dfrac{\phi_0 + 10\phi_1 + \phi_2 + f_{1-\alpha,0} + 10f_{1-\alpha,1} + f_{1-\alpha,2}}{12} + \displaystyle\sum_{k=1}^{n-1} a_k^n \dfrac{u_0^k - 2u_1^k + u_2^k}{h^2} \\[2ex] \dfrac{\phi_1 + 10\phi_2 + \phi_3 + f_{1-\alpha,1} + 10f_{1-\alpha,2} + f_{1-\alpha,3}}{12} + \displaystyle\sum_{k=1}^{n-1} a_k^n \dfrac{u_1^k - 2u_2^k + u_3^k}{h^2} \\[2ex] \dots \\[1ex] \dfrac{\phi_{M-1} + 10\phi_M + f_{1-\alpha,M-1} + 10f_{1-\alpha,M}}{12} + \displaystyle\sum_{k=1}^{n-1} a_k^n \dfrac{u_{M-1}^k - 2u_M^k}{h^2} \end{bmatrix},
$$

where $\mathbf{I_2^{*}}$ is defined in an analogous manner by

$$
\mathbf{I_2^{*}} = \begin{bmatrix} \dfrac{10}{12} + \dfrac{a_n^n}{h^2} & \dfrac{1}{12} - \dfrac{a_n^n}{2h^2} & 0 & 0 & \dots & 0 \\[2ex] \dfrac{1}{12} - \dfrac{a_n^n}{2h^2} & \dfrac{10}{12} + \dfrac{a_n^n}{h^2} & \dfrac{1}{12} - \dfrac{a_n^n}{2h^2} & 0 & \dots & 0 \\[2ex] 0 & \dfrac{1}{12} - \dfrac{a_n^n}{2h^2} & \dfrac{10}{12} + \dfrac{a_n^n}{h^2} & \dfrac{1}{12} - \dfrac{a_n^n}{2h^2} & \dots & 0 \\[1ex] & & \dots & & & \\[1ex] 0 & 0 & 0 & 0 & \dots & \dfrac{10}{12} + \dfrac{a_n^n}{h^2} \end{bmatrix}.
$$

This naturally extends to a general γ-order approximation scheme, which can be defined

similarly to the previous two. In this manner, we obtain

$$
\begin{bmatrix} u_0^n \\ u_1^n \\ u_2^n \\ \dots \\ u_M^n \end{bmatrix} = \mathbf{I}_{\lceil\gamma\rceil}^{*}{}^{-1}
\begin{bmatrix}
\dfrac{10\phi_0 + \phi_1 + 10f_{1-\alpha,0} + f_{1-\alpha,1}}{12} + \displaystyle\sum_{k=1}^{n-1}\sum_{j=0}^{\lceil\gamma\rceil-1} \tilde{c}_j^k \dfrac{-2u_0^k + u_1^k}{h^2} \\[4mm]
\dfrac{\phi_0 + 10\phi_1 + \phi_2 + f_{1-\alpha,0} + 10f_{1-\alpha,1} + f_{1-\alpha,2}}{12} + \displaystyle\sum_{k=1}^{n-1}\sum_{j=0}^{\lceil\gamma\rceil-1} \tilde{c}_j^k \dfrac{u_0^k - 2u_1^k + u_2^k}{h^2} \\[4mm]
\dfrac{\phi_1 + 10\phi_2 + \phi_3 + f_{1-\alpha,1} + 10f_{1-\alpha,2} + f_{1-\alpha,3}}{12} + \displaystyle\sum_{k=1}^{n-1}\sum_{j=0}^{\lceil\gamma\rceil-1} \tilde{c}_j^k \dfrac{u_1^k - 2u_2^k + u_3^k}{h^2} \\[4mm]
\dots \\[2mm]
\dfrac{\phi_{M-1} + 10\phi_M + f_{1-\alpha,M-1} + 10f_{1-\alpha,M}}{12} + \displaystyle\sum_{k=1}^{n-1}\sum_{j=0}^{\lceil\gamma\rceil-1} \tilde{c}_j^k \dfrac{u_{M-1}^k - 2u_M^k}{h^2}
\end{bmatrix},
$$

where now

$$
\mathbf{I}_{\lceil\gamma\rceil}^{*}{}^{-1} =
\begin{bmatrix}
\dfrac{10}{12} + \dfrac{\tilde{c}_0^n}{h^2} & \dfrac{1}{12} - \dfrac{\tilde{c}_0^n}{2h^2} & 0 & 0 & \dots & 0 \\[4mm]
\dfrac{1}{12} - \dfrac{\tilde{c}_0^n}{2h^2} & \dfrac{10}{12} + \dfrac{\tilde{c}_0^n}{h^2} & \dfrac{1}{12} - \dfrac{\tilde{c}_0^n}{2h^2} & 0 & \dots & 0 \\[4mm]
0 & \dfrac{1}{12} - \dfrac{\tilde{c}_0^n}{2h^2} & \dfrac{10}{12} + \dfrac{\tilde{c}_0^n}{h^2} & \dfrac{1}{12} - \dfrac{\tilde{c}_0^n}{2h^2} & \dots & 0 \\[2mm]
& & \dots & & & \\[2mm]
0 & 0 & 0 & 0 & \dots & \dfrac{10}{12} + \dfrac{\tilde{c}_0^n}{h^2}
\end{bmatrix}.
$$

Here,

$$
\tilde{c}_j^k = \int_{t_{k-1}}^{t_k} c_j^k(s) K(t_n - s)\,ds,
$$

$$
\tilde{c}_0^n = \int_{t_{n-1}}^{t_n} c_0^n(s) K(t_n - s)\,ds,
$$

where $c_k^n(s)$ and $c_0^n(s)$ are determined from the γ-order accurate scheme. Naturally, for the first order scheme presented above, $c_0^n(s) = 1$, so then $\tilde{c}_0^n = a_n^n$, as expected. This method naturally extends to the results stated in Chapter 3.

APPENDIX C

CONDITION NUMBERS FOR NUMERICAL EXPERIMENTS

Featured here are the tabulated values of the condition numbers $\kappa_{2,2}$ and $\kappa_{2,\alpha}$ for the two major numerical experiments featured in Chapter 2. For the scheme (15), we consider the exact solution $u(x,t) = sin(\pi x)t^{1.01}$, $\phi(x) = 0$, $u(0,t) = u(1,t) = 0$, given $N = 10, 20, 40, 80, 160$ and $M = 25$. Similarly, for the scheme (11), the condition number $\kappa_{2,\alpha}$ is calculated for a numerical experiment with $u(x,t) = sin(\pi x)t^{\alpha}$, $\phi(x) = 0$, $u(0,t) = u(1,t) = 0$, given $N = 10, 20, 40, 80, 160$ and $M = 25$. In both cases, the α values considered are $\alpha = 0.05, 0.1, 0.15, 0.2, 0.25, 0.3, 0.35, 0.4, 0.45, 0.5, 0.55, 0.6,$
$0.65, 0.7, 0.75, 0.8, 0.85, 0.9, 0.95$. As α and N increase, the condition number decreases and the problem becomes more numerically stable.

Table 15: Condition Number $\kappa_{2,2}$ for $u(x,t) = \sin(\pi x)t^{1.01}$, using scheme (15), where $0 < \alpha \leq 0.25$

Condition Number $\kappa_{2,2}$ for $u(x,t) = \sin(\pi x)t^{1.01}$, using scheme (15)		
α	N	$\kappa_{2,2}$
0.05	10	206.9724
	20	205.6623
	40	204.3234
	80	202.9556
	160	201.5587
0.1	10	203.427
	20	200.6241
	40	197.7049
	80	194.6693
	160	191.5179
0.15	10	199.5268
	20	195.0378
	40	190.2884
	80	185.2831
	160	180.0298
0.2	10	195.2557
	20	188.8822
	40	182.0576
	80	174.8045
	160	167.1572
0.25	10	190.6
	20	182.146
	40	173.0228
	80	163.3002
	160	153.076

Table 16: Condition Number $\kappa_{2,2}$ for $u(x,t) = \sin(\pi x)t^{1.01}$, using scheme (15), where $0.25 < \alpha \le 0.5$

Condition Number $\kappa_{2,2}$ for $u(x,t) = \sin(\pi x)t^{1.01}$, using scheme (15)		
α	N	$\kappa_{2,2}$
0.3	10	185.5491
	20	174.8306
	40	163.2278
	80	150.9055
	160	138.0816
0.35	10	180.0973
	20	166.9535
	40	152.754
	80	137.826
	160	122.5749
0.4	10	174.2445
	20	158.5503
	40	141.7218
	80	124.3294
	160	107.0253
0.45	10	167.9978
	20	149.6763
	40	130.2886
	80	110.7271
	160	91.9160
0.5	10	161.3723
	20	140.4072
	40	118.6418
	80	97.3461
	160	77.6851

Table 17: Condition Number $\kappa_{2,2}$ for $u(x,t) = \sin(\pi x)t^{1.01}$, using scheme (15), where $0.5 < \alpha \leq 0.75$

Condition Number $\kappa_{2,2}$ for $u(x,t) = \sin(\pi x)t^{1.01}$, using scheme (15)		
α	N	$\kappa_{2,2}$
0.55	10	154.3922
	20	130.8379
	40	106.9871
	80	84.4986
	160	64.6765
0.6	10	147.0911
	20	121.0793
	40	95.5351
	80	72.453
	160	53.1123
0.65	10	139.5124
	20	111.2540
	40	84.4856
	80	61.4129
	160	43.0892
0.7	10	131.7089
	20	101.4905
	40	74.0141
	80	51.5071
	160	34.5949
0.75	10	123.7414
	20	91.9165
	40	64.2610
	80	42.7907
	160	27.5354

Table 18: Condition Number $\kappa_{2,2}$ for $u(x,t) = \sin(\pi x)t^{1.01}$, using scheme (15), where $0.75 < \alpha < 1$

Condition Number $\kappa_{2,2}$ for $u(x,t) = \sin(\pi x)t^{1.01}$, using scheme (15)		
α	N	$\kappa_{2,2}$
0.8	10	115.6776
	20	82.6522
	40	55.3256
	80	35.2543
	160	21.7655
0.85	10	107.5901
	20	73.8042
	40	47.2647
	80	28.8388
	160	17.1158
0.9	10	99.5533
	20	65.4610
	40	40.0954
	80	23.4516
	160	13.4126
0.95	10	91.6412
	20	57.6897
	40	33.8015
	80	18.9809
	160	10.4921

Table 19: Condition Number $\kappa_{2,\alpha}$ for $u(x,t) = \sin(\pi x)t^\alpha$, using scheme (11), where $0 < \alpha \leq 0.25$

Condition Number $\kappa_{2,\alpha}$ for $u(x,t) = \sin(\pi x)t^\alpha$, using scheme (11)		
α	N	$\kappa_{2,2}$
0.05	10	227.5294
	20	226.735
	40	225.9185
	80	225.0793
	160	224.2171
0.1	10	225.3691
	20	223.6372
	40	221.8105
	80	219.8856
	160	217.8594
0.15	10	222.9534
	20	220.1207
	40	217.061
	80	213.7644
	160	210.2221
0.2	10	220.2595
	20	216.1424
	40	211.5996
	80	206.6121
	160	201.1663
0.25	10	217.2637
	20	211.6594
	40	205.3609
	80	198.3434
	160	190.6

Table 20: Condition Number $\kappa_{2,\alpha}$ for $u(x,t) = \sin(\pi x)t^\alpha$, using scheme (11), where $0.25 < \alpha \leq 0.5$

Condition Number $\kappa_{2,\alpha}$ for $u(x,t) = \sin(\pi x)t^\alpha$, using scheme (11)		
α	N	$\kappa_{2,2}$
0.3	10	213.9415
	20	206.6304
	40	198.29
	80	188.9054
	160	178.5081
0.35	10	210.2682
	20	201.0185
	40	190.3497
	80	178.2939
	160	164.9831
0.4	10	206.22
	20	194.794
	40	181.5285
	80	166.5694
	160	150.245
0.45	10	201.7746
	20	187.9376
	40	171.8485
	80	153.8685
	160	134.6452
0.5	10	196.9126
	20	180.4443
	40	161.3723
	80	140.4072
	160	118.6418

Table 21: Condition Number $\kappa_{2,\alpha}$ for $u(x,t) = \sin(\pi x)t^\alpha$, using scheme (11), where $0.5 < \alpha \leq 0.75$

Condition Number $\kappa_{2,\alpha}$ for $u(x,t) = \sin(\pi x)t^\alpha$, using scheme (11)		
α	N	$\kappa_{2,2}$
0.55	10	191.6186
	20	172.3268
	40	150.2073
	80	126.4732
	160	102.7518
0.6	10	185.8827
	20	163.619
	40	138.5056
	80	112.4043
	160	87.486
0.65	10	179.702
	20	154.3782
	40	126.4586
	80	98.5579
	160	73.2843
0.7	10	173.0823
	20	144.6857
	40	114.2864
	80	85.2749
	160	60.4692
0.75	10	166.0394
	20	134.6458
	40	102.2228
	80	72.8465
	160	49.2246

Table 22: Condition Number $\kappa_{2,\alpha}$ for $u(x,t) = \sin(\pi x)t^\alpha$, using scheme (11), where $0.75 < \alpha < 1$

Condition Number $\kappa_{2,\alpha}$ for $u(x,t) = \sin(\pi x)t^\alpha$, using scheme (11)		
α	N	$\kappa_{2,2}$
0.8	10	150.8027
	20	124.3825
	40	90.4969
	80	61.4911
	160	39.6024
0.85	10	150.8027
	20	114.0344
	40	79.3164
	80	51.3433
	160	31.5471
0.9	10	142.6984
	20	103.7471
	40	68.8529
	80	42.4559
	160	24.9293
0.95	10	164.3488
	20	93.6653
	40	59.2332
	80	34.8116
	160	19.5782

By comparison, the condition numbers of the scheme presented in [56] are presented below. Recall that in [56], the time-fractional diffusion equation is written in differential form without the application of the Laplace transform. The L1-method is used to discretize the time-fractional diffusion equation (1) for $u \in C^2[0,T]$ and the same discrete Laplacian operator from the numerical experiments here is applied in the space variable. The resulting regularity requirements for the results in [56] require $u \in C^2([0,T]; C^6[0,1])$. The numerical experiment considered here has the exact solution $u(x,t) = \sin(\pi x)t^2$, consistent with the numerical experiment featured in [56]. To accurately compare the conditioning of both schemes, we consider $N = 10, 20, 40, 80, 160$ and $M = 25$. Similarly, the α values considered are $\alpha = 0.05, 0.1, 0.15, 0.2, 0.25, 0.3, 0.35, 0.4, 0.45, 0.5, 0.55, 0.6, 0.65, 0.7, 0.75, 0.8, 0.85, 0.9,$ 0.95. The condition numbers $\kappa_{2,2}$ are computed below. On average, the condition number for the integral formulation is 15 times smaller than the differential form of the time-fractional diffusion equation.

Table 23: Condition Number $\kappa_{2,2}$ for $u(x,t) = \sin(\pi x)t^2$, using L1 method in [56], where $0 < \alpha \leq 0.25$

Condition Number $\kappa_{2,2}$ for $u(x,t) = \sin(\pi x)t^2$, using L1 method in [56]		
α	N	$\kappa_{2,2}$
0.05	10	3631.00
	20	3617.74
	40	3604.11
	80	3590.01
	160	3575.73
0.1	10	3577.76
	20	3547.95
	40	3516.54
	80	3483.50
	160	3448.76
0.15	10	3519.56
	20	3469.62
	40	3415.82
	80	3358.04
	160	3296.17
0.2	10	3456.37
	20	3382.42
	40	3301.29
	80	3212.76
	160	3116.76
0.25	10	3388.09
	20	3286.20
	40	3172.72
	80	3047.59
	160	2911.05

Table 24: Condition Number $\kappa_{2,2}$ for $u(x,t) = \sin(\pi x)t^2$, using L1 method in [56], where $0.25 < \alpha \leq 0.5$

Condition Number $\kappa_{2,2}$ for $u(x,t) = \sin(\pi x)t^2$, using L1 method in [56]		
α	N	$\kappa_{2,2}$
0.3	10	3314.82
	20	3181.03
	40	3030.45
	80	2863.56
	160	2618.75
0.35	10	3236.70
	20	3067.23
	40	2875.35
	80	2663.03
	160	2433.96
0.4	10	3153.99
	20	2945.10
	40	2709.02
	80	2449.62
	160	2174.84
0.45	10	3067.06
	20	2816.45
	40	2533.65
	80	2228.07
	160	1912.24
0.5	10	2976.53
	20	2681.49
	40	2351.99
	80	2003.80
	160	1656.94

Table 25: Condition Number $\kappa_{2,2}$ for $u(x,t) = \sin(\pi x)t^2$, using L1 method in [56], where $0.5 < \alpha \leq 0.75$

Condition Number $\kappa_{2,2}$ for $u(x,t) = \sin(\pi x)t^2$, using L1 method in [56]		
α	N	$\kappa_{2,2}$
0.55	10	2882.43
	20	2541.93
	40	2167.14
	80	1782.42
	160	1414.77
0.6	10	2785.94
	20	2399.33
	40	1982.39
	80	1569.15
	160	1192.47
0.65	10	2687.59
	20	2255.36
	40	1800.93
	80	1368.38
	160	993.90
0.7	10	2588.13
	20	2111.73
	40	1625.68
	80	1183.33
	160	820.71
0.75	10	2488.38
	20	1970.11
	40	1459.11
	80	1016.04
	160	672.69

Table 26: Condition Number $\kappa_{2,2}$ for $u(x,t) = \sin(\pi x)t^2$, using L1 method in [56], where $0.75 < \alpha < 1$

Condition Number $\kappa_{2,2}$ for $u(x,t) = \sin(\pi x)t^2$, using L1 method in [56]		
α	N	$\kappa_{2,2}$
0.8	10	2389.15
	20	1832.04
	40	1303.11
	80	867.31
	160	548.28
0.85	10	2291.24
	20	1689.03
	40	1158.98
	80	737.01
	160	445.14
0.9	10	2954.44
	20	1571.84
	40	1027.44
	80	624.25
	160	360.54
0.95	10	2102.51
	20	1451.78
	40	908.68
	80	527.66
	160	291.72

APPENDIX D

NUMERICAL EXPERIMENT ILLUSTRATIONS

The figures for numerical experiments (27), (28) and (56) are presented below. For numerical experiments (27) and (28), we present the approximate solution u_i^n when compared to the exact solution $u(x,t)$, and the grid error over the entire mesh is presented as well. The first series of figures presents the exact solution $u(x,t) = \sin(\pi x)t^\alpha$ using the C^α approximation to solve the discrete approximation equation (11). The second series of figures presents the exact solution $u(x,t) = \sin(\pi x)t^{1.01}$ using the C^1 approximation to solve the discrete approximation equation (15). For numerical experiment (56), we present the approximation to the scalar equation first where u is unknown, but where $f(t) = t^\alpha$ and subsequently where $f(t) = t^{2\alpha}$. Then, the scalar equation is presented for the third and fourth-order approximate schemes where u is now known, where $u(t) = t^{6+\alpha} - t^{9/2}$. The latter examples feature $\alpha = 0.1, 0.25, 0.4, 0.5, 0.7, 0.9$ to showcase the necessity of the invertibility criterion that is presented in Chapter 2.
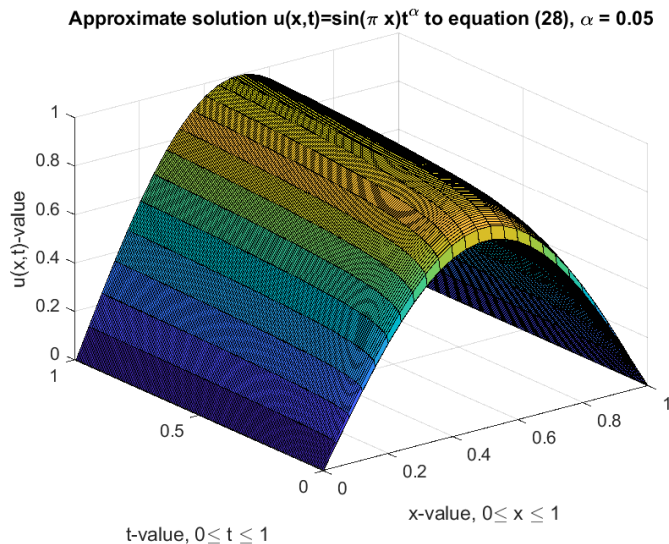
Figure 1: Numerical simulation of (28) with $u(x,t) = \sin(\pi x)t^\alpha$, $\alpha = 0.05$, $M = 25$ and $N = 160$ time steps

Approximate solution u(x,t)=sin(π x)t$^{\alpha}$ to equation (28), α = 0.25
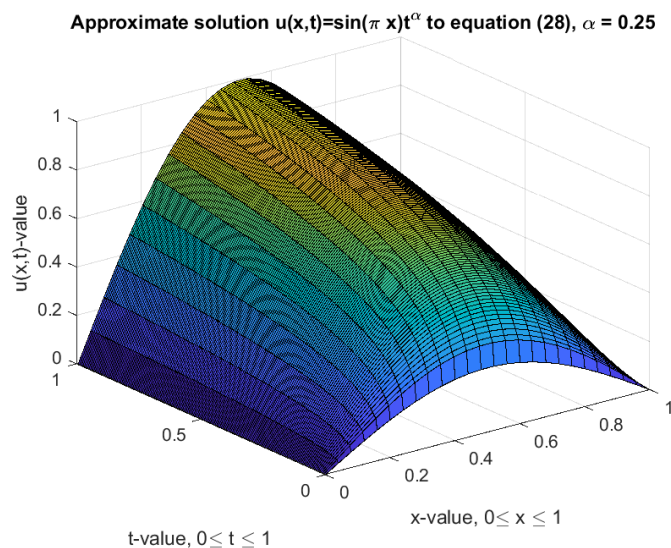
Figure 2: Numerical simulation of (28) with $u(x,t) = \sin(\pi x)t^{\alpha}$, $\alpha = 0.25$, $M = 25$ and $N = 160$ time steps

Approximate solution u(x,t)=sin(π x)t$^{\alpha}$ to equation (28), α = 0.5
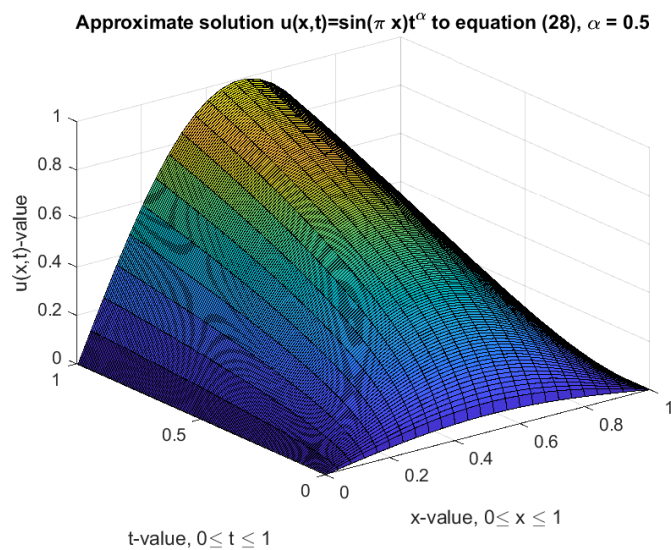
Figure 3: Numerical simulation of (28) with $u(x,t) = \sin(\pi x)t^{\alpha}$, $\alpha = 0.5$, $M = 25$ and $N = 160$ time steps

Approximate solution u(x,t)=sin(π x)t$^\alpha$ to equation (28), α = 0.75
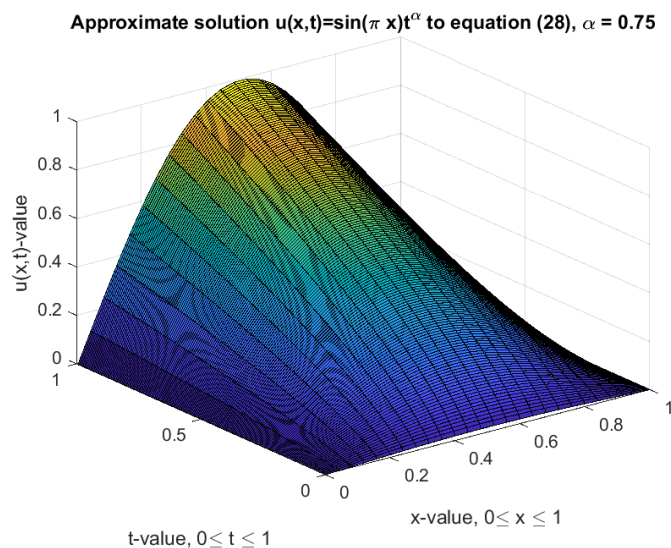
Figure 4: Numerical simulation of (28) with $u(x,t) = \sin(\pi x)t^\alpha$, $\alpha = 0.75$, $M = 25$ and $N = 160$ time steps

Approximate solution u(x,t)=sin(π x)t$^\alpha$ to equation (28), α = 0.95
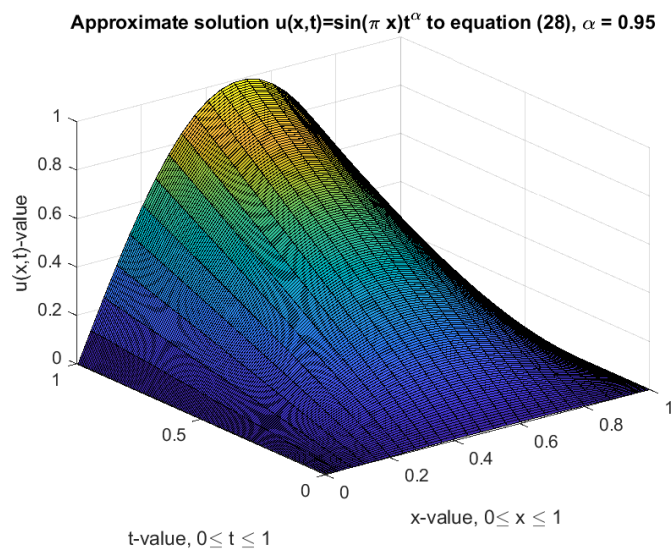
Figure 5: Numerical simulation of (28) with $u(x,t) = \sin(\pi x)t^\alpha$, $\alpha = 0.95$, $M = 25$ and $N = 160$ time steps
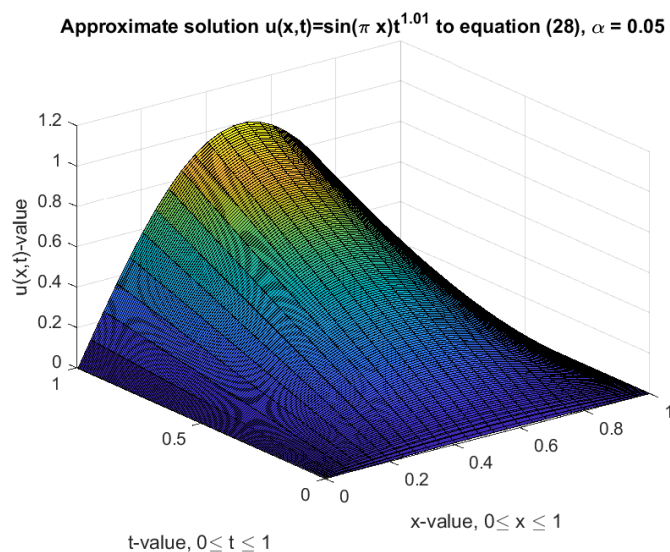
Figure 6: Numerical simulation of (28) with $u(x,t) = \sin(\pi x)t^{1.01}$, $\alpha = 0.05$, $M = 25$ and $N = 160$ time steps
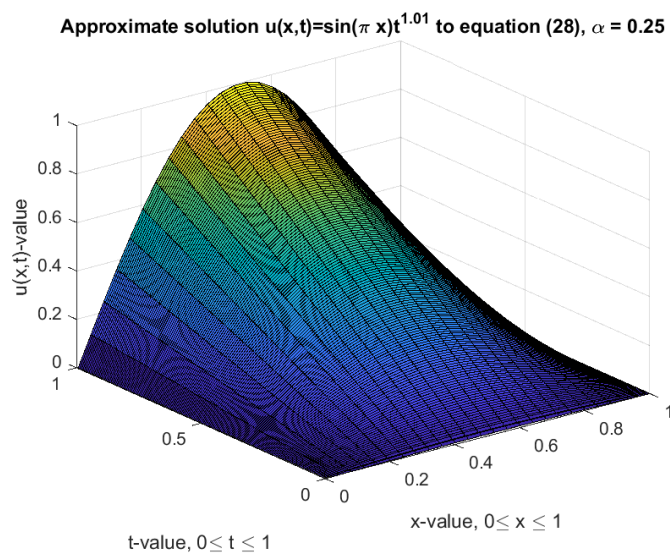
Figure 7: Numerical simulation of (28) with $u(x,t) = \sin(\pi x)t^{1.01}$, $\alpha = 0.25$, $M = 25$ and $N = 160$ time steps
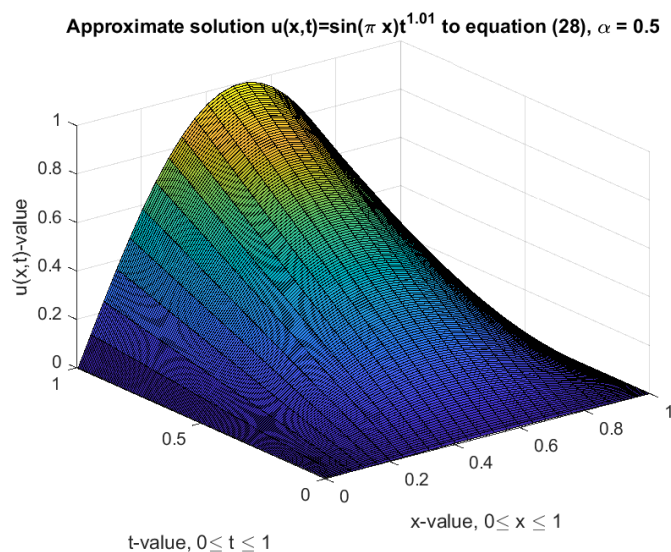
Figure 8: Numerical simulation of (28) with $u(x,t) = \sin(\pi x)t^{1.01}$, $\alpha = 0.5$, $M = 25$ and $N = 160$ time steps
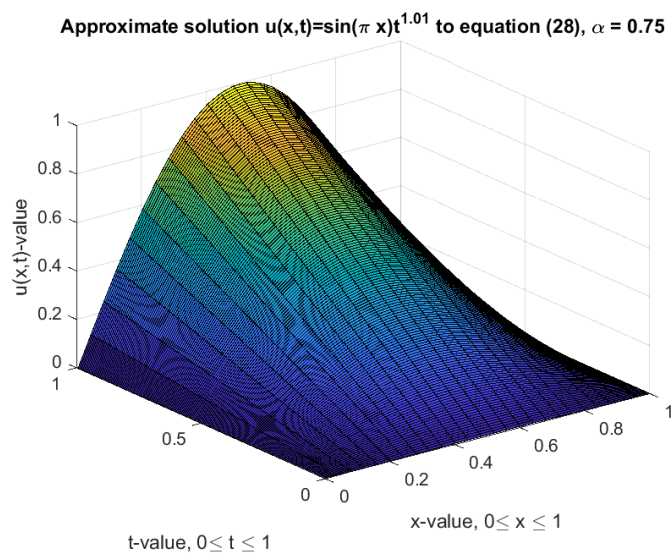
Figure 9: Numerical simulation of (28) with $u(x,t) = \sin(\pi x)t^{1.01}$, $\alpha = 0.75$, $M = 25$ and $N = 160$ time steps

Approximate solution u(x,t)=sin(π x)t$^{1.01}$ to equation (28), α = 0.95
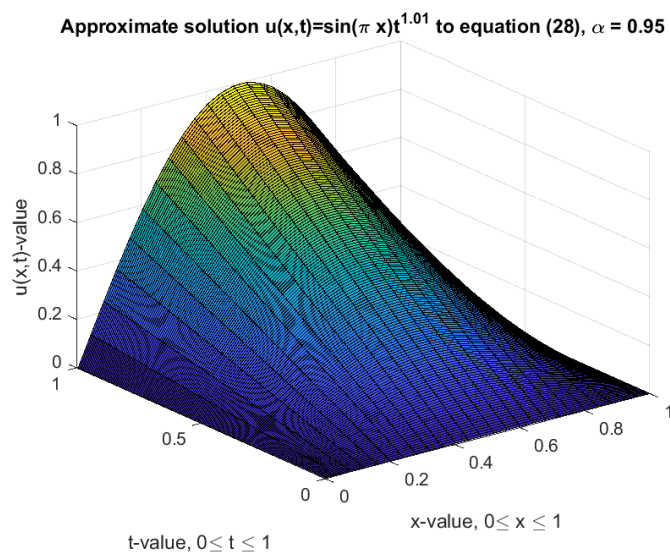
Figure 10: Numerical simulation of (28) with $u(x,t) = \sin(\pi x)t^{1.01}$, $\alpha = 0.95$, $M = 25$ and $N = 160$ time steps

Approximate solution to scalar equation (56) where f(t) = t$^{\alpha}$, α = 0.05
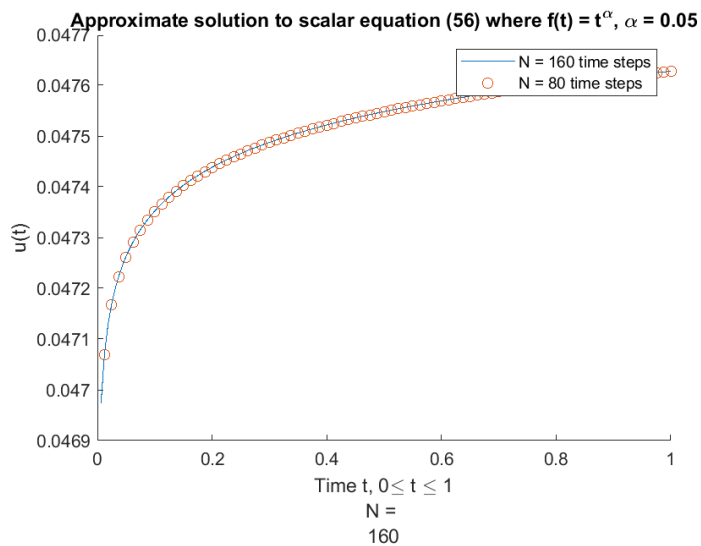
Figure 11: Numerical simulation of (56) with u unknown, $f(t) = t^\alpha$, $\alpha = 0.05$, $N = 80$ and $N = 160$ time steps
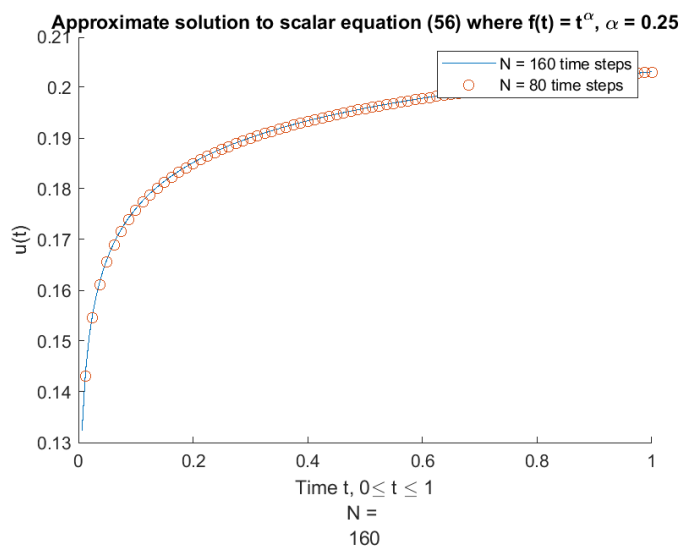
Figure 12: Numerical simulation of (56) with u unknown, $f(t) = t^\alpha$, $\alpha = 0.25$, $N = 80$ and $N = 160$ time steps
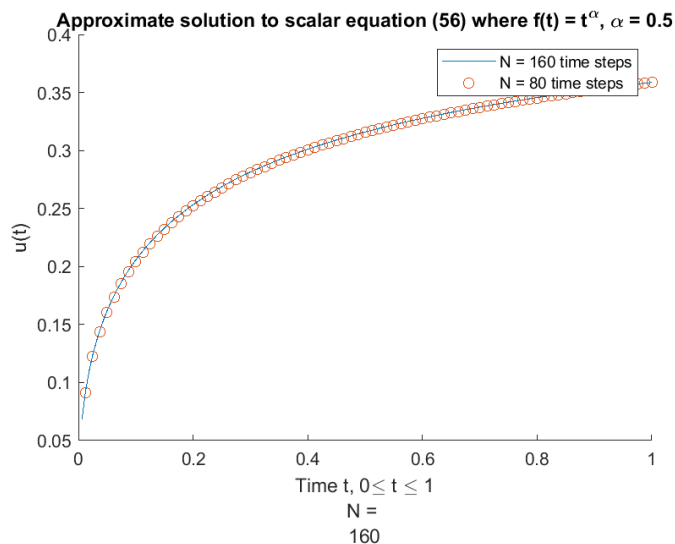
Figure 13: Numerical simulation of (56) with u unknown, $f(t) = t^\alpha$, $\alpha = 0.5$, $N = 80$ and $N = 160$ time steps
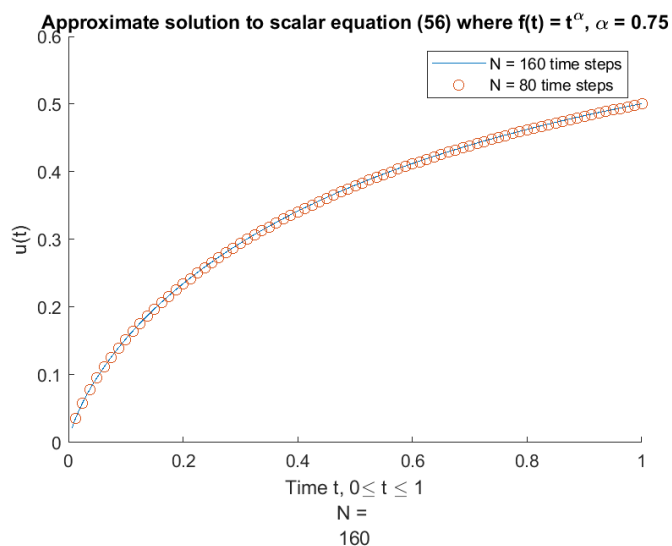
Figure 14: Numerical simulation of (56) with u unknown, $f(t) = t^\alpha$, $\alpha = 0.75$, $N = 80$ and $N = 160$ time steps
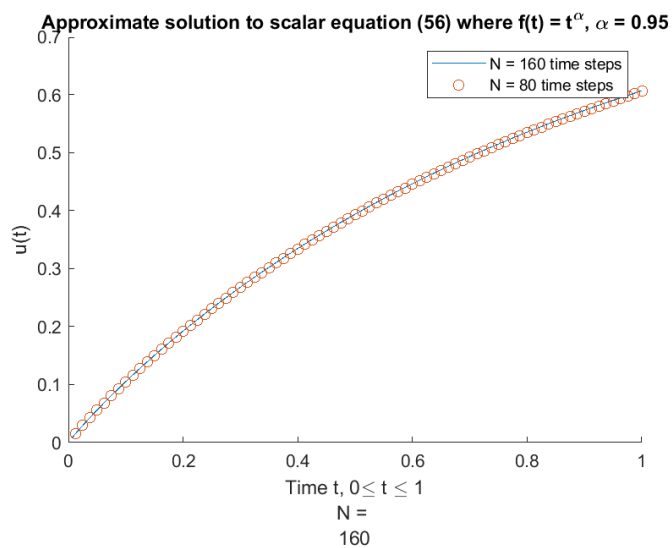
Figure 15: Numerical simulation of (56) with u unknown, $f(t) = t^\alpha$, $\alpha = 0.95$, $N = 80$ and $N = 160$ time steps
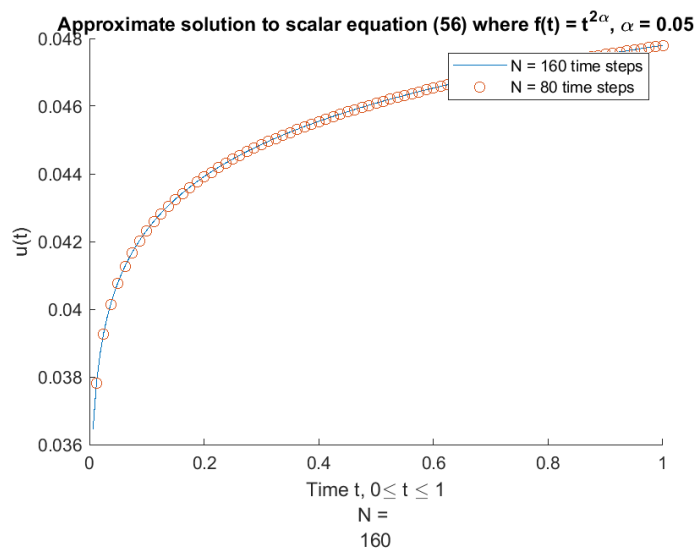
Figure 16: Numerical simulation of (56) with u unknown, $f(t) = t^{2\alpha}$, $\alpha = 0.05$, $N = 80$ and $N = 160$ time steps
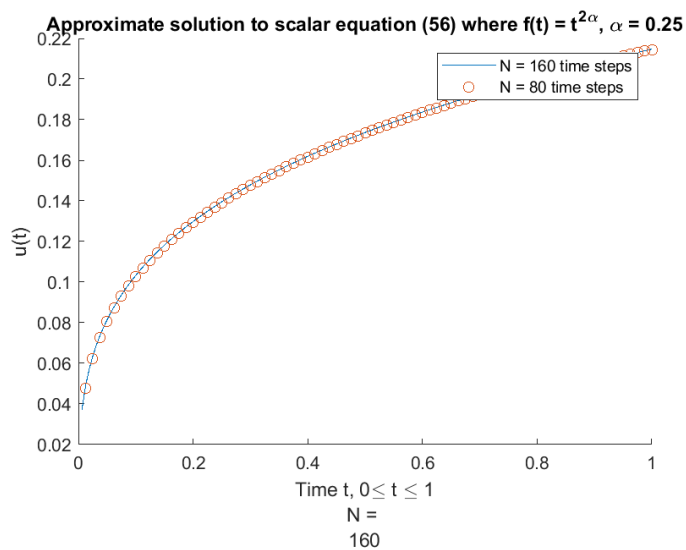
Figure 17: Numerical simulation of (56) with u unknown, $f(t) = t^{2\alpha}$, $\alpha = 0.25$, $N = 80$ and $N = 160$ time steps
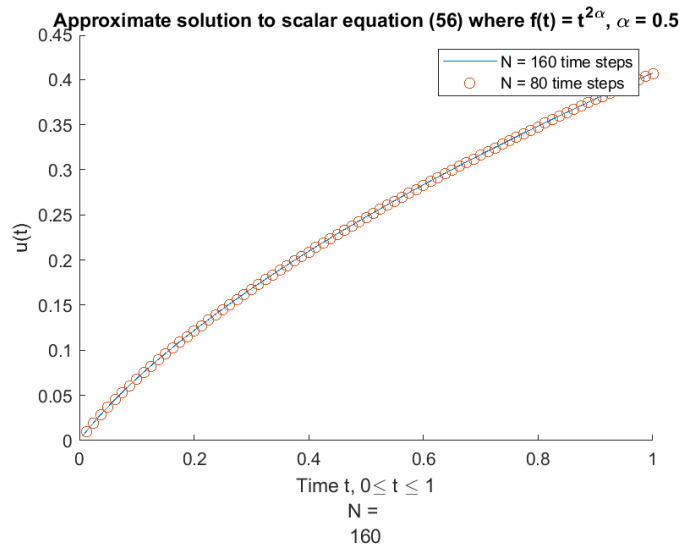
Figure 18: Numerical simulation of (56) with u unknown, $f(t) = t^{2\alpha}$, $\alpha = 0.5$, $N = 80$ and $N = 160$ time steps
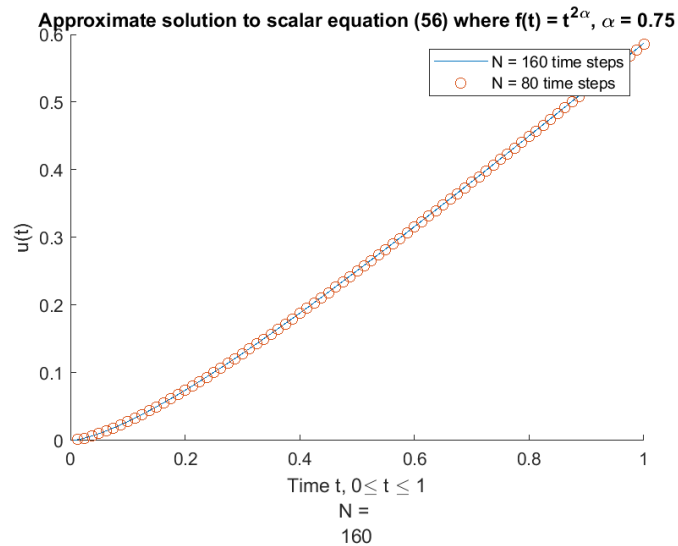
Figure 19: Numerical simulation of (56) with u unknown, $f(t) = t^{2\alpha}$, $\alpha = 0.75$, $N = 80$ and $N = 160$ time steps
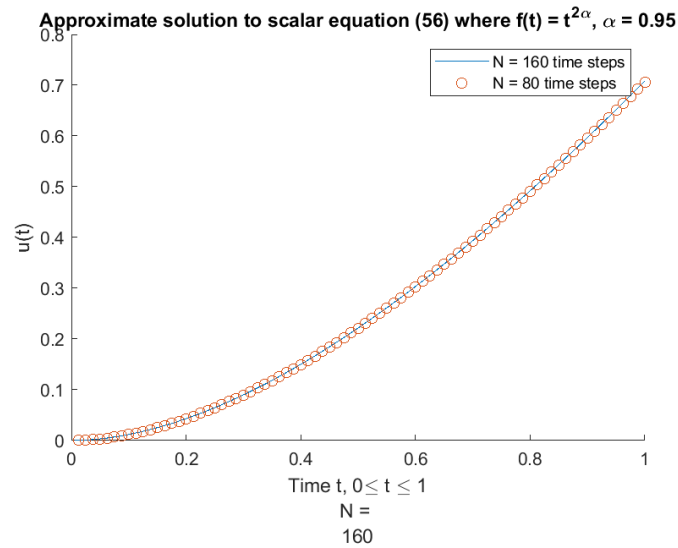
Figure 20: Numerical simulation of (56) with u unknown, $f(t) = t^{2\alpha}$, $\alpha = 0.95$, $N = 80$ and $N = 160$ time steps
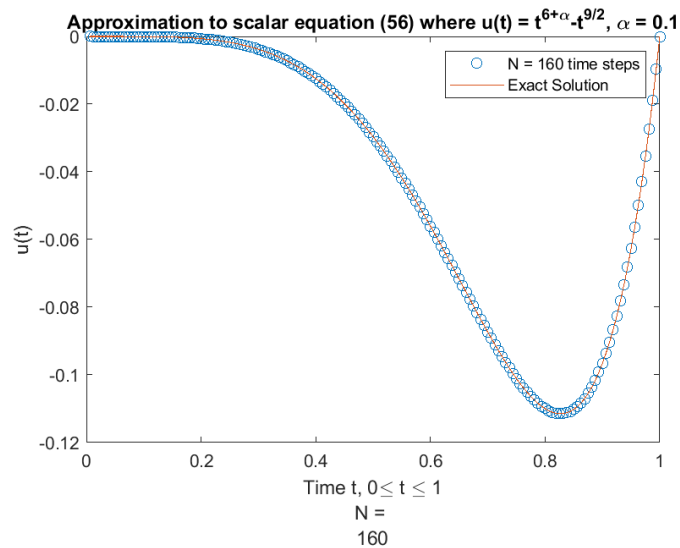
Figure 21: Numerical simulation of (56) with $u(t) = t^{6+\alpha} - t^{9/2}$, $\gamma = 3$, $\alpha = 0.1$, $N = 160$ time steps
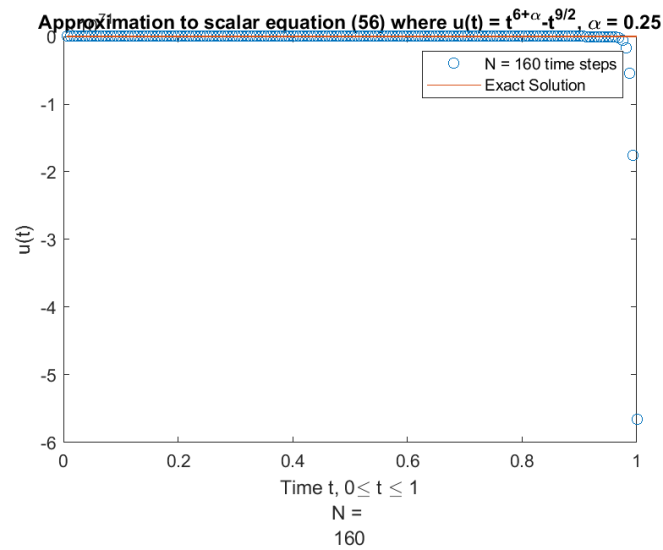
Figure 22: Numerical simulation of (56) with $u(t) = t^{6+\alpha} - t^{9/2}$, $\gamma = 3$, $\alpha = 0.25$, $N = 160$ time steps
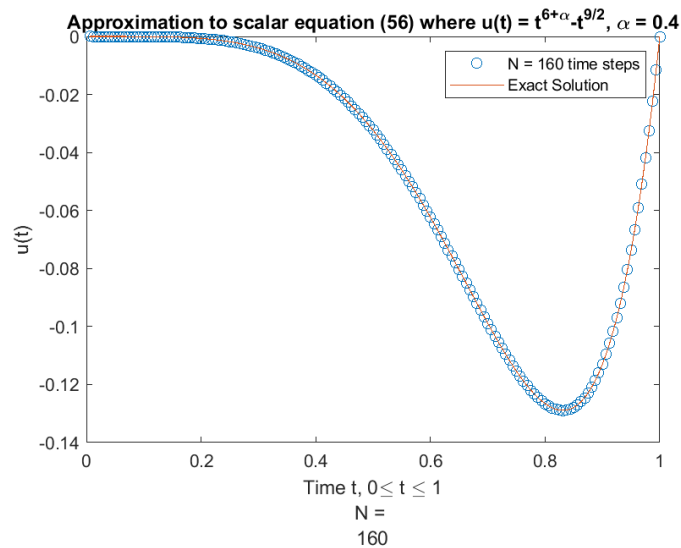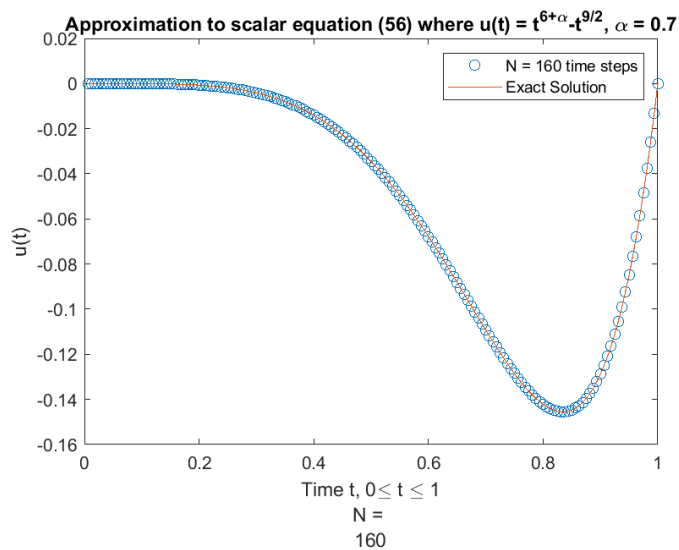

Figure 23: Numerical simulation of (56) with $u(t) = t^{6+\alpha} - t^{9/2}$, $\gamma = 3$, $\alpha = 0.4$, $N = 160$ time steps
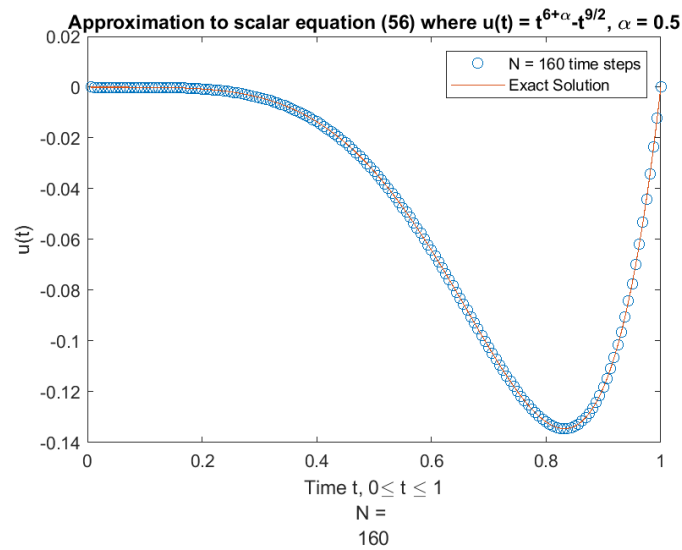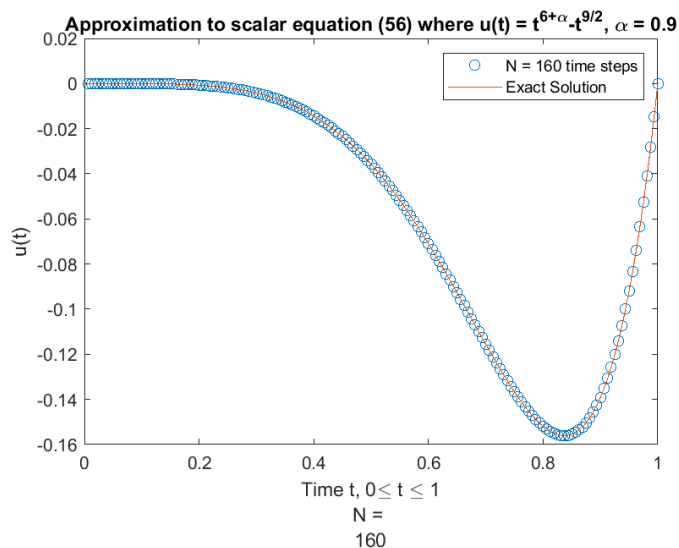
Figure 24: Numerical simulation of (56) with $u(t) = t^{6+\alpha} - t^{9/2}$, $\gamma = 3$, $\alpha = 0.5$, $N = 160$ time steps
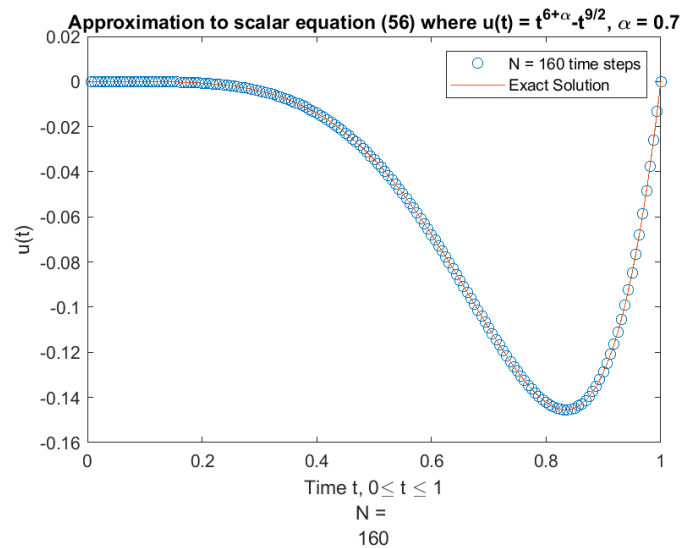
Figure 25: Numerical simulation of (56) with $u(t) = t^{6+\alpha} - t^{9/2}$, $\gamma = 3$, $\alpha = 0.7$, $N = 160$ time steps
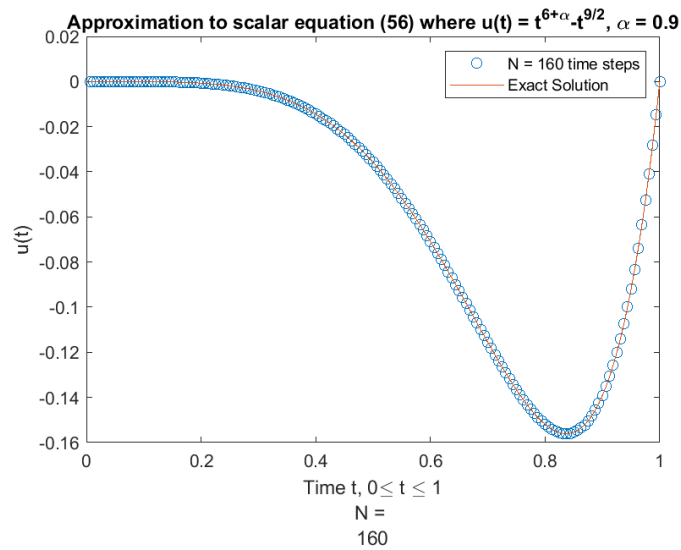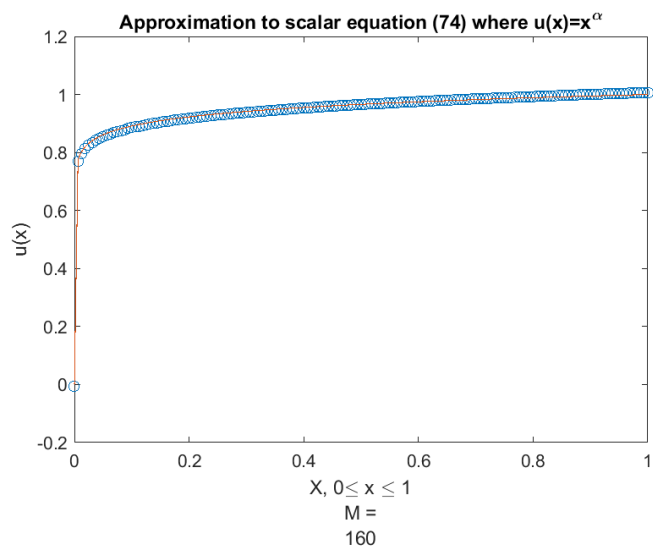
Figure 26: Numerical simulation of (56) with $u(t) = t^{6+\alpha} - t^{9/2}$, $\gamma = 3$, $\alpha = 0.9$, $N = 160$ time steps
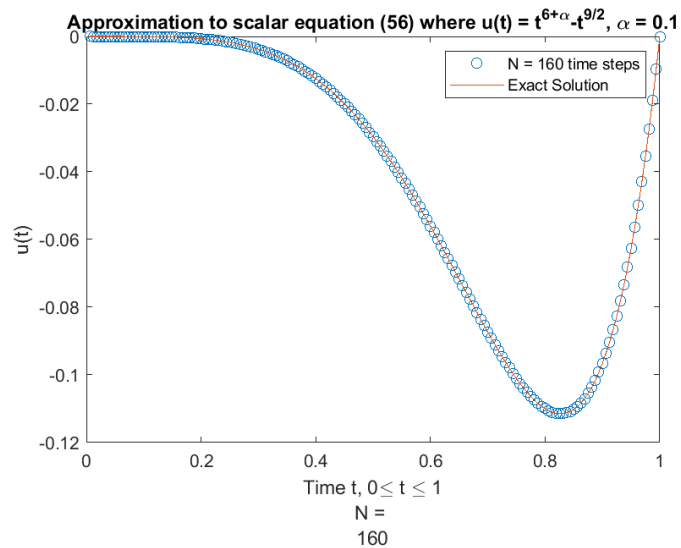
Figure 27: Numerical simulation of (56) with $u(t) = t^{6+\alpha} - t^{9/2}$, $\gamma = 4$, $\alpha = 0.1$, $N = 160$ time steps
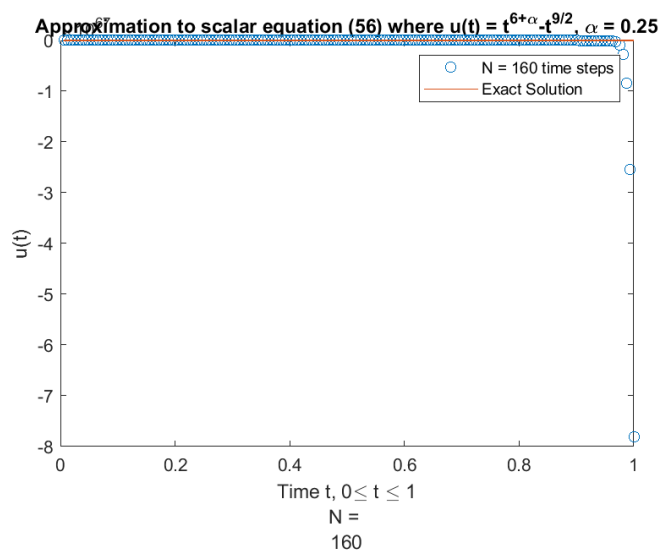
Figure 28: Numerical simulation of (56) with $u(t) = t^{6+\alpha} - t^{9/2}$, $\gamma = 4$, $\alpha = 0.25$, $N = 160$ time steps
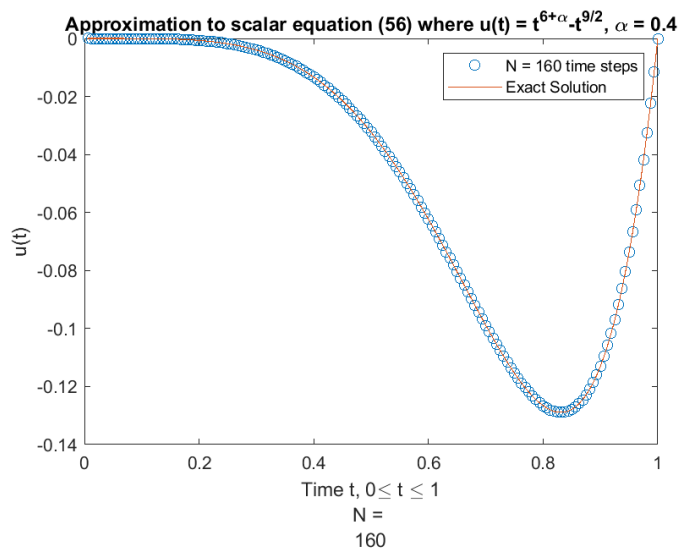
Figure 29: Numerical simulation of (56) with $u(t) = t^{6+\alpha} - t^{9/2}$, $\gamma = 4$, $\alpha = 0.4$, $N = 160$ time steps
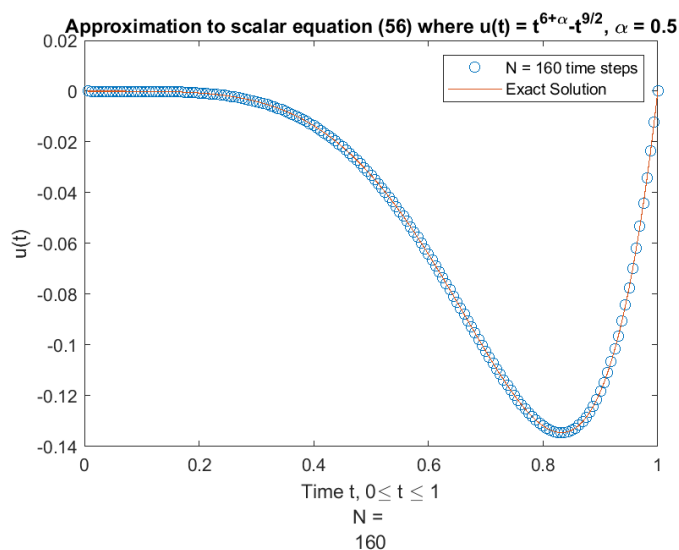
Figure 30: Numerical simulation of (56) with $u(t) = t^{6+\alpha} - t^{9/2}$, $\gamma = 4$, $\alpha = 0.5$, $N = 160$ time steps

Figure 31: Numerical simulation of (56) with $u(t) = t^{6+\alpha} - t^{9/2}$, $\gamma = 4$, $\alpha = 0.7$, $N = 160$ time steps

Figure 32: Numerical simulation of (56) with $u(t) = t^{6+\alpha} - t^{9/2}$, $\gamma = 4$, $\alpha = 0.9$, $N = 160$ time steps
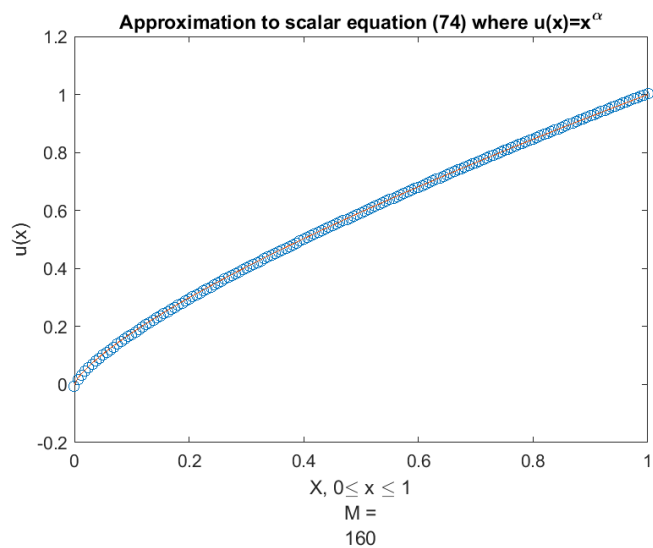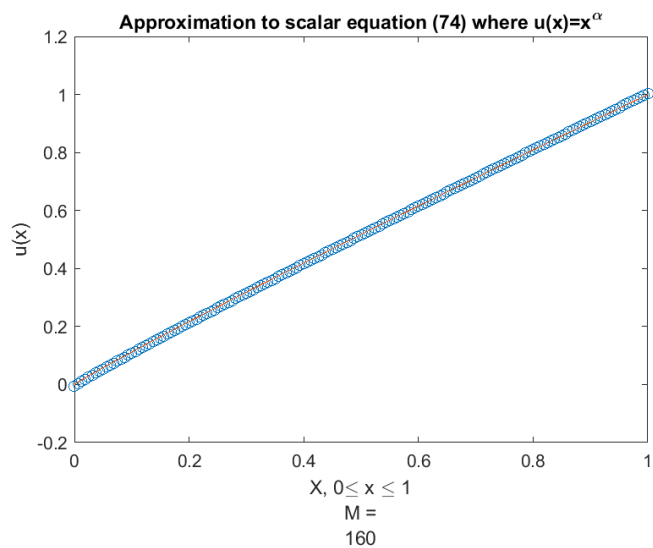

Figure 33: Numerical simulation of (74) with $u(x) = x^\alpha$, $\gamma = 1$, $\alpha = 0.05$, $M = 160$ space steps
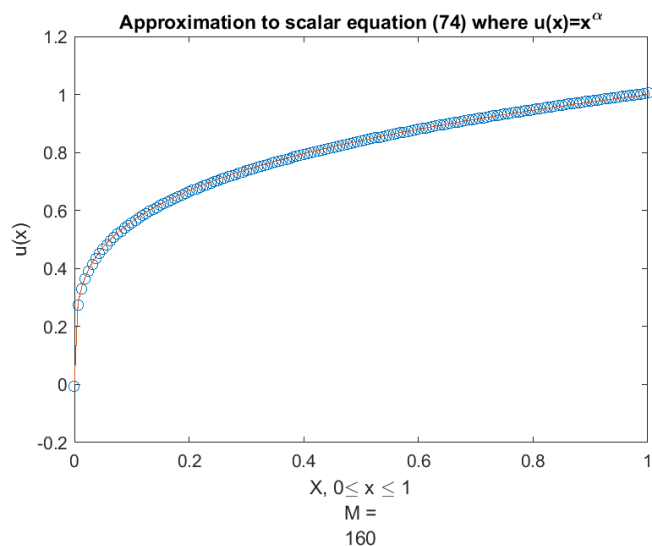
Figure 34: Numerical simulation of (74) with $u(x) = x^\alpha$, $\gamma = 1$, $\alpha = 0.25$, $M = 160$ space steps
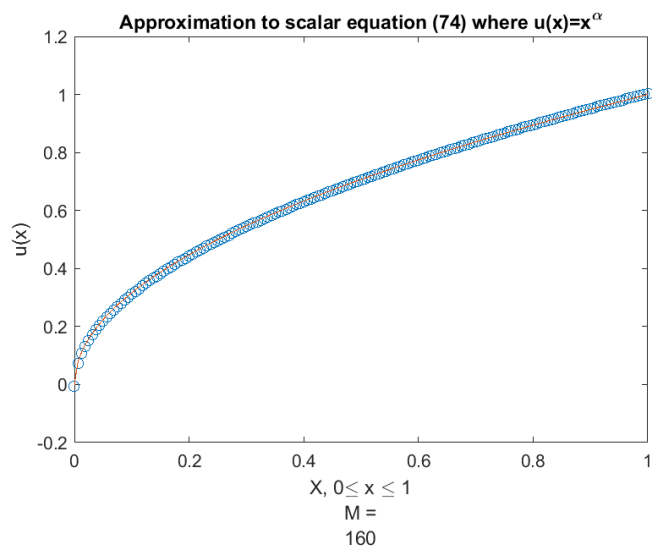
Figure 35: Numerical simulation of (74) with $u(x) = x^\alpha$, $\gamma = 1$, $\alpha = 0.5$, $M = 160$ space steps

Figure 36: Numerical simulation of (74) with $u(x) = x^\alpha$, $\gamma = 1$, $\alpha = 0.75$, $M = 160$ space steps

Figure 37: Numerical simulation of (74) with $u(x) = x^\alpha$, $\gamma = 1$, $\alpha = 0.95$, $M = 160$ space steps
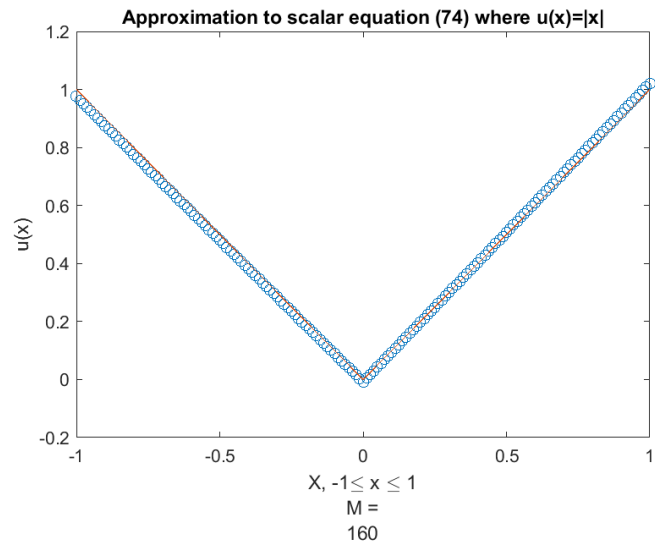
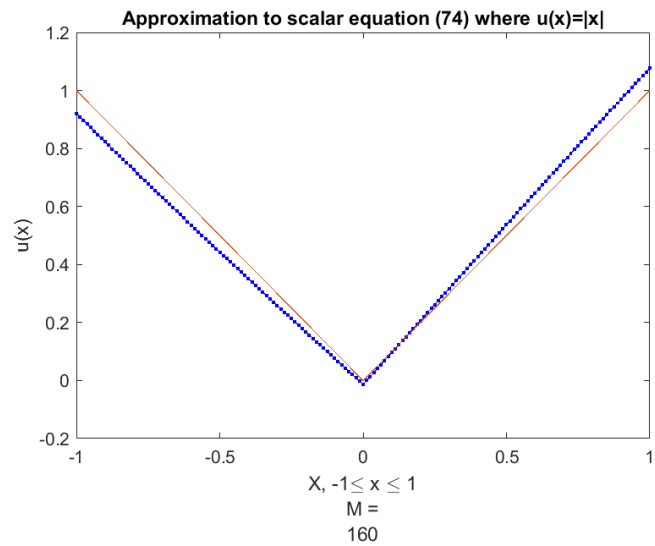Figure 38: Numerical simulation of (74) with $u(x) = |x|$, $\gamma = 1$, $M = 160$ space steps

Figure 39: Numerical simulation of (74) with $u(x) = |x|$, $\gamma = 2$, $M = 160$ space steps

VITA

Wesley C. Davis

Department of Mathematics and Statistics

Old Dominion University

Norfolk, VA, 23529

Education
Old Dominion University, M. S. Applied and Computational Mathematics,
Graduated Fall 2016

Virginia Wesleyan College (University), Graduated May 2014

Journal Publications and Accepted Articles
W. Davis, R. Noren, K. Shi, *A C^α Finite Difference method for the Caputo Time-Fractional Diffusion Equation*, Numer. Methods Partial Differential Equations, Accepted November 2020, published March 2021, https://doi.org/10.1002/num.22686.

W. Davis, R. Noren, *Stable and Convergent Difference Schemes for Weakly Singular Convolution Integrals*, Submitted to JIE Jan 2021, accepted Mar 30, 2021.

Conference Presentations
An Analysis of the Caputo Fractional Derivative Using Transform Methods, presented November 2016 and April 2018 at SEARCDE 2016 and at the ODU SIAM Mathematics Awareness Conference.